MEMBRANE DISTILLATION

a new approach using composite membranes

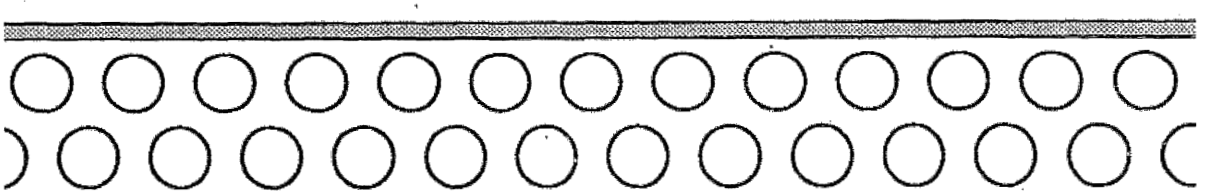

Tonnie Franken

11

MEMBRANE DISTILLATION

a new approach using composite membranes

PROEFSCHRIFT

ter verkrijging van
de graad van doctor aan de Universiteit Twente,
op gezag van de rector magnificus
prof.dr.ir. J.H.A. de Smit
volgens besluit van het College van Dekanen
in het openbaar te verdedigen
op vrijdag 23 september 1988 te 14.00 uur

door

ANTONIUS CHRISTIANUS MARIA FRANKEN

geboren op 9 mei 1957 te Klarenbeek

Dit proefschrift is goedgekeurd door de promotor prof. dr. C.A. Smolders
Assistent promotor: dr. ing. M.H.V. Mulder

Acknowledgement:

This paper is based upon work financially supported by the Ministry of Economical Affairs in The Netherlands and by Enka A.G. (Product Group Membrane), Wuppertal, Federal Republic of Germany.

Dit onderzoek werd uitgevoerd met geldelijke steun van het Ministerie van Economische Zaken en Enka A.G.

ISBN 90-9002420-4
Druk: Alfa, Enschede

"Tegenover enkele onverklaarbare feiten moet je proberen vele algemene wetten te bedenken waarvan je nog niet het verband ziet met de feiten waar je je mee bezighoudt: en plotseling, in het onverwachte verband van een resultaat, een geval en een wet, tekent zich een redenering voor je af die je overtuigender lijkt dan de andere."

(Umberto Eco in "De naam van de roos")

Velen hebben een bijdrage geleverd tot de verwezenlijking van dit proefschrift. Zonder iedereen bij name te noemen wil ik hen hiervoor langs deze weg hartelijk bedanken.

Tonnie

CONTENTS

Chapter 1:

INTRODUCTION

A.C.M. Franken

1.1: Terminology

A thesis concerning membrane technology should start with a definition of the subject itself. The problem, however, is that every definition has its limitations and everyone trying to define membrane technology takes the risk of being incomplete or not precise enough. Nevertheless, I think that one of the definitions worth mentioning is a (Dutch) definition of professor Smolders: 'Membraantechnologie is in feite schei-kunde in de letterlijke betekenis van het woord'. Translating this sentence into English while saving the pun is impossible, because 'schei-kunde' stands for both 'chemistry' and 'separation-science' at the same time; it will not be tried to do the impossible.

Many authors have tried to give a definition of 'membrane' itself. A new definition will not be added here, but attention is drawn to the definition given in a report of the European Society of Membrane Science and Technology on terminology: 'a **membrane** is an intervening phase separating two phases and/or acting as an active or passive barrier to the transport of matter between phases adjacent to it' (1). Although defined and accepted by the European Society of Membrane Science and Technology, there will always be scientists who will not be fully satisfied with this definition. Nevertheless, standardization of terminology and symbols will diminish the confusion of tongues and will contribute to a better understanding between membranologists. In this thesis a report on terminology for membrane distillation is given as an appendix. This report has also been published by the European Society of Membrane Science and Technology (2).

1.2: Membrane technology

In the last fifteen years membranes and membrane processes have evolved from a useful laboratory tool to an industrial product of significant tech-

nical and commercial importance. Membrane processes have not only replaced some of the conventional separation techniques in all kinds of industries, but they have also successfully been utilized to solve mass separation problems where conventional techniques failed or were too expensive.

Because membrane technology is in fact nothing more or less than a new separation technology, it has to compete with and prove its superiority over existing separation techniques. This is one of the reasons why the development of membrane technology does not show such an explosive growth as for instance biotechnology. Although in some cases membranes are accepted as the best alternative for a separation problem, this does not imply that from one day to the other membrane technology is the only separation technique to solve that specific problem. The fact that already huge investments into an existing technology have been made or the fact that membrane technology is not a 'proven' technique yet are some other factors for the relatively slow development of membrane technology.

The development of membrane technology can be illustrated by the example of the production of chlorine and sodium hydroxide by means of electrolysis of a salt-rich brine solution. Although membrane electrolysis offers several advantages over the conventional techniques (mercury electrolysis and diaphragm electrolysis), due to economical reasons only a few plants in the world operate using membranes. Only when replacement investments or new investments are made, in more than 90% of the cases membranes will be used (3). Due to this (slow) replacement of the existing technologies, it takes a relatively long time before this electrolysis process is an 'all-membrane' process. However, in this case a 'break-through' could be expected if the environmental legislation on the use of mercury and/or asbestos should be made more strict.

The though competition with the existing separation techniques (which are also being improved!), the 'conservative' investment policy of the industry and the fact that membranes and membrane processes cannot fulfil all the expectations ascribed to them in the recent history, are the main reasons that a real 'break-through' of membrane technology has not taken place. Nevertheless, membrane technology is a firmly growing technique with a growth of the annual turnover of 12 to 15% (4).

In figure 1.1 the turnover is presented as a function of the stage of development for various membrane processes (5).

The processes in the first stage (research) are processes which are technically known and available, but have not been developed commercially. Examples of this stage are thermo-osmosis (TO), membrane sensors (MS) and active transport (AT).

The second stage (development) is marked by a high rate of growth. In this stage the technical development and the maintenance of the pilot-plants are the most important variables and the price of the technique is of less importance. Pervaporation (PV), membrane distillation (MD) and liquid membranes (LM) are, among others, typical examples of this group.

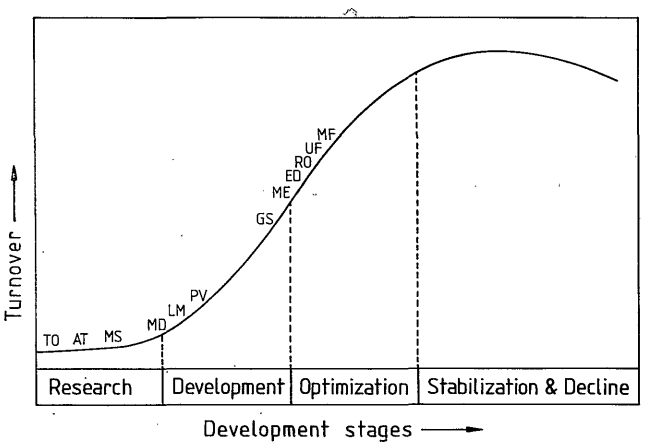

FIGURE 1.1: Stages of development of various membrane processes (5).

The processes, which are mentioned in the third stage (optimization), are so-called state-of-the-art processes. The development of the processes in this group is as good as finished and optimization of the process design is the most important variable. The rate of growth in this stage is high, only diminishing for the 'older' processes. Examples of this stage are microfiltration (MF), ultrafiltration (UF), reverse osmosis (RO) and electrodialysis (ED). Membrane electrolysis (ME) and gas separation (GS) are somewhere between the second and the third group.

The fourth stage of development (stabilization and decline) is marked by a levelling off or decline of turnover. In this stage the processes are replaced by other technologies. Until now, no membrane process has reached this stage of 'development'.

Some of the technically interesting membrane processes are summarized in table 1.1. The first five processes in this table are from a commercial point of view the most important processes. Microfiltration has about 30% of annual turnover in membrane technology and dialysis and reverse osmosis each have about 15% of the world market in membranes. Electrodialysis and ultrafiltration together possess about 15 to 20% of the market [6], resulting in a total market-share of these five processes of about 80%. From figure 1.1 it can be seen that these processes are already in the stage of optimization and the expectations are that the market-share of these processes will reach a saturation point in the near future [4,5,6].

Table 1.1: Some membrane separation processes.

Membrane Process	Phases	Driving Force	Some Applications
Dialysis	L/L	Concentration difference	Hemodialysis (artificial kidney)
Micro-filtration	L/L	Pressure difference (0.01 - 0.1 MPa)	Sterile filtration Cell harvesting Production of ultrapure water
Ultra-filtration	L/L	Pressure difference (0.1 - 1 MPa)	Separation of oil/water emulsions Recovery of proteins from whey, milk and blood
Reverse Osmosis	L/L	Pressure difference (2 - 10 MPa)	Desalination of sea and brackish water Concentration of whey and juice
Electro-dialysis	L/L	Electric potential difference	Desalination of brackish water Desalination of food (e.g. whey) Removal of metals from waste water
Gas Separation	G/G	Pressure difference (4 - 10 MPa)	Recovery of hydrogen Oxygen enriched air Purification of methane in biogas
Pervaporation	L/V	Partial vapour pressure difference	Concentration of ethanol Separation of azeotropic mixtures
Membrane Distillation	L/V/L	Partial vapour pressure difference	Desalination of sea water and brackish water Boiler feed water production
Liquid Membranes	L/L	Concentration difference	Nitrate removal from ground water

The other membrane processes do not have such a high annual turnover, but it must be remembered that these processes are still in a stage of development. The expected growth of these processes (especially membrane electrolysis, gas separation and pervaporation) is considerable.

A point of interest for membrane technology are the developments in biotechnology. The need for sophisticated separation technologies is of essential importance for the development of this field of research. In contrast to most other applications, membrane technology has equal chances compared to the other separation technologies, because for every type of technology chosen investments must be made. Since the most important criteria to be considered are selectivity and low operation temperatures, membrane technology is slightly preferred. Furthermore, the price of the separation technique has not the highest importance, because the separation costs are often low compared to the value of the product (4).

Less spectacular, but nevertheless interesting, are the possibilities for membrane technology as an environmental technology. In a recent report membrane technology is mentioned as an interesting alternative for solving and preventing environmental problems. Especially the use of reverse osmosis in treatment of polluted water (for instance percolation water of a refuse-dump) and the use of vapour permeation for the recovery of organic solvents from air are mentioned (7,8).

1.3: Thermo-osmosis

Thermally driven membrane processes are known for more than one hundred years. Mass transport of gases by thermo-osmosis was observed for the first time in 1873 by Feddersen, who called this effect 'thermo-diffusion' (9,10). Since these investigations the thermo-osmosis of gases has been studied by several authors (11-15).

Thermo-osmosis of liquids is of more recent date. The first observations were made by Lippman in 1907 and Aubert in 1912 (10,16). Because no stationary state was reached, these observations are rather obscure and can also be a result of osmosis and/or electro-osmosis. The first steady-state observations on thermo-osmosis were made in 1950, as Alexander and Wirtz investigated thermo-osmosis of water through cellophane and nitro-cellulose membranes (9,10). At a given temperature difference a constant pressure

difference between the two phases adjacent to the membrane was found. These measurements and also further investigations by other authors were conducted on aqueous solutions (17-21).

Thermo-osmosis has been described by Haase as 'mass transport through a membrane as a result of a temperature difference' (9). By that time (1959) Haase did not realize that other thermally driven membrane processes (e.g. membrane distillation) would be developed to which this definition can also be applied. The main difference between thermo-osmosis and membrane distillation is that the membranes in the former process can be porous or non-porous and that no phase transition occurs between the feed side and the permeate side of the membrane. In a membrane distillation operation, (selective) evaporation of the liquid feed takes place and the permeant is transported as a vapour through the pores of a non-wetted membrane. Although it is difficult to give an exact definition of membrane distillation containing all the characteristics of the membrane operation (2), the previous statement is accurate enough to explain the difference between membrane distillation and thermo-osmosis.

Nevertheless Haase was one of the first to realize that not every thermally driven membrane process can be called thermo-osmosis. For instance, he described that the transport of gases through porous membranes is in fact Knudsen diffusion.

Later authors were not as careful as Haase in defining thermo-osmosis and used terms like 'thermo-dialysis' (21-25) to describe the same phenomenon. In some of these cases it can be doubted whether a thermo-osmotic effect is observed at all (21,24,25). Pagliuca et al. (24) noticed that 'the transmembrane pressure produced in the TF-450 membranes far exceeds thermo-osmotic pressures ever found in dense membranes under comparable conditions'. Considering that they were doing experiments on the transport of water through porous Teflon membranes, it is most likely that they were performing membrane distillation experiments without knowing it.

Although thermo-osmosis has quite a long history, in figure 1.1 the process is listed as being in the first stage of development (research) and probably this process will never come out of this stage. This is due to a lack of practical applications of thermo-osmosis, since small solvent fluxes and small separation factors are normally obtained (26).

1.4: Membrane distillation

1.4.1: Historical development

The renewed interest in thermally driven processes has been generated by a relatively new process, called membrane distillation. This process is generally used to remove water from aqueous solutions of inorganic solutes. Desalination of sea water and the production of boiler feed water are the best-known applications.

Although the concept of membrane distillation is known for about twenty years, the process is still in its developing stage. The first patent on membrane distillation was obtained by Weyl in 1967 (applied for in 1964) (27) and the first publication on this subject was made by Findley in 1967 (28). The reason why membrane distillation did not become directly a well-respected separation technique was the lack of good membranes. Findley concluded that 'if low cost, high temperature, long-life membranes with desirable characteristics can be obtained, this method would become an economical method of evaporation (..)'. Even though Findley et al. (29) were able to make the surface of the membranes more hydrophobic by using Teflon, the membranes did not have the desired properties for the development of membrane distillation by that time.

It took till about 1980 before membrane distillation as a separation technique was rediscovered. By that time the conditions, stated by Findley, were (at least to a certain extent) fulfilled. Microporous membranes, made of polypropylene (PP), poly(vinylidene fluoride) (PVDF) and poly(tetrafluoro ethylene) (PTFE, Teflon), were available for the use in membrane distillation.

1.4.2: Description of the membrane operation

Membrane distillation is a distillation process in which two aqueous solutions with different temperatures are separated by a microporous hydrophobic membrane. In this process the pores of the microporous membrane, which are not wetted by the liquid mixtures at the feed side or the permeate side, act as the vapour phase. The vapour pressure difference, resulting from the temperature difference across the membrane, causes vapour molecules to be transported from the warm feed side to the cold permeate side.

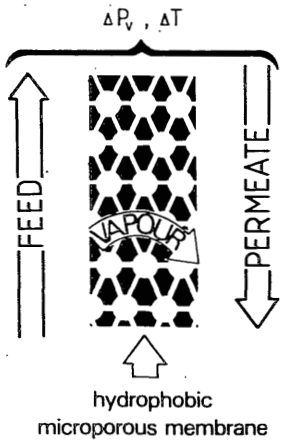

FIGURE 1.2:
Schematic representation
of membrane distillation.

The characteristics of a membrane distillation operation, which are given explicitly in the report on terminology (2), can be reduced to one important point, being that the permeant is transported as a vapour through the pores of a porous membrane, which is at least at one side in direct contact with the liquid.

The transport mechanism of membrane distillation involves three steps:

1. evaporation at the feed side of the membrane;
2. transport of the vapour through the pores of the hydrophobic membrane;
3. condensation of the vapour at the permeate side of the membrane.

On the basis of this transport mechanism, it can be understood that the separation mechanism of membrane distillation is formed by the vapour-liquid equilibrium. The maximum selectivity that can be obtained will never exceed the selectivity which is calculated from this vapour-liquid equilibrium. Therefore, membrane distillation is not a real alternative for distillation, because it cannot be used in difficult separation problems, such as azeotropic mixtures.

1.4.3: Applications

Most publications, both patents and articles, concern desalination of saline water (30-42), but in recent years a number of investigators doubt the feasibility of this application (39,43,44). Desalination of brackish water or sea water can be performed more economically by reverse osmosis or MSF-distillation, especially if large-scale applications are concerned. According to these authors, the special advantages of membrane distillation should be emphasized and applications of this process must be found in

area's where i) high osmotic pressures are involved, ii) a high purity of the permeate is necessary, iii) waste heat is available and/or iv) small-scale applications are concerned. Special applications, mentioned in literature, are the concentration of a feed up to very high solute concentrations (39,48), production of boiler feed water for power plants (44,45) and the use of membrane distillation in applications where waste heat can be used (41,49).

Only a few authors considered the possibility of separating organic aqueous solutions by membrane distillation (50-52). Honda et al. (50) were the first to discuss the possibility of separating aqueous solutions of alcohols and carboxylic acids. More recently Gostoli et al. (51) and Franken et al. (52) published on the separation of ethanol and water by membrane distillation. However, membrane distillation of these mixtures is only possible if the restrictive condition, that the pores of the hydrophobic membrane should not be filled with liquid, is fulfilled. Therefore, Franken et al. (53) have defined a maximum allowable concentration of the organic component in water and have developed a method to determine this value.

1.4.4: Different embodiments of membrane distillation

A number of different embodiments of membrane distillation exists, which all are consistent with the characteristics of the membrane operation as described in section 1.4.2 and in the report on terminology for membrane distillation (2).

Direct-contact membrane distillation is the oldest (27-29) and the most simple embodiment of membrane distillation, in which the liquid on both sides of the membrane is in direct contact with the membrane and in which the liquid on the downstream side is used as the condensing medium (see figure 1.3). The main advantage of this system is that it can be used in any desired membrane configuration (flat sheets, spiral wound, capillaries or hollow fibers). The direct-contact system is used by Enka A.G. in a process called "Trans Membrane Distillation" (44-47). Enka uses modules with capillary membranes, which have the additional advantage that they can be used without any modification in microfiltration as well. The possibilities for heat recovery when the process is conducted in counter-current flow makes this process especially suitable for commercial applications (44,45).

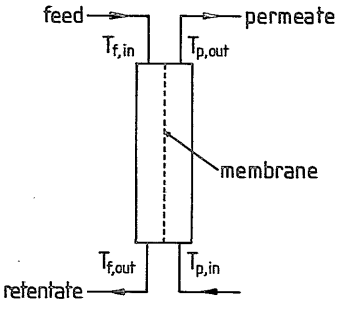

FIGURE 1.3:
Direct-contact
membrane distillation.

The second type of embodiment is **gas-gap membrane distillation.** This system makes use of a cooling surface inside the module and the condensed liquid on the downstream side does not have to be in contact with the membrane. Among others, the Svenska Utvecklings Aktiebolaget makes use of a spacer to separate the membrane from the cooling surface (40-42). In this case the membrane and the cooling surface are strictly separated from each other by the spacer.

Advantages of this system compared to direct-contact membrane distillation are that the gas-gap (or air-gap as it is commonly called) reduces the heat loss through the membrane considerably and that wetting of some of the pores of the membrane does not spoil the permeate quality at once. A disadvantage of this system is that only plate-and-frame or spiral-wound modules can be used due to the existence of a condensation surface. Furthermore, the construction of the modules is rather complicated (and relatively expensive) compared to the modules used in direct-contact membrane distillation. These disadvantages make this system rather unattractive for commercialization.

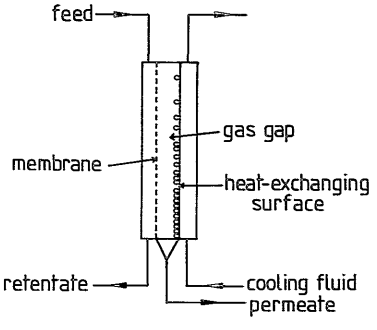

FIGURE 1.4:
Gas-gap membrane distillation.

Low pressure membrane distillation is a system in which a low pressure ('vacuum') is applied downstream and in which the condensation of the permeating vapour takes place outside the module (2). Until so far, this system is only used on a laboratory scale by a few investigators (54,55). Due to a removal of inert gases from the membrane an enhanced diffusion of the permeate through the membrane takes place, resulting in an increase of the flux through the membrane by about a factor 4 as compared to other process designs (55).

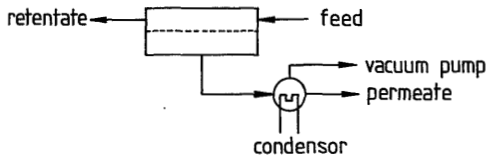

FIGURE 1.5: Low pressure membrane distillation.

The last embodiment mentioned in the terminology report is **sweeping gas membrane distillation** (2). In this system a sweeping gas is used downstream to remove the permeating vapour, which is condensed outside the module. Basini et al. have performed measurements on the permeation of water through PTFE and PP membranes and came to the conclusion that the flux is higher and the heat loss through the membrane is comparable when these experiments are compared with experiments with gas-gap membrane distillation (56). In our own experiments on ethanol/water mixtures, we found that fluxes are in the order of magnitude of direct-contact membrane distillation. Depending on the flow rate of the sweeping gas, selectivities up to the selectivities as predicted by the vapour-liquid equilibrium could be reached (55).

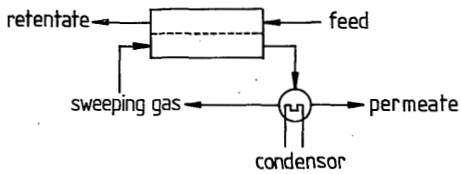

FIGURE 1.6: Sweeping gas membrane distillation.

An embodiment of membrane distillation which cannot be directly assigned to one of the descriptions above is the membrane distillation module as described by Gore (35). The module consists of a thin flexible microporous membrane which is positioned against an impermeable, rigid condensor sheet. The permeating vapour diffuses through the membrane and condenses against the condensor sheet. According to the definitions, this process should be called 'gas-gap membrane distillation'. However, in steady-state operation no gas gap is present in this module and, furthermore, the membrane is in direct contact with a thin film of the condensed permeate. Considering the thin liquid film as the condensing medium, this system is a representative of 'direct-contact' membrane distillation.

Lefebvre (57) described a system, which was called 'osmotic membrane distillation'. This system, which belongs to the group of direct-contact membrane distillation, differs from a conventional membrane distillation unit by the use of a highly concentrated salt solution at the permeate side. Due to this concentrated solution, the vapour pressure at the permeate side of the membrane is reduced, resulting in a higher flux across the membrane.

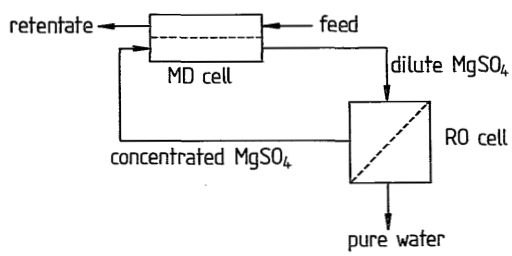

FIGURE 1.7: Osmotic membrane distillation.

The diluted salt solution (preferably magnesium sulfate) can be concentrated again by reverse osmosis. A practical application of this process can be found in the concentration of solutions which cannot be heated. Although this process is an interesting object for the study of mass transport in membrane distillation, it is thought that the practical value of this process is low. Sarti et al. calculated that a temperature difference of 0.6°C is enough to overcome an osmotic pressure of 50 bars (5 MPa) at room temperature (58). In the same way it can be calculated that the reduction of the partial vapour pressure due to a concentration of 15% $MgSO_4$ in compari-

son with clean water can be achieved more easily by the reduction of the permeate temperature by less than 1°C.

1.5: Pervaporation

The most common definition of pervaporation is: a membrane process in which a liquid is in direct contact with one side of the membrane (feed side) and in which the permeating product is removed as a vapour at the other side of the membrane (permeate side) by applying a reduced partial pressure. If this definition is used without any further specification, one might think that membrane distillation is a special case of pervaporation. To make a distinction between membrane distillation and pervaporation, it should be added to the above definition that the name pervaporation is used for the selective permeation of a liquid through a dense polymer matrix, whereas membrane distillation describes the permeation through the pores of a membrane. Unfortunately, Japanese authors do not distinguish between both processes and use the term 'pervaporation' for both.

Although the principle of pervaporation is known since the beginning of this century (the term 'pervaporation' was already introduced in 1917 by Kober), it took until the beginning of the sixties before the research on pervaporation was intensified (59). Binning et al. reported on a number of possible applications for pervaporation, but unfortunately the membranes used in their investigations showed insufficient flux and selectivity to compete with existing separation techniques (60).

A new revival came in the early seventies when energy prices raised to such an extent that alternatives for energy-consuming separation techniques became interesting. As a result of this 'energy-crisis', the research into pervaporation was intensified and many groups throughout the world were searching for superior membranes. The development of asymmetric membranes by Loeb and Sourirajan (61) and the subsequent research into thin composite membranes (see next paragraph), were of great importance for the development of pervaporation.

Nevertheless, it took until 1982 before the German company GFT patented a composite membrane for the separation of aqueous mixtures of ethanol (62) and started to commercialize the pervaporation process. Since this time about 25 pervaporation installations with a total capacity of about 250

m^3/day have been installed, all using GFT membranes (60). Although membranes with superior properties have been developed (63,64), the instability of these membranes does not permit a commercialization at this moment.

A more detailed description of pervaporation with respect to transport mechanism and different embodiments of the process is given in chapter 6 of this thesis.

1.6: Composite membranes

1.6.1: Preparation methods

The evolution of ultrathin synthetic membranes started with the development of asymmetric membranes by Loeb and Sourirajan (61). This invention led almost immediately to a search for alternative ways to make thin membranes. Most of the methods to make composite membranes were developed in the late sixties and early seventies of this century (65).

Commercially interesting methods to make composite membranes are casting, dip-coating, plasma polymerization and interfacial polymerization. Other methods of making composite membranes are water-casting (spreading of a polymer solution on water), dynamic membrane formation and spray-coating. For various reasons these methods are commercially not interesting and are only used on laboratory scale.

Although casting is not a method to make ultrathin composites, membranes with a thickness of about 3 to 5 μm can be obtained. Advantages of this method are that hardly any defects occur and that the selectivities obtained are very close to the intrinsic selectivity of the polymer membrane material. The disadvantage of these relatively thick membranes is of course the low flux. This method is mainly used for the production of membranes to be used in separation problems which demand a high selectivity. GFT describes the use of this method for the production of pervaporation membranes, consisting of a poly(vinyl alcohol) toplayer on a polyacrylonitrile support (62).

A preparation technique, which is commonly known under the name of 'dip-coating', was described for the first time by Carnell and Cassidy (66,67). Riley et al. (68) succeeded in making ultrathin reverse osmosis membranes, made from cellulose acetate. In their investigations, they dipped a clean glass plate into a dilute polymer solution. After evaporation of the

solvent and drying of the films, they were floated off onto a water surface and placed on molecular filter supports. Despite the tricky preparation method, useful membranes as thin as 60 nm were prepared reproducibly by this method.

The more common way to prepare 'dip-coated' membranes is to bring the porous sublayer directly into contact with the polymer solution. The coating of elastomers onto an ultrafiltration sublayer is one of the most used methods for the preparation of membranes for vapour permeation (69,70). The best-known example of a thin silicone-rubber coating applied by dip-coating is the Prism membrane of Monsanto (71).

The pioneer of the use of plasma polymerization to prepare thin membranes is without any doubt Yasuda (72). He observed that under certain conditions organic vapours become a partially ionized gas or 'plasma', which will deposit on nearby solid surfaces as a very thin polymer film with an ill-defined chemistry. Although a lot of research is being performed on this subject, the relative complicated process design and the bad reproducibility of the membranes are the malefactor that plasma polymerized membranes have not been commercialized yet (65).

Probably the most successful method to make composite membranes is interfacial polymerization (73). In this method a condensation polymerization is carried out at the interface of two immiscible solutions. By choosing the conditions in such a way that the reaction takes place at the surface of a finely porous membrane, a thin film composite of the condensation polymer is obtained. All the membranes obtained by this method are used in reverse osmosis. Commercial examples are NS-100 membranes of North Star and FT-30 of Film Tec (65).

1.6.2: Influence of the support

The most frequently mentioned support in composite membranes is an asymmetric membrane made of polysulfone (69,71,73). The advantage of polysulfone is that it can be easily manufactured into an asymmetric membrane with the desired surface porosity and surface pore sizes of less than 20 nm. Depending on the application, the surface porosity can be adjusted within certain limits. For instance, for gas separation (in case of the Monsanto membrane) the surface porosity should be as low as possible, whereas on the other hand for vapour permeation a high surface porosity is desired. As an example of the latter application, it can be mentioned that Strathmann has

published that a support having a surface porosity of 25% with pore sizes of about 20 nm can be prepared (69). Other supports which are mentioned in literature are porous films of cellulose nitrate / cellulose acetate (CNCA) (72) and porous asymmetric membranes of polyacrylonitrile (PAN) (62).

Although most authors involved in the fabrication of thin composite membranes do not discuss the influence of the sublayer, it appears that the sublayer is often as important as the toplayer. From investigations at our institute (74) and communications with other investigators, it appeared that, once a sublayer can be made reproducibly without defects, the actual manufacturing of the composite membrane itself is a minor problem.

Another aspect of the porous sublayer, besides supporting the selective layer, is its role in the actual separation process. As far as the above applications are concerned, the sublayer is mainly used as a support. Only the Monsanto Prism-membrane makes use of the separation characteristics of the sublayer and the silicone-rubber coating is used to reduce the effect of 'pin-holes' (71).

1.6.3: Composite membranes in membrane distillation

Membrane distillation is only possible if the restrictive condition, that the pores should not be filled with liquid is guaranteed. To prevent the hydrophobic membrane from being wetted, a thin polymer layer can be applied to this hydrophobic membrane. In such a composite membrane the hydrophobic sublayer determines the separation characteristics of the membrane distillation process.

The use of composite membranes in membrane distillation was described by Cheng et al. (30-34) in a series of patents. While performing membrane distillation experiments on saline water with microporous hydrophobic membranes, Cheng observed water-logging of the membranes after several days of operation. It is believed that water-logging occurs in desalination due to a growth of salt crystals through the membrane (30). To prevent or at least to reduce the effect of water-logging, the hydrophobic membrane is coated with a hydrophilic membrane. The coating can be applied at both sides of the membrane, but should at least be applied at the feed side of the membrane (31). The hydrophilic coating can be made of, for instance, cellulose acetate or polysulfone (32). Although the hydrophylic layer can be non-porous, also good results were obtained with pore sizes in the range of 25 till 50 nm (32).

As soon as organic solutes are present in an aqueous solution, the surface tension of this solution will decrease rapidly. When the concentration of the organic material in the feed exceeds a certain limit, the hydrophobic microporous membrane will be filled with liquid instantaneously and the membrane distillation process cannot be used.

A solution for this problem is to use a composite membrane, consisting of a hydrophilic selective toplayer and a porous hydrophobic sublayer. In this thermally driven membrane operation the toplayer is permselective to water. Because the toplayer shows a permselectivity towards one of the components, this process differs essentially from the above description by Cheng et al. The use of the hydrophobic porous sublayer is, however, still very essential for this process since the pores of this sublayer contain the vapour phase. As far as wetting of the microporous hydrophobic membrane is concerned, only the liquid at the permeate side of the composite membrane has to fulfil the non-wetting condition. In chapter 6 of this thesis the separation of mixtures of ethanol and water, using this 'modified' membrane distillation operation, is described.

Although the title of this paragraph suggests that this membrane operation is a modification of the membrane distillation operation, it is a new process design of pervaporation. Because the separation characteristics of this membrane operation are determined by the permselective toplayer, the name 'membrane distillation' should not be applied.

1.7: Structure of this thesis

The main objective of the research project was to develop composite membranes, consisting of a hydrophilic selective toplayer and a porous hydrophobic sublayer, which can be used in a thermally driven pervaporation process for the dehydration of aqueous organic components. In this thesis several aspects concerning the development of these composite membranes are described.

Chapters 2 and 3 both deal with the characterization of the microporous sublayer. In these chapters the criteria for the applicability of a membrane distillation operation and a thermally driven pervaporation process are described. In **chapter 2** theoretical considerations about wetting of polymers are given and an experimental method is described to measure the maximum allowable concentration of an organic component in water at which

the liquid is on the verge of penetration into the membrane.

In **chapter 3** the influence of the structure of a hydrophobic microporous membrane on its wettability is discussed. Theoretical considerations on the penetration of a liquid into different pore structures are confirmed by experiments, using the experimental method of the previous chapter.

The next two chapters discuss the possibility of separating a mixture of ethanol and water by membrane distillation. A model, in which vapour-liquid equilibria data are combined with an effect of temperature and concentration polarization, is described in **chapter 4**.

In **chapter 5** membrane distillation experiments with ethanol/water mixtures are described and the experimental selectivities and fluxes are compared with the calculated values.

Chapter 6 describes a new process design for pervaporation in which a composite membrane, consisting of a hydrophilic selective toplayer and a porous hydrophobic sublayer, is used. The driving force for this process is caused by the thermal gradient existing between the warm feed side of the membrane and the cold permeate side of the membrane. In this chapter the characteristics of this new process design and its advantages over other pervaporation designs are described.

In **chapter 7** a method for the application of a homogeneous permselective layer onto a porous hydrophobic sublayer, called the evaporation-deposition method, is described. Several coating variables are discussed and results of the application of a poly(vinyl alcohol) layer onto microporous polypropylene capillaries are evaluated by pervaporation experiments.

The report on 'Terminology for Membrane Distillation' as published by the European Society of Membrane Science and Technology is given as an **appendix** to this thesis.

1.8: References

1. V. Gekas; Terminology for Pressure Driven Membrane Operations; European Society of Membrane Science and Technology, June 1986.
2. A.C.M. Franken & S. Ripperger; Terminology for Membrane Distillation; European Society of Membrane Science and Technology, January 1988 (given as an appendix to this thesis).
3. Interview with J. Zwinkels, production manager of AZC's Rotterdam Botlek site; Saltgram 36 (Facts figures features from Akzo Zout Chemie), 1983.
4. A. Schrauwers; Machevo '86, Membraantechnologie een solide groeier; PT/Procestechniek 41 (1986) nr.9, 140-143.

5. H. Strathmann & H. Chmiel; Membranen in der Verfahrenstechnik; Chemie Ingenieur Technik 57 (1985) 581-596.
6. H. Finken & T. Krätzig; Industrielle Anwendungen der Gaspermeation; Chemie Technik 13 (1984) nr.8, 75-85.
7. L.J. Kuijvenhoven, M.M.J. Allessie, C.P.M. van Ginneken; Membraantechnonologie als Milieutechnologie; PT/Procestechniek 42 (1987) nr.1, 17-21.
8. C.P.M. van Ginneken & L.J. Kuijvenhoven (Tebodin); Verkennende studie naar de toepassingsmogelijkheden van membraantechnologie in het milieuveld; rapport 81774, januari 1987.
9. R. Haase; Thermoosmose in Flüssigkeiten, I. Grundlagen; Zeitschrift für Physikalische Chemie Neue Folge 21 (1959) 244-269.
10. H. Voellmy & P. Läuger; Untersuchungen über Thermoosmose in Flüssigkeiten; Berichte der Bunsengesellschaft Physikalische Chemie 70 (1966) 165-170.
11. E.A. Mason & A.P. Malinauskas; Gaseous Diffusion in Porous Media, IV. Thermal Diffusion; The Journal of Chemical Physics 41 (1964) 3815-3819.
12. R.P. Rastogi & H.P. Singh; Heats of Transport of Gases, II. Thermoosmosis of Binary Gaseous Mixtures without Chemical Reaction; The Journal of Physical Chemistry 74 (1970) 1946-1949.
13. R.P. Rastogi & Byas Misra; Thermoosmotic Studies on Argon Gas and Binary Gaseous Mixtures of Argon and Ethylene Through an Unglazed Porcelan Membrane; Journal of Membrane Science 4 (1978) 1-15.
14. R.P. Rastogi & A.P. Rai; Thermoosmosis of Gaseous Mixtures, IV. Thermoosmotic Concentration Difference; Journal of Membrane Science 4 (1979) 291-304.
15. R. Ash, R.M. Barrer, A.V. Edge & T. Foley; Thermo-osmosis of Sorbable Gases in Porous Media, part I: Theoretical Basis of Two Methods of Mixture Separation; Journal of Membrane Science 10 (1982) 183-207.
16. K. Sollner; The Early Developments of the Electrochemistry of Polymer Membranes; pages 46-47. In: E. Sélègny (editor); Charged Gels and Membranes, part I; Reidel Publishing Company, Dordrecht, Holland, 1976.
17. R. Haase & C. Steinert; Thermoosmose in Flüssigkeiten, II. Messungen; Zeitschrift für Physikalische Chemie Neue Folge 21 (1959) 270-297.
18. R.P. Rastogi, R.L. Blokhra & R.K. Agarwal; Cross-phenomenological Coefficients, Part 1. Studies on Thermo-osmosis; Transactions of the Faraday Society 60 (1964) 1386-1390.
19. R. Haase & H.J. de Greiff; Thermoosmose in Flüssigkeiten, III. Richtungsumkehr und Zeitverlauf; Zeitschrift für Physikalische Chemie Neue Folge 44 (1965) 301-313.
20. J.I. Mengual, J. Aguilar & C. Fernandez-Pineda; Thermoosmosis of Water Through Cellulose Acetate Membranes; Journal of Membrane Science 4 (1978) 209-219.
21. N. Pagliuca, D.G. Mita & F.S. Gaeta; Isothermal and Non-isothermal Water Transport in Porous Media, I. The Power Balance; Journal of Membrane Science 14 (1983) 31-57.
22. F.S. Gaeta & D.G. Mita; Non-isothermal Mass Transport in Porous Media; Journal of Membrane Science 3 (1978) 191-214.
23. F. Bellucci, E. Drioli, F.S. Gaeta, D.G. Mita, N. Pagliuca & D. Tomadacis; Temperature Gradient Affecting Mass Transport in Synthetic Membranes; Journal of Membrane Science 7 (1980) 169-183.
24. N. Pagliuca, G. Perna, D.G. Mita, F.S. Gaeta, B. Karamalis & F. Bellucci; Perspectives of Practical Applications of Thermodialysis; Journal of Membrane Science 16 (1983) 91-108.
25. F.S. Gaeta & D.G. Mita; Thermal Diffusion Across Porous Partitions. The Process of Thermodialysis; Journal of Physical Chemistry 83 (1979) 2276-2285.

26. F. Bellucci; Temperature Polarization Effects in Thermo-osmosis; Journal of Membrane Science 9 (1981) 285-301.
27. P.K. Weyl; Recovery of Demineralized Water from Saline Waters; United States Patent US 3,340,186.
28. M.E. Findley; Vaporization Through Porous Membranes; Industrial & Engineering Chemistry, Process Design & Development 6 (1967) 226-230.
29. M.E. Findley, V.V. Tanna, Y.B. Rao & C.L. Yeh; Mass and Heat Transfer Relations in Evaporation through Porous Membranes; AIChE Journal 15 (1969) 483-489.
30. D.Y. Cheng & S.J. Wiersma; Apparatus and Method for Thermal Membrane Distillation; United States Patent US 4,419,187.
31. D.Y. Cheng & S.J. Wiersma; Composite Membrane for a Membrane Distillation System; United States Patent US 4,419,242.
32. D.Y. Cheng; Method and Apparatus for Distillation; United States Patent US 4,265,713.
33. D.Y. Cheng & S.J. Wiersma; Composite Membrane for a Membrane Distillation System; United States Patent US 4,316,772.
34. D.Y. Cheng; Thermal Membrane Distillation System; European Patent EP 0149666.
35. W.L. Gore, R.W. Gore & D.W. Gore; Desalination Device and Process; European Patent EP 0088315.
36. D.J. Curtin; Membrane Distillation Method; United States Patent US 4,460,473.
37. E. Drioli, N. Chlubek & A. Punzo; Studio sui Processi a Membrana Condotti sotto Gradiente Termico; La Chimica e l'Industria 66 (1984) 147-152.
38. E. Drioli, V. Calabro & Y. Wu; Microporous Membranes in Membrane Distillation; Pure & Applied Chemistry 58 (1986) 1657-1662.
39. E. Drioli, Y. Wu & V. Calabro; Membrane Distillation in the Treatment of Aqueous Solutions; Journal of Membrane Science 33 (1987) 277-284.
40. A.-S. Jönsson, R. Wimmerstedt & A.-C. Harrysson; Membrane Distillation - A Theoretical Study of Evaporation Through Microporous Membranes; Desalination 56 (1985) 237-249.
41. S.-I. Andersson, N. Kjellander & B. Rodesjö; Design and Field Tests of a New Membrane Distillation Desalination Process; Desalination 56 (1985) 345-354.
42. N. Kjellander & B. Rodesjö; Apparatus for Desalting Salt Water by Membrane Distillation; Patent PCT WO 87/00160.
43. W.T. Hanbury & T. Hodgkiess; Membrane Distillation - An Assessment; Desalination 56 (1985) 287-297.
44. S. Ripperger; Transmembraandestillatie; PT/Procestechniek 41 (1986) nr.8, 50-53.
45. K. Schneider & T.J. van Gassel; Membrandestillation; Chemie Ingenieur Technik 56 (1984) 514-521.
46. K. Ostertag; Verfahren und Vorrichtung zur Transmembrandestillation; German Patent DE 3312359.
47. K. Ostertag; Verfahren zum Trennen eines Flüssigkeitsgemisches oder einer Lösung mittels einer porösen Trennwand; German Patent DE 3334640.
48. S. Kimura, S. Nakao & S. Shimatani; Transport Phenomena in Membrane Distillation; Journal of Membrane Science 33 (1987) 285-298.
49. A.G. Fane, R.W. Schofield & C.J.D. Fell; The Efficient Use of Energy in Membrane Distillation; Desalination 64 (1987) 231-243.
50. Z. Honda, H. Komada, K. Okamoto & M. Kai; Nonisothermal Mass Transport of Organic Aqueous Solution in Hydrophobic Porous Membrane; pages 587-594. In: E. Drioli & M. Nakagaki (editors); Membranes and Membrane Processes (Proceedings of the Europe-Japan Congress on Membranes and Membrane Processes; Stresa (Italy), June 18-22, 1984); Plenum Press, New York, 1986.

51. C. Gostoli, G.C. Sarti & S. Bandini; Membrane Distillation of Ethanol-Water Mixtures; chapter 29, pages 383-394. In: M.S. Verral & M.J. Hudson (editors); Separation for Biotechnology; Publishing Co. Ellis Horwood; 1987.
52. A.C.M. Franken, J.A.M. Nolten, M.H.V. Mulder & C.A. Smolders; Ethanol/Water Separation by Membrane Distillation: Effect of Temperature Polarization, pages 531-540. In: B. Sedlacek & J. Kahovec (editors); Synthetic Polymeric Membranes; De Gruyter, Berlin, 1987.
53. A.C.M. Franken, J.A.M. Nolten, M.H.V. Mulder, D. Bargeman & C.A. Smolders; Wetting Criteria for the Applicability of Membrane Distillation; Journal of Membrane Science 33 (1987) 315-328. (also chapter 2 of this thesis)
54. S. Nakao, F. Saitoh, T. Asakura, K. Toda & S. Kimura; Continuous Ethanol Extraction by Pervaporation from a Membrane Bioreactor; Journal of Membrane Science 30 (1987) 273-287.
55. A.C.M. Franken; to be published.
56. L. Basini, G. D'Angelo, M. Gobbi, G.C. Sarti & C. Gostoli; A Desalination Process through Sweeping Gas Membrane Distillation; Desalination 64 (1987) 245-257.
57. M.S.M. Lefebvre; Osmotic Concentration by Membrane; PCT International Application WO 86 03,135.
58. G.C. Sarti, C. Gostoli & S. Matulli; Low Energy Cost Desalination Processes Using Hydrophobic Membranes; Desalination 56 (1985) 277-286.
59. M.H.V. Mulder; Pervaporation, Separation of Ethanol-Water and of Isomeric Xylenes; Ph.D. thesis, University of Twente, 1984.
60. J.W.F. Spitzen; Pervaporation, Membranes and Models for the Dehydration of Ethanol; Ph.D. thesis, University of Twente, 1988.
61. S. Loeb & S. Sourirajan; Sea Water Demineralization by Means of an Osmotic Membrane. In: R.F. Gould (editor); Saline Water Conversion II; Advances in Chemistry Series 38 (1962) 117.
62. H. Brüschke; Mehrschichtige Membran und ihre Verwendung zur Trennung von Flüssigkeitsgemischen nach dem Pervaporationsverfahren; German Patent DE 3220570.
63. I. Cabasso, E. Korngold & Z.-Z. Liu; On the Separation of Alcohol/Water Mixtures by Polyethylene Ion Exchange Membranes; Journal of Polymer Science: Polymer Letters Edition 23 (1985) 577-581.
64. G. Ellinghorst; Optimale Trennung von Stoffgemischen; Chemische Industrie 7/86 592-594.
65. H.K. Lonsdale; The Evolution of Ultrathin Synthetic Membranes; Journal of Membrane Science 33 (1987) 121-136.
66. P.H. Carnell & H.G. Cassidy; The Preparation of Membranes; Journal of Polymer Science 55 (1961) 233-249.
67. P.H. Carnell; Preparation of Thin Polymer Films; Journal of Applied Polymer Science 9 (1965) 1863-1872.
68. R.L. Riley, H.K. Lonsdale, C.R. Lyons & U. Merten; Preparation of Ultrathin Reverse Osmosis Membranes and the Attainment of Theoretical Salt Rejection; Journal of Applied Polymer Science 11 (1967) 2143-2158.
69. H. Strathmann, C.-M. Bell & K. Kimmerle; Development of Synthetic Membranes for Gas and Vapor Separation; Pure & Applied Chemistry 58 (1986) 1663-1668.
70. R.W. Baker, N. Yoshioka, J.M. Mohr & A.J. Khan; Separation of Organic Vapors from Air; Journal of Membrane Science 31 (1987) 259-271.
71. J.M.S. Hennis & M.K. Tripodi; Composite Hollow Fiber Membranes for Gas Separation: the Resistance Model Approach; Journal of Membrane Science 8 (1981) 233-246.

72. H. Yasuda & H.C. Marsh; Preparation of Composite Reverse Osmosis Membranes by Plasma Polymerization of Organic Compounds. III. Plasma Polymers of Acetylene/CO/H2O; Journal of Applied Polymer Science 19 (1975) 2981-2990.
73. L.T. Rozelle, J.E. Cadotte, K.E. Cobian & C.V. Kapp; Nonpolysaccharide Membranes for Reverse Osmosis: NS-100 Membranes; chapter 12, pages 249-261. In: S. Sourirajan (editor); Reverse Osmosis and Synthetic Membranes, Theory - Technology - Engineering; Ottawa, 1977.
74. J.A. van 't Hoff; Bereiding van Komposietmembranen voor Waterontzouting via een Grensvlakpolymerisatie; Master thesis; University of Twente, 1983.

Chapter 2:

WETTING CRITERIA FOR THE APPLICABILITY OF MEMBRANE DISTILLATION

A.C.M. Franken, J.A.M. Nolten, M.H.V. Mulder, D. Bargeman and C.A. Smolders

Summary

Membrane distillation can only be applied on liquid mixtures which do not wet a microporous hydrophobic membrane. Solutions of inorganic material in water have such high values of the surface tension ($\gamma_L \geq 72 \cdot 10^{-3}$ N/m) that the non-wetting condition is fulfilled for a number of hydrophobic membranes. As soon as organic solutes are present in the solution, the surface tension γ_L will be lowered and if the concentration of organic material becomes too high, wetting of the membrane will occur.

By means of theoretical considerations a critical solute concentration or surface tension at which a homogeneous smooth material will be wetted ($\theta < 90°$) can be calculated. For microporous membranes no such theoretical relation can be derived.

Therefore, a simple experimental method is described to measure the maximum allowable concentration for a microporous membrane. On the basis of these measurements, the maximum allowable concentration under process conditions can be determined.

2.1: Introduction

Membrane distillation is a distillation process making use of the pores of a microporous non-wettable membrane as the vapour phase. In this process two aqueous liquids with different temperatures are separated by a hydrophobic microporous membrane. The vapour pressure difference ΔP_v across the membrane, resulting from the temperature difference ΔT, causes vapour molecules to be transported through the pores of the membrane from the warm side (feed) to the cold side (permeate).

The advantages of membrane distillation are that the distillation process takes place at moderate temperatures and that a relatively small temperature difference between the two liquids contacting the microporous hydro-

phobic membrane gives relatively high fluxes. Because entrainment of dissolved particles is avoided a permeate with a high purity is obtained.

However, membrane distillation is only possible if the restrictive condition is fulfilled, that the pores of the membrane should not be filled with liquid. Hence the wetting power of the liquids should be low. Water and solutions of inorganic substances in water have such high values of the surface tension ($\gamma_L \geq 72 \cdot 10^{-3}$ N/m), that for a number of hydrophobic microporous membranes with pores in the range of 1 μm or less (such as polypropylene (PP), poly(vinylidene fluoride) (PVDF) and poly(tetrafluoro ethylene) (PTFE, Teflon)) this non-wetting condition is guaranteed. Therefore, important applications of membrane distillation can be seen in the field of water purification and in concentration of product solutions or waste water solutions [1,2].

As soon as organic solutes are present in an aqueous solution, the surface tension γ_L will decrease rapidly. If the concentration of organic material does not exceed a certain critical value (so the liquid on both sides of the membrane does not wet the membrane), the membrane distillation process can still be used. On the other hand, if the concentration of organic material exceeds this critical value, the microporous membrane will be filled with liquid. In this case membrane distillation is no longer possible.

The aim of this investigation is to find out which concentration of organic material in water is allowed before the liquid will penetrate into the membrane.

2.2: Background

The value of the contact angle θ of a liquid droplet on an ideal smooth homogeneous surface is described by Young's equation:

$$\gamma_L \cdot \cos\theta = \gamma_S - \gamma_{SL} \qquad (2.1)$$

A droplet of water on a hydrophobic surface (e.g. PP, PVDF or PTFE) will give a contact angle which is larger than 90°. If surface active agents (or in general: organic materials) are dissolved in water, the surface tension of the liquid will decrease. As a consequence, the contact angle θ will decrease and if θ becomes smaller than 90° the liquid will wet the solid

surface. In the case that the material is non-porous the contact angle will have a value between 0° and 90°. On the other hand, if the material is porous (which is the case for membranes used in the membrane distillation process) it is possible that the droplet will penetrate into the pores of the material.

Lucassen-Reynders (3) stated that any of the interfacial tensions in equation 2.1 can be affected by surfactant adsorption by virtue of Gibb's law:

$$\frac{d\,\gamma_i}{d\,\ln a_i} = -R.T.\Gamma_i \qquad (2.2)$$

a_i being the activity of the surfactant and Γ_i its surface excess at any interface.

Adsorption of surfactants can only influence the contact angle if they affect the ratio $(\gamma_S - \gamma_{SL})/\gamma_L$. Changes in contact angle can be shown conveniently by plotting $\gamma_S - \gamma_{SL}$ as a function of γ_L. Combination of equation 2.1 and 2.2 then yields the following expression:

$$\frac{d(\gamma_L.\cos\theta)}{d\gamma_L} = \frac{\Gamma_S - \Gamma_{SL}}{\Gamma_L} \qquad (2.3)$$

For low energy surfaces (such as PP, PVDF or PTFE) it is expected that hardly any interaction exists between the surface active agents and the surface, in which case $\Gamma_{SL} \approx \Gamma_L$.

It is also expected that $\Gamma_S << \Gamma_{SL}$ (4) and consequently the slope of the curve as represented by equation 2.3 will be:

$$\frac{d(\gamma_L.\cos\theta)}{d\gamma_L} \approx -1 \qquad (2.4)$$

Bargeman et al. (4) indeed found this relation for solutions of sodium decane-1-sulphonate and sodium dodecane sulphate in water on non-polar solids like parafin wax and PTFE. For conditions as assumed up till now the influence of surfactants on the contact angle on non-polar solids can be described by:

$$\gamma_L.\cos\theta = -\gamma_L + C \qquad (2.5)$$

This lineair equation with a slope equal to -1 has the advantage that only one contact angle measurement needs to be performed: the measurement of the contact angle of pure water on the solid material. If the surface tension of the solution as a function of the composition is known, the value of γ_L and therefore the value of the contact angle θ can be calculated for each solution composition. This situation is represented by the dotted line in figure 2.1.

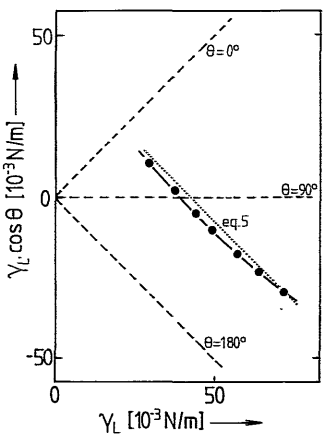

FIGURE 2.1: $\gamma_L.\cos\theta$ as a function of γ_L for ethanol/water mixtures on a homogeneous PTFE surface.

In figure 2.1 the value of γ_L^{90} is given by the intercept on the abcissa. γ_L^{90} is the surface tension of a liquid mixture which has a contact angle of 90° when brought in contact with a homogeneous smooth solid material. In the membrane distillation process the value of γ_L^{90} is very important. If the surface tension of a liquid is lower than γ_L^{90} it could be possible that the liquid penetrates into the pores of the porous material spontaneously.

The surface tension of a liquid that is on the verge of penetration into the pores of a microporous membrane, is defined as γ_L^p (p stands for penetration). As far as membrane distillation is concerned the value of γ_L^p is even more important than the value of γ_L^{90}.

Although the above described method for the determination of γ_L^{90} seems to be promising, it cannot be used as an accurate determination of γ_L^p. This is mainly due to three effects:

1. the experimental error for points on a line with a certain inaccuracy in its slope drawn through one experimental point with a certain inherent error, increases with the distance to that point;

2. the use of equation 2.5 is limited to surface active agents of a certain molecular structure (rather long chain amphipolar molecules, so called surfactants);
3. the value of γ_L^{90} does not always coincide with the value of γ_L^p for porous media.

ad 1. Although contact angle measurements can be made very accurately some deviations are inevitable. Mostly a deviation of about 1° is given. In literature the differences between the measured contact angles may differ considerably. For example, for a droplet of water on a Teflon surface, contact angles varying from 108° to 115° have been reported (5-8). This effect is mainly due to different specimens of Teflon. Another source of error is the inaccuracy in the slope of the curve: the slope is not exactly -1. For different series of measurements Bargeman et al. (4) found that the slope varied between -0.96 and -1.02. So, the effect of an experimental error in the contact angle is reinforced by the uncertainty in the tangent of the slope. For example, if for a droplet of water on Teflon a contact angle $\theta = 114° \pm 1°$ is found and the tangent of the slope is uncertain within 2%, then the extreme values for γ_L^{90} are $40 \cdot 10^{-3}$ N/m and $46 \cdot 10^{-3}$ N/m respectively.

ad 2. Equation 2.5 is used to describe the influence of surfactants on the contact angle of non-polar solids and a good agreement with experimental results is found (4). On the other hand this relation cannot be used in general for mixtures of water and low molecular weight organic components, such as alcohols (methanol, ethanol) or carboxylic acids (formic acid, acetic acid). In these cases the lineair behaviour as described by equation 2.5 is not always found. As an example the curve for ethanol/water mixtures on a homogeneous PTFE surface is given in figure 2.1 (the experimental results were obtained from Bernett et al. (6)).

ad 3. The difference between γ_L^{90} and γ_L^p will be demonstrated and explained on the basis of the results of our experiments.

The restrictions mentioned above do not permit an accurate determination of γ_L^{90} on the basis of the measurement of the contact angle of a droplet of water on a solid. Furthermore it is doubtful whether the value for γ_L^{90} is the same as the value for γ_L^p.

From the above considerations it can be concluded that the value of γ_L^p has to be determined experimentally for the microporous membranes used.

2.3: Method of investigation

2.3.1: Determination of γ_L^p

The value of γ_L^p is determined by the 'penetrating drop method'. In this method a droplet is brought in contact with the microporous membrane. By trials with narrowing series of solution compositions the composition of a liquid mixture is determined at which the liquid is on the verge of penetration into the membrane. The amount of organic material in water at this composition is called the 'maximum allowable concentration' and the value of the surface tension belonging to this composition is defined as γ_L^p.

The advantages of the penetrating drop method are:

- the value of γ_L^p can be measured directly;
- the measurements can be carried out on the membrane material itself;
- the method is experimentally simple and requires no special equipment;
- the measurements can be carried out very quickly;
- the method has a high accuracy (compared to the contact angle measurement).

The accuracy of the penetrating drop method can be fairly illustrated with the following example. A droplet will have a height of less than 5 mm and therefore will exert a gravitational force of about 50 N/m^2 which might form an inaccuracy in determining γ_L^p. Suppose the maximum pore size of the membrane material is smaller than 10 µm. According to the Laplace equation,

$$\Delta P = - \frac{2.B.\gamma_L.\cos\theta}{r_{max}} \qquad (2.6)$$

the value of $\gamma_L.\cos\theta$ can be measured with an accuracy of less than $0.25 \cdot 10^{-3}$ N/m. In the above equation B is a pore geometry coefficient, being 1 for cylindrical pores. Using equation 2.4 for an estimation of the uncertainty in γ_L^p, in this case $\Delta\gamma_L^p$, it follows that $\Delta\gamma_L^p < 0.25 \cdot 10^{-3}$ N/m.

2.3.2: Calculation of γ_L^p under process conditions $(\gamma_{L,pc}^p)$

The preceding explanation about γ_L^p and its determination is only partly applicable to hydrophobic microporous membranes under process conditions. As far as intrinsic membrane properties are concerned the preceding discussion

remains unaltered.

Nevertheless, it can be easily understood that a liquid mixture with a composition just beneath the maximum allowable concentration can give problems in the membrane distillation process. In practical applications the pressure, exerted by the liquid on the membrane, will be higher than zero as a result of, among other things, pumping pressure. If in that case the liquid has a surface tension γ_L, which is only slightly higher than γ_L^p, it is possible that the liquid penetrates into the microporous membrane.

Therefore, $\gamma_{L,pc}^p$ is introduced. The surface tension $\gamma_{L,pc}^p$ is defined as the 'minimum allowable surface tension under process conditions'. The concentration corresponding to $\gamma_{L,pc}^p$ is called 'maximum allowable concentration under process conditions'.

The relation between the applied pressure and the surface tension is given by the Laplace equation (equation 2.6). If the value of the maximum pore size is known and an estimation is made for the applied pressure, then the value of $\gamma_L.\cos\theta$ can be calculated. If the curve for $\gamma_L.\cos\theta$ as a function of the concentration is known, the value of $\gamma_{L,pc}^p$ can be obtained graphically. Determination of $\gamma_{L,pc}^p$ in this way makes use of the assumption that $\gamma_L^{s\,o} = \gamma_L^p$ and as will be shown later this assumption is not always correct.

A better approach is provided by making use of equation 2.5. Combination of this equation and equation 2.6 with the boundary condition that $\gamma_L = \gamma_L^p$ if $\gamma_L.\cos\theta = 0$, then yields the following equation:

$$\gamma_L = \gamma_L^p + \frac{\Delta P.r_{max}}{2.B} \qquad (2.7)$$

If in the above equation the values for a membrane distillation process are substituted, then the calculated value of γ_L is equal to $\gamma_{L,pc}^p$. For a proper use of equation 2.7 it is important that the value of ΔP, which is substituted, is higher than the maximum pressure to be applied in the system.

2.3.3: Experimental determination of $\gamma_{L,pc}^p$

The above calculation of $\gamma_{L,pc}^p$ reproduces reliable results. If, however, an accurate determination of $\gamma_{L,pc}^p$ is desired, the value of $\gamma_{L,pc}^p$ has to be determined experimentally.

This can be done by determining the 'liquid entry pressure' as a function of the surface tension of the liquid (in other words: as a function of the concentration of organic material in water). For these measurements a dry microporous membrane is put into a cell and the liquid is brought into contact with the membrane. The liquid is put under pressure and this pressure is slowly raised. The pressure at which the liquid penetrates into the membrane is defined as the liquid entry pressure. By changing the liquid composition, the liquid entry pressure is obtained as a function of the concentration of organic material in water. In order to minimize the number of experiments, the calculated value of $\gamma^p_{L,pc}$ can be used as a first estimate. In figure 2.2 the liquid entry pressure is given as a function of the weight fraction of ethanol in the mixture, using a microporous polypropylene membrane (Accurel 0.1).

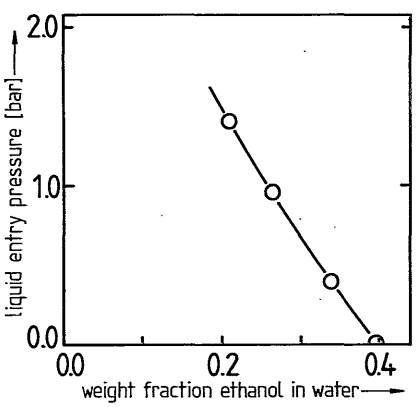

FIGURE 2.2: Liquid entry pressure as a function of the weight fraction of ethanol in water for a flat PP membrane (Accurel 0.1).

Note that the point where the liquid entry pressure is zero, the concentration is equal to the maximum allowable concentration and the surface tension of the liquid is equal to γ^p_L.

Of course, a margin of safety should be taken. The point of operation should always be situated on the left hand side of the curve in figure 2.2 and preferably not too close to this curve.

2.3.4: Summary of the method

The experimental method involves the following steps:

- determination of γ_L^p by means of the 'penetrating drop method';
- calculation of $\gamma_{L,pc}^p$ by means of equation 2.7, in which $\gamma_L = \gamma_{L,pc}^p$;
- determination of the 'liquid entry pressure' as a function of the liquid composition (in case the calculation of $\gamma_{L,pc}^p$ is not accurate enough).

2.4: Experimental

We have seen that in this investigation two different experimental techniques were used, namely:

- the penetrating drop method;
- the liquid entry pressure method.

Both techniques are rather simple and have already been described in the previous paragraph.

Penetrating drop method (PDM) measurements were carried out using two different kinds of polymers (PVDF and PP) with different characteristics. An overview of the characteristics of the membranes used is given in table 2.1.

Table 2.1: Properties of membranes used.

Property	Acc.0.1	R 5/1	PV 159	F 0030
material	PP	PP	PVDF	PVDF
configuration	flat		capillary	
outer diameter (µm)	-	1800	1230	1500
inner diameter (µm)	-	1200	830	1000
membrane thickness(µm)	160	300	200	250
porosity (%)	ca. 80	ca.80	75	82
av. pore diameter (µm)	0.1	0.1		
max.pore diameter (µm)	0.40	0.38	0.25	0.60

Liquid entry pressure (LEP) measurements were carried out on flat PP membranes and on capillary PVDF membranes.

The measurements, both PDM measurements and LEP measurements, were conducted with new untreated membranes which were only used in one experiment.

All the membranes were kindly supplied by Enka A.G. (Product Group Membrana).

2.5: Results

In this paragraph the results of the penetrating drop method and the liquid entry pressure measurements will be presented. In order to be able to compare the results of these measurements with the results of the measurements on homogeneous, smooth surfaces the literature results of the latter are presented in table 2.2. In this table the results of the measurements on PTFE surfaces are also given.

Table 2.2: Some properties of hydrophobic materials.

Property	PP	PVDF	PTFE
$\gamma_L^{90}(10^{-3}$ N/m)	55	50	40.5 (6)
$\gamma_c(10^{-3}$ N/m)*	29 (10)	25 (9)	18 (9)

* γ_c is the critical surface tension of wetting of a homogeneous smooth material by a liquid mixture, which is defined by the intercept of the experimental line in figure 1 with the line where $\theta = 0$ (9).

The results of the penetrating drop method measurements are given in table 2.3 and some of these measurements are also plotted in figures 2.3 and 2.4. Although the values obtained for γ_L^p deviate strongly from γ_L^{90}, some interesting conclusions can be drawn from these measurements.

First, it is remarkable that the liquid penetrates into PVDF membranes at a higher value of γ_L than it does into PP membranes. This result is unexpected since PVDF is a more hydrophobic material than PP.

The second conclusion which can be obtained from these measurements is that all the values of γ_L^p are lower than the value of γ_L^{90}. Some of the measurements (e.g. alcohol/water mixtures in contact with flat PP membranes) give values for γ_L^p which are almost as low as γ_c. This means that contact

angle measurements on homogeneous smooth materials form not at all a good criterion for the applicability of membrane distillation. The only measurements in which values of γ_L^p are roughly equal to γ_L^{90} are the experiments with aqueous mixtures of DMF, DMAc and DMSO on PVDF porous membranes and even for different types of PVDF membranes differences occur.

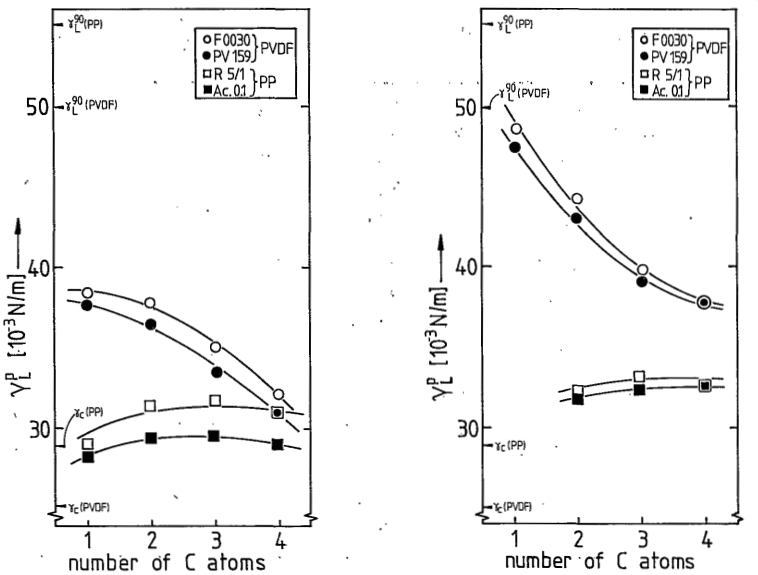

FIGURE 2.3: γ_L^p for aqueous mixtures of alcohols.
FIGURE 2.4: γ_L^p for aqueous mixtures of carboxylic acids.

The third conclusion that can be drawn from the PDM-experiments is that for a specific membrane γ_L^p can be dependent upon the composition of the liquid mixture. For PP membranes the value of γ_L^p seems to be dependent upon the class of organic solutes only and not on the molecular size within a series. For instance, for a flat PP membrane (Accurel 0.1) the following values for γ_L^p are found:

alcohols ~ 29 . 10^{-3} N/m;
carboxylic acids ~ 32 . 10^{-3} N/m;
DMF/DMAc ~ 36 . 10^{-3} N/m.

On the other hand, for PVDF membranes this dependence is different. Both for a series of aqueous mixtures of alcohols and for a series of aqueous mixtures of carboxylic acids the values of γ_L^p decrease when the number of C-atoms increases (see also figures 2.3 and 2.4).

Table 2.3: Penetrating drop measurements of aqueous mixtures of organic components.

Organic component	Membrane							
	PV 159		F 0030		R 5/1		Acc. 0.1	
	wt.%	γ_L^p	wt.%	γ_L^p	wt.%	γ_L^p	wt.%	γ_L^p
methanol	37	37.8	35	38.5	69	29.0	74	28.0
ethanol	23.5	36.5	21	38.0	35	31.5	41	29.5
propanol-1	11.5	33.5	10.5	35.0	13	32.0	15.5	29.5
butanol-1	4.5	31.0	3.5	32.0	4.5	31.0	5.5	29.0
butanol-2	9	29.0	7.5	31.0	8.5	29.5	9	29.0
formic acid	59	47.5	53	48.9	100	--	100	--
acetic acid	31	43.4	27	44.7	81	32.2	83	31.8
propionic acid	17	39.0	15.5	39.8	37	33.3	43	32.5
butyric acid	5	38	5	38	9	32.5	9	32.5
DMAc	41	48	39	50	91	36	94	35.5
DMF	43	48	39	50	95	36	98	35.5
DMSO	61	50	57	51	100	--	100	--
acetone	33	35.0	31	35.8	47	31.2	54	29.8
1-4 dioxane	37	44.3	35	45.0	61	38.2	64	37.7

Liquid entry pressure measurements were carried out to find out whether the values of the PDM-measurements and the use of these values for the calculation of $\gamma_{L,pc}^p$ by means of equation 2.7 are correct. The LEP-measurements were carried out on flat PP membranes and on capillary PVDF membranes with aqueous mixtures of ethanol. The results of the measurements are given in figure 2.5. In this figure the LEP-value is plotted as a function of the surface tension of the aqueous ethanol mixture. The values of $\gamma_{L,pc}^p$ which are calculated by means of equation 2.7 are represented in figure 2.5 by dashed lines.

From this figure it can be seen that:

- the value of γ_L^p, measured by the PDM is in good accordance with the LEP-measurements;
- the values of $\gamma_{L,pc}^p$ which are calculated by equation 2.7, differ from the values measured by means of the LEP. A reason for this deviation might be that $d(\gamma_L.\cos\theta)/d\gamma_L$ is not exactly -1. Furthermore, the membrane structure might be a factor of importance;

- the slope of the LEP-curve is not constant. This means that the use of equation 2.7 is limited as was already discussed before. The deviation might be caused by the fact that ethanol is not a surfactant and its mixtures with water are far from ideal.

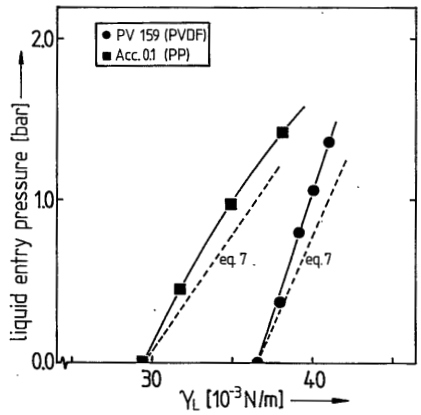

FIGURE 2.5: Liquid entry pressure as a function of the surface tension of ethanol/water mixtures.

In spite of the slight difference between the measured and the calculated curves it can be concluded that the description of the wettability criteria for a membrane distillation system by means of the penetrating drop method and the calculation of the values of $\gamma^p_{L,pc}$ is rather good.

2.6: Discussion

From the results that are presented here it becomes clear that the calculation of a maximum allowable concentration of organic material on the basis of simple contact angle measurements of a droplet on a homogeneous material is not possible. The measured values of γ^{90}_L obtained in that way cannot be used to describe the penetration of a liquid into a porous material. The values of γ^p_L, measured by means of the PDM, are lower than γ^{90}_L and higher than γ_c and its exact value can only be obtained by measurement.

In this paragraph a qualitative explanation for the difference between the values of γ^p_L on one hand and γ^{90}_L and γ_c on the other will be given. The value of γ^p_L will depend upon the polymer material, the porous structure of

the membrane and the composition of the liquid mixture. The value of γ_L^{so} (and γ_c) depends upon the polymer material and in some cases also on the composition of the liquid mixture. For instance, Bernett et al. (6) found different values for γ_c of polyethylene and Teflon when measured with different aqueous solutions (PE: γ_c (ethanol, butanol-1) = 27.5 . 10^{-3} N/m; γ_c (1,4-dioxane) = 31.5 . 10^{-3} N/m). Although no other values for PP and PVDF are known except for the ones given in table 2.2, it is expected that γ_c might be slightly different for different liquid mixtures in contact with these materials.

However, the above explanation for the possible difference in γ_c does not explain why the value of γ_L^p is (much) lower than γ_L^{so}. This experimental fact can be explained by the extremely high surface porosity of the membrane material. Davies et al. (11) stated that on rough or hairy surfaces always higher contact angles are obtained than on a smooth surface of the same material. This can be understood by the following relation, derived by Cassie and Baxter (12):

$$\cos\theta' = f_1.\cos\theta - f_2, \qquad (2.8)$$

which gives a relation between the contact angle measured on a rough surface (θ') and the contact angle measured on a smooth surface (θ). In equation 2.8 f_1 and f_2 are the fractions of the composite surface which are liquid/solid and liquid/air respectively. This equation can only be used in case $f_2 < f_1$. In the other case ($f_2 > f_1$) cos θ' would be smaller than zero, which would imply that θ' is always larger than 90°. This should mean that such a surface never could be wetted. But it can be easily understood that, if θ becomes zero or approaches zero, the surface of the material (even inside the pores) becomes completely wetted.

For highly porous membranes, like the ones that are used in our investigations, the value of f_2 will have a substantial value and may even be larger than 0.5, in which case equation 2.8 no longer is valid. (Note: the fact that the overall porosity of a membrane is 80% does not mean that f_2 is equal to 0.8; probably this value is much lower). In cases where equation 2.8 is valid, θ' is a function of the porosity.

In case of membrane distillation the membrane will be wetted only if $\theta' < 90°$. For different values of f_2, the contact angle on a smooth surface θ is listed in table 2.4.

f_2	θ (°)
0	90
0.2	75
0.4	48
0.45	35
0.48	23
0.5	0

Table 2.4:
Contact angle on a smooth surface (θ) for which a porous substrate with pore fraction f_2 will be wetted ($\theta' = 90°$).

The values in this table are calculated by means of equation 2.8 with the boundary condition that $\cos \theta' = 0$. From this table it can be seen that for f_2 in the range of 0.45 till 0.5 a small variation in porosity (or better: in liquid/air surface fraction) leads to an enormous difference in required contact angle and will also lead to differences in γ_L^p.

It must be mentioned again that not all the results can be explained by this qualitative description. For instance, the fact that γ_L^p for alcohols and carboxylic acids on PVDF membranes is lowered as the number of C-atoms increases, whereas the values on the PP membranes remain constant, cannot be explained by the above discussion. Therefore, more investigations especially on the influence of the membrane structure on wetting phenomena, will be carried out.

2.7: Conclusions

The main conclusion that can be drawn from our investigations is that the maximum allowable concentration of organic material in water cannot be calculated, but has to be determined experimentally.

The 'penetrating drop method' is a good and experimentally simple method for determining the maximum allowable concentration of organic material in water and its corresponding surface tension (called γ_L^p).

The semi-empirical way to determine the surface tension at process conditions, $\gamma_{L,pc}^p$, making use of the penetrating drop method and equation 2.7 gives fairly good results, which can be used to safely estimate the maximum allowable concentration at process conditions.

2.8: Symbols

The symbols that are used in this chapter are conform the terminology of membrane distillation (13). Additional symbols or symbols which are defined a different way are marked with the *-symbol.

Latin symbols

a	activity of surfactant	-	*
B	pore geometry coefficient	-	*
C	(eq. 5) constant	N/m	*
f_1	(eq. 8) liquid-solid surface fraction	-	*
f_2	(eq. 8) liquid-air surface fraction	-	*
ΔP	pressure difference	N/m^2	
ΔP_v	vapour pressure difference	N/m^2	*
R	gas constant ($\equiv 8.310$)	J/mol°C	
r_{max}	maximum pore radius	µm	*
ΔT	temperature difference	°C	

Greek symbols

Γ	surface excess activity of surfactant	mol/m^2	*
γ	surface tension	N/m	
γ_c	critical surface tension of wetting	N/m	*
$\gamma_L^{s°}$	surface tension of a liquid (mixture) which has a contact angle of 90° when brought in contact with a homogeneous smooth solid material	N/m	*
γ_L^p	surface tension of a liquid (mixture) that is on the verge of penetration into the pores of a (micro)porous membrane	N/m	*
$\gamma_{L,pc}^p$	γ_L^p under process conditions	N/m	*
θ	contact angle	°	*
θ'	(eq. 8) contact angle on a rough surface	°	*

Subscripts

i	index	
L	liquid	*
S	solid	*
SL	solid-liquid	*

2.9: References

1. K. Schneider & T.J. van Gassel; Membrandestillation; Chemie-Ingenieur-Technik 56 (1984) 514.
2. N. Kjellander; Applications and Engineering Aspects of Membrane Distillation; Summer School on Engineering Aspects of Membrane Processes, Aarhus, Denmark; June 2-6, 1986.
3. E.H. Lucassen-Reynders; Contact angles and Adsorption on Solids; Journal of Physical Chemistry 67 (1963) 969.
4. D. Bargeman & F. van Voorst Vader; Effect of Surfactant on Contact Angles at Nonpolar Solids; Journal of Colloid & Interface Science 42 (1973) 467.
5. H.W. Fox & W.A. Zisman; The Spreading of Liquids on Low Energy Surfaces. I. Polyfluoroethylene; Journal of Colloid Science 5 (1950) 514.
6. M.K. Bernett & W.A. Zisman; Wetting of low-energy Solids by Aqueous Solutions of Highly Fluorinated Acids and Salts; Journal of Physical Chemistry 63 (1959) 1241.
7. J.R. Dann; Forces Involved in the Adhesive Process, I. Critical Surface Tensions of Polymeric Solids as Determined with Polar Liquids; Journal of Colloid & Interface Science 32 (1970) 302.
8. D. Bargeman; Contact Angles on Nonpolar Solids; Journal of Colloid & Interface Science 40 (1972) 344.
9. W.A. Zisman; Influence of Constitution on Adhesion; Industrial & Engineering Chemistry 55 (1963) no. 10, 19.
10. H. Schonhorn; Heterogeneous Nucleation of Polymer Melts on Surfaces. I. Influence of Substrates on Wettability; Polymer Letters 5 (1967) 919.
11. J.T. Davies & E.K. Rideal; Interfacial Phenomena; Academic Press, New York (1963).
12. A.B.D. Cassie & S. Baxter; Transactions Faraday Society 40 (1944) 546.
13. A.C.M. Franken & S. Ripperger; Terminology for Membrane Distillation; European Society of Membrane Science and Technology, January 1988 (given as an appendix to this thesis).

Chapter 3:

INFLUENCE OF THE STRUCTURE OF A MICROPOROUS MEMBRANE ON ITS WETTABILITY

A.C.M. Franken, J.A.M. Nolten, D. Bargeman, M.H.V. Mulder & C.A. Smolders

Summary

Wetting of microporous membranes is influenced by three factors: the membrane material, the nature of the penetrating liquid and the membrane structure. In this chapter it is shown that all kinds of membrane structures can be classified into two basic types of structures, the 'sharp-edged' and the 'rounded' pore structure, and that these structures are determined by the membrane preparation method.

Furthermore, it is shown that membranes with a 'sharp-edged' pore structure show more liquid-repellency than those with a 'rounded' pore structure.

3.1: Introduction

Wetting phenomena play an important role in several fields of membrane technology. In microfiltration and ultrafiltration it is important that the membrane is wetted by the liquid which is to be filtered. If the liquid solution does not penetrate into the membrane pores spontaneously an external pressure must be exerted onto the liquid in order to make it penetrate. In cases where this is impossible or unpractical an artifice has to be applied in order to wet the membrane. For instance, membranes made of hydrophobic materials like PTFE or PP are not wetted spontaneously by an aqueous solution and depending on the pore size, sometimes increased pressures up till several bars are necessary to enforce penetration. In this case a wetting-solution (e.g. ethanol) can be used in order to wet the membrane at ambient pressure.

On the other hand, in a process like membrane distillation it is essential that the hydrophobic membrane should not be wetted by the liquid to be treated. Mostly aqueous solutions with a high surface tension are used in which the total amount of organic compounds does not exceed a certain

limit. In the previous chapter wetting criteria for the applicability of membrane distillation have been formulated (1).

Characterization of the wettability of materials is mainly done by contact angle measurements. These measurements provide information about the interaction between a polymer and a liquid. Disadvantages of this technique are that the measurements have to be carried out on smooth homogeneous surfaces and that the measurements often show large deviations. In literature mostly an experimental inaccuracy of about 1° is given. However, the differences between the measurements of different authors are in most cases much larger. For example, for a droplet of water on PTFE surfaces, contact angles varying from 108° to 115° have been reported (2-5). Also the contact angle hysteresis forms a serious experimental and interpretative problem.

Another disadvantage of contact angle measurements is that the method cannot be used on porous materials directly. Therefore, an experimental method, called the 'penetrating drop method', has been developed (1). In this method a droplet is brought into contact with the porous membrane and the conditions for spontaneous penetration of this droplet are found by changing the solute concentration. By trials with narrowing series of solution compositions, the composition of a liquid mixture is determined at which the droplet is on the verge of penetration into the membrane.

As already has been pointed out in the previous chapter, the structure of the porous material plays an important role in wetting phenomena. In this chapter, the influence of the membrane structure will be investigated explicitly.

3.2: Theory

3.2.1: Contact angles and capillary phenomena

Contact angles provide information about the interaction of a solid material in contact with a liquid. If the contact angle, θ, is larger than 90°, then the liquid tends to form a ball (see figure 3.1a). In case of a water droplet, this material is called hydrophobic. When a good interaction between liquid and solid material exists, θ will be lower than 90°. Such a material is called hydrophilic in case of a water droplet (see figure 3.1c).

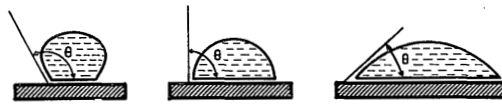

FIGURE 3.1: Contact angles of a liquid droplet on a solid material.

When a porous material is used, the situation can be represented by a capillary. Penetration of a liquid into a capillary is mathematically described by the Laplace equation. This equation (3.1) gives a relation between the pressure difference ΔP across a meniscus in a capillary pore of a certain material using a certain liquid.

$$\Delta P = \frac{-2.B.\gamma_L.\cos\theta}{r} \qquad (3.1)$$

In this equation ΔP is expressed in such a way that it represents the pressure that is needed to make a liquid penetrate into a capillary. B represents a pore geometry factor; in case of a cylindrical capillary B = 1. Furthermore, γ_L is the surface tension of the liquid, r the inner radius of the capillary and θ the contact angle between the solid material and the liquid.

From equation 3.1 it can be seen that a contact angle larger than 90° (i.e. cosine θ is negative) leads to a positive value of ΔP and therefore a certain external pressure will be needed to make the liquid penetrate into the capillary. In an equilibrium situation, as is shown in figure 3.2,

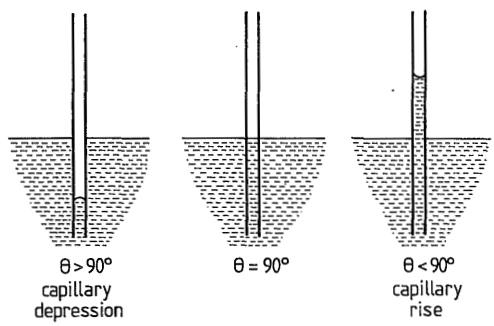

FIGURE 3.2: Contact angles and capillary phenomena.

capillary depression occurs. On the other hand, if θ is lower than 90°, cosine θ is positive, resulting in a negative value of ΔP. In this case the liquid will spontaneously penetrate into the capillary. In the equilibrium situation this results in capillary rise.

In the most simplified model the pores in a membrane can be considered as a number of cylindrical capillaries. However, this situation does not hold when real membranes are considered. The only commercial membranes, for which this requirement is approached, are Nuclepore-membranes and even for these membranes it was shown by Hernandez et al. that the pores cannot be considered as cylindrical capillaries (6).

The fact that a membrane cannot be considered as a number of cylindrical capillaries does not mean that the considerations given above about wetting do not apply. In principle, the deviations from ideality can be covered by adjustment of the pore geometry factor B. This can also be found in literature, among others in an ASTM-method in which the maximum pore size of a membrane is determined by means of the maximum bubble pressure method. In this method, B is fixed at a value of 0.715 (7).

As the factor B can vary between 0.5 and 1.0 (8), this variation can never be responsible for a change in sign of ΔP in equation 3.1. This means that the contact angle is the only parameter which determines whether an external pressure is needed for the penetration of a liquid into a membrane. According to equation 3.1 and figure 3.2, a spontaneous penetration of a liquid into a membrane occurs if the contact angle θ is smaller than 90°. From previous experience, however, it is known that the contact angle can often become (much) lower than 90° before a spontaneous penetration of a liquid into a membrane occurs (1,9,10,11).

3.2.2: Wetting phenomena in relation to pore structure

The pores in a membrane often show an irregular structure which cannot be represented as a bundle of cylindrical capillaries. In figure 3.3 several different pore structures are given. When the constrictions of these pores are considered, all the different pore structures can in fact be condensed to two basic types of constrictions, being a 'rounded' pore type (type I) and a 'sharp-edged' pore type (type II).

Type I pore structures have already been described by Kim and Harriott (9). In their investigations they used Gore-Tex TA 004 PTFE membranes with

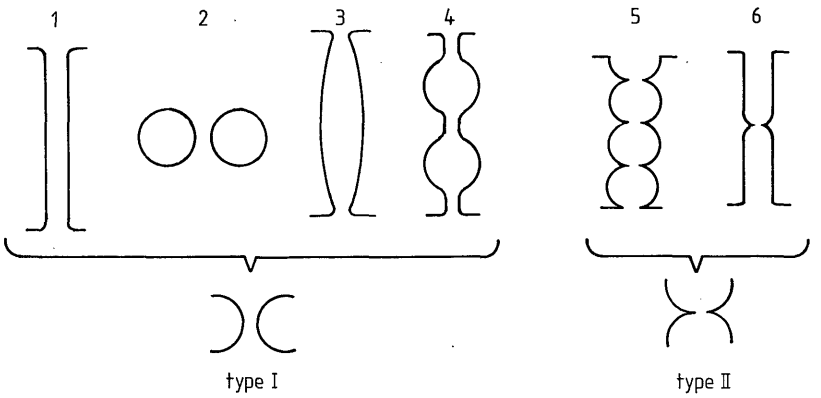

FIGURE 3.3: Several pore structures (side views).

a maximum pore size of 2.0 μm. They considered the pores in these membranes to be similar to the hole in a doughnut. In our investigation such pores are refered to as 'rounded' pores. Schematically a description is given in figure 3.4.

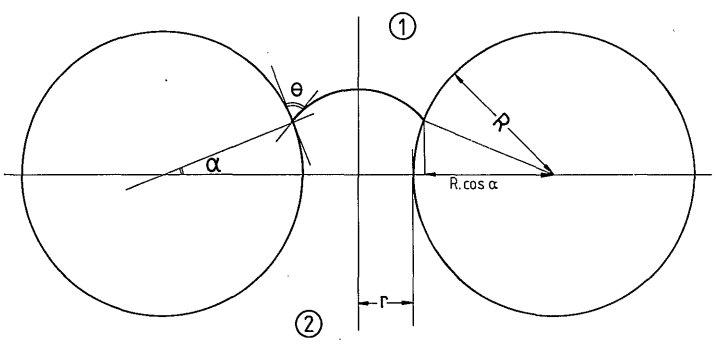

FIGURE 3.4: Side view of the liquid/air interface in a 'rounded' pore; phase (1) is a liquid and phase (2) is air.

For this (circular) geometry the following equation for the pressure difference across the liquid/air interface can be derived (9):

$$P_1 - P_2 = - \frac{2 \cdot \gamma_L \cdot \cos(\theta-\alpha)}{r \cdot \left(1 + (R/r).(1-\cos\alpha)\right)} \qquad (3.2)$$

The maximum pressure difference for penetration, $(P_1-P_2)_{max}$ as a function of the position of the liquid/air interface is obtained when the derivative of (P_1-P_2) with respect to α equals zero. From equation 3.2 we then find:

$$\sin(\theta-\alpha) = \frac{\sin\theta}{(1 + (r/R))} \qquad (3.3)$$

From equations 3.2 and 3.3 it follows that a pressure is needed to force the liquid into the membrane even when θ is smaller than 90°. For instance, if $r = R$ and $\theta = 75°$, it can be calculated from equation 3.3 that $\alpha = -76.1°$. Substituting these values into equation 3.2 gives a maximum pressure of about $0.50*(2.\gamma_L/r)$. Two things become clear from this example. In the first place, it is shown that even when the intrinsic contact angle becomes smaller than 90° a pressure is needed to make the liquid penetrate into the membrane. Secondly one finds that the maximum pressure is not reached at the point where $\alpha = 0°$ and the constriction has its lowest value of 2r.

The second type of constriction is formed by a so-called 'sharp-edged' structure. A schematic representation of this kind of structure is given in figure 3.5.

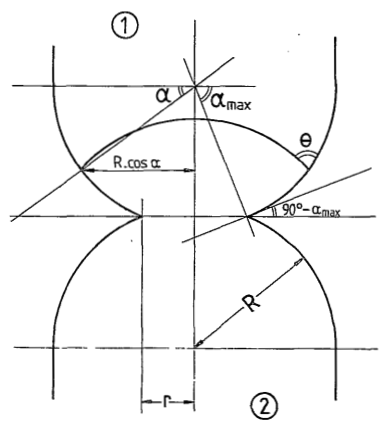

FIGURE 3.5: Side view of the liquid/air interface in a 'sharp-edged' pore; phase (1) is a liquid and phase (2) is air.

Before the penetration of a liquid into a 'sharp-edged' pore can be discussed two assumptions have to be made. The first assumption is that the

structure that is considered is an ideal structure; in other words the sharp edge of the pore is infinitely sharp. The second assumption is that the intrinsic contact angle between solid and liquid does not change unless there is no other way to pass a structural barrier. In fact both assumptions are also implicitly made when a 'rounded' pore is considered. In case of a 'sharp-edged' pore, however, it is necessary to state these assumptions explicitly, because the effects are more pronounced here.

In case of a 'sharp-edged' pore the following equation describes the pressure difference across the liquid/air interface:

$$P_1 - P_2 = - \frac{2 \cdot \gamma_L \cdot \cos(\theta-\alpha)}{r \cdot ((R/r).\cos\alpha)} \qquad (3.4)$$

This equation looks almost similar to the equation that is used to describe the penetration of a liquid into a 'rounded' pore. The difference in the denominater is caused by the fact that the curvature of the pore is convex in the former case (equation 3.3) and concave in the latter (equation 3.4). Until the constriction is reached ($\alpha < \alpha_{max}$), the contact angle θ has a constant value.

When $\alpha = \alpha_{max}$, the value of the contact angle has to change in order to pass the 'sharp-edged' barrier. The changing contact angle is referred to as θ'. In this case the pressure difference across the liquid/air interface is given by the following equation:

$$P_1 - P_2 = - \frac{2 \cdot \gamma_L \cdot \cos(\theta'-\alpha_{max})}{r} \qquad (3.5)$$

If θ is equal to or smaller than α_{max}, the value of (P_1-P_2) reaches its lowest (most negative) value at the point where $\theta' = \alpha_{max}$. An example of this situation is schematically given in the left hand picture of figure 3.6, in which the penetration of a liquid with a contact angle $\theta = 50°$ into a 'sharp-edged' pore with an α_{max} value of 70° is given. In the situation where θ is larger than α_{max}, (P_1-P_2) becomes minimal at the point where $\alpha = \alpha_{max}$. For an example: see situation "a" of the right hand picture of figure 3.6 ($\alpha_{max} = 70°$ and $\theta = 80°$).

The maximum value of ΔP to overcome the 'sharp-edged' barrier, $(P_1-P_2)_{max}$, is reached when θ' becomes equal to $(2.\alpha_{max} + \theta)$. This value is equal to θ again when θ is defined in relation to the wall of the lower part of the capillary. It must be remembered that the value of α at the

other side of the barrier is defined in such a way that its value is negative. For example, if r/R = 0.34 and θ is 50°, then the value of α_{max} is 70° or -70°. The value of $(P_1-P_2)_{min} = -2.\gamma_L/r$ and $(P_1-P_2)_{max} = 0.5*(2.\gamma_L/r)$.

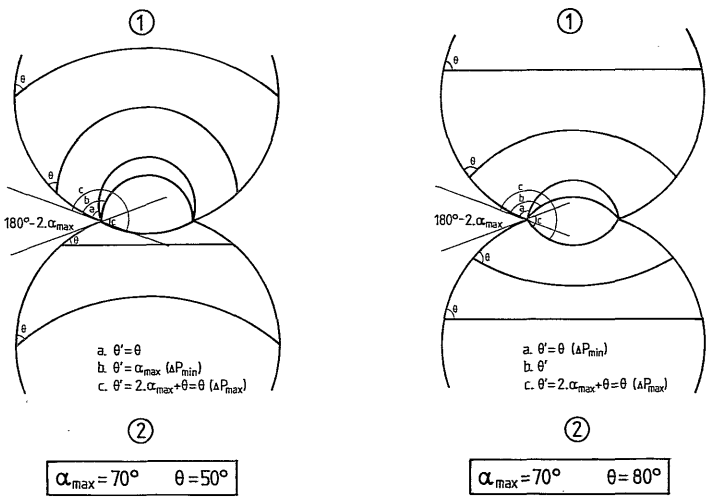

FIGURE 3.6: Interfaces of a penetrating liquid with a contact angle θ = 50°, respectively 80°, into a 'sharp-edged' pore with α_{max} = 70°.

The most interesting variable as far as membrane operations are concerned is the pressure that is needed to make the liquid penetrate into the membrane. In figure 3.7 the relative maximum pressure difference $(P_{rel})_{max}$, defined as $(P_1-P_2)_{max}/(2.\gamma_L/r)$, is given as a function of (r/R) for various contact angles.

Figure 3.7 shows clearly that the penetration pressure P_{rel} becomes higher when the contact angle θ is larger. It also shows that the maximum penetration pressure increases when r/R decreases. This has, for instance, as a consequence that a higher relative pressure is needed to make a liquid with a contact angle of 60° penetrate into a 'sharp-edged' pore with r/R = 0.4 than to make a liquid with a contact angle of 120° penetrate into a cylindrical capillary (r/R = 1).

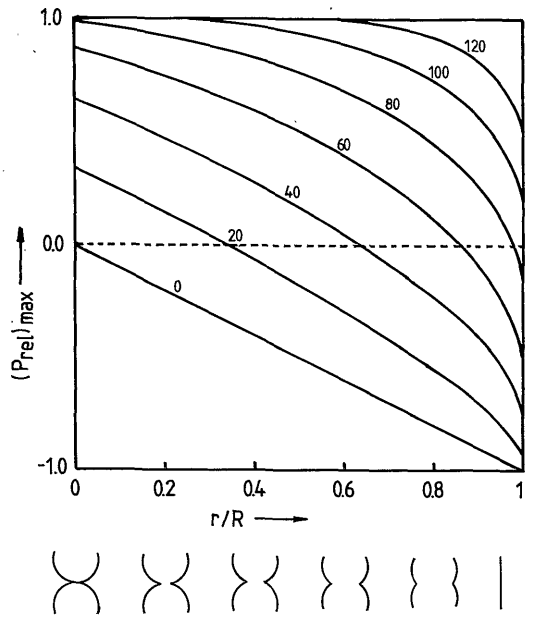

FIGURE 3.7: Relative maximum penetration pressure as a function of (r/R) for 'sharp-edged' pores. The numbers at the curves are the intrinsic contact angles.

The value of θ for which a penetration pressure is needed, can be obtained from figure 3.7 or calculated exactly from equation 3.5. From this equation it follows that (P_1-P_2) is positive when $\cos(\theta'-\alpha_{max}) < 0$. Knowing that the maximum value of (P_1-P_2) is reached when $\theta' = 2.\alpha_{max}+\theta$, it can be calculated that the value of $2.\alpha_{max}+\theta-\alpha_{max} = \alpha_{max}+\theta$ must be larger than 90° in order to have a positive penetration pressure. On the other hand, if $\alpha_{max}+\theta < 90°$, spontaneous penetration into the membrane occurs. For instance, if r/R = 0.4, then $\alpha_{max} = 66.4°$. From the above consideration it follows that spontaneous penetration only occurs when $\theta < 23.6°$.

3.2.3: Membrane formation and pore structure

All the pore structures that are known in membrane literature can be schematically represented by one of the structures shown in figure 3.3. Besides the fact that all these structures can be reduced to two basic types of constriction, it is also possible to predict which type of constriction is likely to occur on the basis of knowledge of the membrane formation mechanism.

A detailed description of membrane formation mechanisms can be found in literature (12,13). In this chapter only a brief description of those aspects of membrane formation, which are necessary for a better understanding of the formation of the different pore types, will be given. There are various methods to obtain microporous membranes: sintering, stretching, track-etching and phase inversion.

Sintering is a membrane formation process that is generally used for the fabrication of membranes from materials that cannot be dissolved in a suitable solvent. Whether the starting-material is a glass, metal, polymer or ceramic material is not so important, the resulting pore structure depends upon the process conditions and the shape of the starting-material. As far as the sintering process is concerned, a distinction is made between two cases.

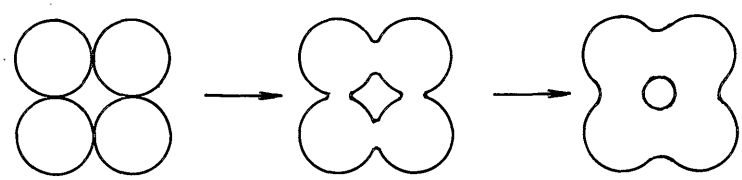

FIGURE 3.8: Sintering of spherical powders.

In the first case, a powder is pressed into the desired shape and additionally subjected to a sintering treatment. This process is generally used for ceramic, glass and metal membranes. For instance, if spherical particles of a ceramic material are used, the holes that are obtained after sintering will be of a 'rounded' type (see figure 3.8). It must be remembered that the pores do not have to be circular (like in a doughnut) in order to belong to the 'rounded' type; the only criterium is that no sharp edges are present. If the starting-material is irregularly shaped, sharp edges cannot be excluded. In most cases, however, the sintering process will have a 'smoothening effect' on these sharp edges, generally resulting in 'rounded' pores.

In the second type of sintering a pore-former or a second phase is added to the powder. This process is generally used for the fabrication of polymer membranes, but can also be used for metal or glass membranes. In case of a polymer (e.g. poly(tetrafluoro ethylene)) a pore-former is added

to the powder before it is pressed into the desired shape and subjected to a sintering treatment. Depending on the situation whether the pore-former or the polymer is forming sphere-like droplets during the process, a structure with 'rounded' pores or a structure with 'sharp-edged' pores is formed. In figure 3.9 an example is given in which the pore-former is forming

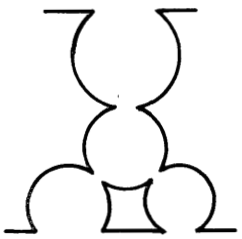

FIGURE 3.9:
Sintering of a polymer material in which the polymer is formed around the pore-former.

droplets and the polymer is pressed around this droplet. In this case a 'sharp-edged' structure is obtained. It must be remembered, however, that the formation of 'rounded' pores can occur as well. For instance, if the pore-former is removed before or during sintering, the sintering process can exert its smoothening effect on the sharp edges.

Stretching of semi-crystalline polymer films, which are obtained by extrusion, is another preparation method which can be used for the fabrication of membranes from polymers. The method is employed for polymers which cannot be dissolved in a suitable solvent (e.g. poly(tetrafluoro ethylene) (12,14)), but can also be used for other polymers that have a high degree of crystallinity (12). An example of the latter kind are Celgard membranes made from polypropylene (15,16). Stretching of the extruded polymer films results in formation of an interconnecting fibrous network of slitlike voids between the crystalline areas. As the polymer film will try to reduce the effect of deformation, it can be easily understood that the polymer 'fibers' forming the interconnecting network have a circular cross-section. Therefore, all the membranes that are obtained by this method have 'rounded' pore shapes (schematically represented by type I-2 of figure 3.3 (see also figures 3.10 (a,b) and 3.11 (a,b,c)).

The third method to obtain porous membranes is by **track etching.** The method is used to obtain Nuclepore membranes and membranes obtained by

this method are often referred to as 'nucleation track membranes'. As etching has more or less the same smoothening effect on sharp edges as the sintering process, the surfaces of the membranes do not show any sharp edges. A number of photographs of Nuclepore membranes support this preposition (12,13,17). Hernandez et al. (6) showed that the pores cannot be considered as cylindrical capillaries. Although their schematical representation of a pore (with sharp edges at the membrane surfaces) is a good description as far as the transport mechanism through the membrane is concerned, the sharp edges are conflicting with the surface photographs mentioned above. Therefore the best representation of the pore shape of track-etched membranes is given by type I-3 in figure 3.3. In conclusion it can be stated that membranes obtained by (track) etching will have pores with a 'rounded' shape.

The last method that is considered is membrane formation by the **phase inversion** process. There are several ways of making porous membranes by means of phase inversion of which 'immersion precipitation' (18, 19,20), in which liquid-liquid demixing of a polymer/solvent/non-solvent system takes place, and the 'thermal inversion process' (21), in which the process of demixing and solidification takes place through lowering the temperature, are the most important.

In analogy to our discussion above it depends on the fact whether the pore-former or the polymer is forming sphere-like droplets during the phase inversion process. If a liquid-liquid demixing takes place, it will always be the polymer phase which is solidifying. As the solidifying polymer tends to minimize its energy a 'rounded' structure will always be obtained.

On the other hand if the membranes are obtained by thermal inversion it depends on the solidifying phase whether a structure with 'rounded' pores or a structure with 'sharp-edged' pores is obtained. If the solution is cooled slowly, then a spherical cell structure with type II pores is obtained (22). For example, the typical Accurel-structure is obtained by a solidification of the pore-former and the polymer is built around this phase (23). After removal of the pore-former a membrane with 'sharp-edged' pores is obtained (see figure 3.10c).

Concluding this paragraph it can be stated that in most cases a structure with 'rounded' constrictions is obtained and that only in special cases a 'sharp-edged' structure is formed.

3.3: Experimental

To determine at which concentration of organic material in water a membrane is wetted an experimental method, called the 'penetrating drop method', has been developed (1). In this method a droplet is brought in contact with the porous membrane. By trials with narrowing series of solution compositions the composition of a liquid mixture on the verge of penetration into the membrane is determined. This method has been described in detail in the previous chapter.

The membranes used in this investigation were all flat microporous membranes. All membranes have a symmetrical structure, except for "FS 3.0" which is a composite membrane consisting of a poly(tetrafluoro ethylene) (PTFE) toplayer (10 μm) on a polyethylene (PE) non-woven. In table 3.1 an overview of the characteristics of the membranes used is given. All experiments were performed with new untreated membranes which were only used once.

Table 3.1: Properties of membranes used.

Property	Celgard		Accurel	Fluoropore			Mitex
	2400	2500	0.1	FG 0.2	FH 0.5	FS 3.0	LC 10.0
Material	PP	PP	PP	PTFE	PTFE	PTFE	PTFE
Membr.thickness (μm)	20	20	160	40	40	10	100
Porosity (%)	38	51	75				
Av. pore size (μm)	0.02	0.04	0.1	0.2	0.5	3.0	10.0
Max. pore size (μm)	0.2	0.2	0.45				

Both types of Celgard membranes were obtained from the Celanese Corporation, the Accurel membranes were obtained from Enka A.G. and the Fluoropore and Mitex membranes are products of the Millipore Corporation.

3.4: Results

In this section the results of the penetrating drop method will be presented. In order to be able to compare the results of these measurements with the results of (contact angle) measurements on homogeneous, smooth

Table 3.2: Some properties of hydrophobic materials.

Property	PP	PTFE
γ_L^{90} (10^{-3} N/m)	55	40.5 (3)
γ_c (10^{-3} N/m)	29 (24)	18 (25)

surfaces, literature data of the latter are presented in table 3.2.

In this table γ_L^{90} is the surface tension of a liquid mixture which has a contact angle of 90° when brought in contact with a homogeneous smooth material and γ_c is the critical surface tension of wetting, which is defined as the surface tension at which $\theta = 0°$ when a liquid mixture is brought into contact with a homogeneous smooth material.

The results of the experiments with the penetrating drop method are given in table 3.3 and 3.4. Table 3.3 shows the data with the PP membranes and table 3.4 gives the results of the experiments with PTFE membranes. For every membrane the weight percentage of the organic component in water, at which this liquid is on the verge of penetration, is given. The surface

Table 3.3: Penetrating drop measurements of aqueous mixtures of organic components using polypropylene membranes.

Organic component	Membrane					
	Celgard 2400		Celgard 2500		Accurel 0.1	
	wt.%	γ_L^p	wt.%	γ_L^p	wt.%	γ_L^p
methanol	65	29.8	67	29.3	74	28.0
ethanol	35	31.4	35	31.4	41	29.5
propanol-1	13	32.0	15	30.5	16	29.5
butanol-1	4.5	32.5	4.5	32.5	5.5	29.0
formic acid	100	-	100	-	100	-
acetic acid	73	33.8	75	33.4	83	31.8
propionic acid	29	34.6	31	34.2	43	32.5
DMAc	91	36.0	93	35.7	94	35.5
DMF	91	36.5	91	36.5	98	35.5
DMSO	100	-	100	-	100	-
acetone	45	31.7	47	31.2	54	29.8
1,4-dioxane	53	39.7	53	39.7	64	37.7

tensions, corresponding with the measured concentrations, are calculated using literature data.

From these measurements some interesting conclusions can be drawn. First of all, it can be seen very clearly that the surface tension upon penetration, γ_L^p, is much lower than γ_L^{90}. In some of the above experiments γ_L^p is even as low as the critical surface tension, γ_c.

The second conclusion is that, although the concentration of organic component is different, the surface tension upon penetration, γ_L^p, is practically constant for a class of organic solutes. This same conclusion has already been obtained in previous measurements (1).

The third conclusion is that γ_L^p for Accurel membranes ('sharp-edged' pores) is lower than γ_L^p for Celgard membranes ('rounded' pores). The difference between these membranes, which are representatives of the two basic types of structure, will be discussed in the next paragraph.

For the penetrating drop experiments with PTFE membranes (see table 3.4) the same conclusions as obtained for PP membranes can be drawn. In these experiments γ_L^p is also much lower than γ_L^{90}, but in this case the surface tension upon penetration is not as low as γ_c. The measurements in

Table 3.4: Penetrating drop measurements of aqueous mixtures of organic components using poly(tetrafluoro ethylene) membranes.

Organic component	Membrane FG 0.2		FH 0.5		FS 3.0		LC 10.0	
	wt.%	γ_L^p	wt.%	γ_L^p	wt.%	γ_L^p	wt.%	γ_L^p
methanol	99	22.3	99	22.3	99	22.3	100	-
ethanol	83	24.1	81	24.3	77	24.8	87	23.6
propanol-1	51	25.0	45	25.2	31	25.8	71	24.5
butanol-1	7	26.0	7	26.0	5.5	29.0	7	26.0
formic acid	100	-	100	-	100	-	100	-
acetic acid	97	28.5	97	28.5	95	28.9	99	28.0
propionic acid	85	28.7	83	28.8	81	29.0	95	27.5
DMAc	100	-	100	-	100	-	100	-
DMF	100	-	100	-	100	-	100	-
DMSO	100	-	100	-	100	-	100	-
acetone	91	24.8	89	25.1	87	25.4	95	24.1
1,4-dioxane	100	-	100	-	100	-	100	-

which γ_L^p is closest to γ_c are the measurements with aqueous methanol mixtures.

The conclusion that γ_L^p is constant for a class of solutes, which was obtained for PP membranes, is not observed for PTFE membranes. From the measurements in table 3.4 using mixtures of alcohols in water, a slight increase in γ_L^p with the number of C-atoms is observed.

The differences between the two types of structure (LC 10.0 has 'sharp-edged' pores, whereas the others have 'rounded' pores) is not so clear as in the case of PP membranes, but nevertheless in this case it is also found that the 'sharp-edged' pores are more liquid-repellent than the 'rounded' pores.

The existence of a 'sharp-edged' or 'rounded' pore structure can be seen on electron microscope photographs. In figure 3.10 photographs of the investigated PP membranes are given and in figure 3.11 those of PTFE membranes.

These photographs indicate that the pore structure of the Celgard membranes (figure 3.10a and 3.10b) belongs to type I ('rounded' pore shape)

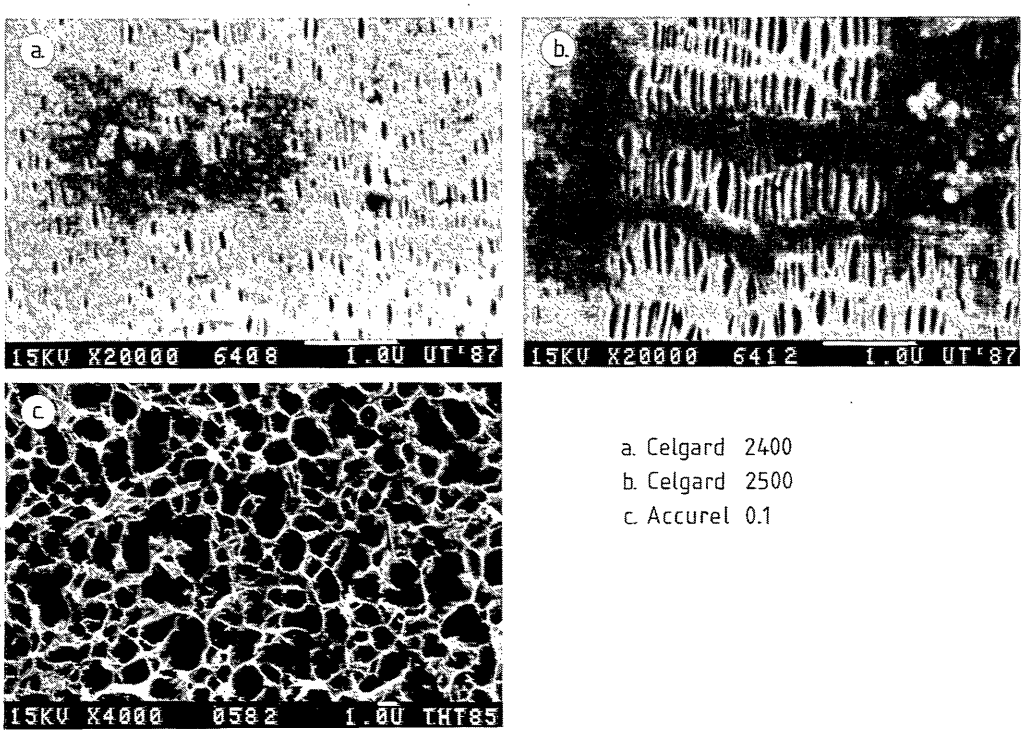

a. Celgard 2400
b. Celgard 2500
c. Accurel 0.1

FIGURE 3.10: Electron microscope photographs of polypropylene membranes.

and Accurel 0.1 (figure 3.10c) belongs to type II ('sharp-edged' pore shape). The fact that the Celgard membranes belong to type I can also be predicted on the basis of the membrane formation mechanism. These membranes are obtained by stretching of semi-crystalline films, and according to the theory this membrane preparation method always leads to a 'rounded' pore structure. Accurel membranes (figure 3.10c) are obtained by a thermal inversion process in which the the pore-former (i.c. a fatty oil) solidifies, resulting in a 'sharp-edged' pore structure.

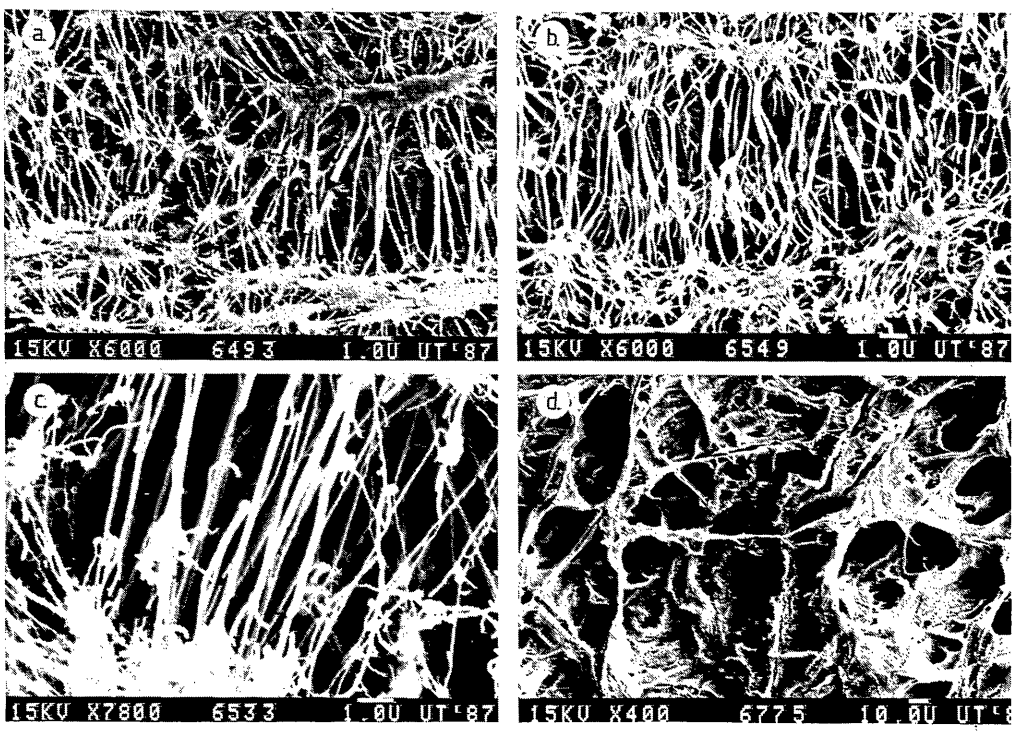

FIGURE 3.11: Electron microscope photographs of poly(tetrafluoro ethylene) membranes (a; FG 0.2; b. FH 0.5; c. FS 3.0; d. LC 10.0).

The PTFE membranes, shown in figure 3.11a till 3.11c belong to type I and are obtained by sintering and additional stretching. The PTFE membrane shown in figure 3.11d (tradename: Mitex) is made by sintering and additional leaching of the pore-former. As can be seen from the electron microscope photograph, the resulting structure contains 'sharp-edged' pores. Although the pore structure is not as regular as for Accurel membranes, this Mitex membrane is also a representative of a type II structure.

3.5: Discussion

An explanation for the fact that a liquid does not spontaneously penetrate into a membrane if the intrinsic contact angle becomes lower than 90° was already given by Cassie and Baxter (10). They stated that the apparent contact angle θ_{app}, measured on a porous surface, is a function of the intrinsic contact angle θ_{int}, measured on a smooth homogeneous surface, and the surface porosity. According to their derivation, membranes with a high surface porosity will not be spontaneously wetted even if $\theta_{int} = 0°$. The derivation of the equation of Cassie and Baxter has been given in chapter 2 (equation 2.8).

Kim and Harriott agree with Cassie and Baxter on the point that an intrinsic contact angle lower than 90° might be needed before spontaneous penetration of a liquid into the membrane occurs, but they derived that the intrinsic contact angle has a lower limit below which spontaneous penetration does occur (9).

According to their derivation penetration occurs when (P_1-P_2) goes through a maximum or when α reaches -90° and the adjoining interfaces merge. For instance, if $r = R$ and $\alpha = -90°$, then the lower limit for θ_{int} is about 63.5°. This means that if θ_{int} is lower than 63.5°, spontaneous penetration always would occur in case of 'rounded' pores. Although their theory is partially confirmed by their experimental results, Kim and Harriott are not correct as far as their theoretical derivation is concerned. The conclusion in the above example that a maximum penetration pressure is not reached anymore if θ_{int} is lower than 63.5° is correct, but a penetration pressure is still needed. Using equation 3.2 it can be derived that if $(\theta-\alpha) > 90°$, cosine $(\theta-\alpha) < 1$ which again leads to a positive value of P_1-P_2. Using this derivation it can be seen that even if θ_{int} is almost 0° and α is approaching -90°, a penetration pressure would still be necessary.

However, it must be realized that this reasoning only applies if the liquid front passing a 'rounded' pore does not get in contact with the next pore or a neighbouring liquid front. In a membrane this ideal situation is not likely to occur and therefore it is expected that a liquid penetrates spontaneously into a membrane at contact angles which are higher than 0°. Unfortunately, it cannot be predicted at which value of θ_{int} the liquid will spontaneously penetrate into a membrane with 'rounded' pores.

The description of the penetration of a liquid for 'sharp-edged' pores can also be done according to the theory of Cassie and Baxter. In the previous chapter, it has been shown however that this description is not very precise, especially if the pore fraction f_2 has a value between 0.45 and 0.5 (1).

The theoretical derivation, given in this chapter, is more precise and only uses the values of r/R and θ_{int}. The intrinsic contact angle can in principle be measured by contact angle measurement on homogeneous smooth material and the value of r/R can be estimated using electron microscope photographs. For instance, for Accurel membranes (see figure 3.10c) the value of r/R will be about 0.20 ($\pm$ 0.05). From figure 3.7 we can read that a penetration pressure is then necessary if θ_{int} is about 15° and larger. Although it is difficult to give an accurate value of r/R for the Mitex membrane (see figure 3.11d) it still can be estimated that r/R will be in the range of 0.4 ($\pm$ 0.1). This would imply that θ_{int} of a liquid, which is on the verge of penetration, is about 25°.

Two remarkable observations become clear from the theoretical considerations on 'sharp-edged' pores. First, it is shown that a positive pressure always has to be applied if the sum of the intrinsic contact angle of a penetrating liquid and α_{max} is larger than 90° and, secondly, the maximum penetration pressure is always reached at the 'sharp-edged' constriction. The second observation is very important in relation to deviations from ideality. In contrast to a membrane with 'rounded' pores in which interference with other pores or neighbouring liquid fronts might occur, this does not happen in a membrane with 'sharp-edged' pores. Therefore, deviations from the ideal situation as described for one pore are not expected if membranes with 'sharp-edged' pores are considered.

The above description uses intrinsic contact angles. In our investigations porous materials were used, which do not allow a direct measurement of the intrinsic contact angles. It is possible to define an 'effective contact angle' (9) or an 'apparent contact angle' (10) for a porous material, but in our opinion these descriptions are not accurate enough.

Moreover, since we are mostly interested in penetration pressures or maximum allowable solute concentrations at which a membrane is wetted, the penetrating drop method is much more practical. On the basis of these measurements a rough estimation of the intrinsic contact angles, using γ_c and γ_L^p, can still be made. The description in the previous chapter on low ener-

gy surfaces resulted in equation 2.5. Using this equation for this specific case yields:

$$\gamma_L^p.\cos\theta = -\gamma_L^p + 2.\gamma_c \qquad (3.6)$$

This equation gives us the possibility to calculate the intrinsic contact angle of the penetrating liquid. For instance, γ_c for alcohol/water mixtures on PP is about 29 . 10^{-3} N/m (24) and γ_L^p for Celgard 2400 membranes is about 32 . 10^{-3}, leading to an intrinsic contact angle of the penetrating solution of about 35°.

As Celgard membranes have type I constrictions, it is shown that the ideal situation (spontaneous penetration of a liquid into a 'rounded' pore only occurs if θ is about 0°) is not occuring for these membranes. Even if an uncertainty in the calculated value of θ_{int} is considered, its value will not become as low as 0°. Also the situation as calculated by Kim and Harriott is not realistic as their theoretical derivation (θ = 63.5° for r = R) would imply (using equation 3.6) a value of γ_L^p of about 40 . 10^{-3} N/m.

In case of type II constrictions, equation 3.6 can also be used to calculate the value of γ_L^p. On the basis of an electron microscope photograph from which the value of r/R can be obtained and the use of figure 3.7, an estimation of θ_{int} for the penetrating liquid can be made. When γ_c is known, the value of γ_L^p can then be calculated from equation 3.6. For instance, for Accurel membranes θ_{int} for a penetrating liquid will be about 15° and γ_c for alcohol/water mixtures on PP is about 29 . 10^{-3} N/m. This leads to a value of γ_L^p of 29.5 . 10^{-3} N/m, which is only slightly higher than γ_c. Even if the contact angle of the penetrating liquid would be 20°, then the value of γ_L^p would not be higher than 30 . 10^{-3} N/m. These estimations are confirmed by our experiments with Accurel membranes.

Comparison of the non-alcoholic mixtures from table 3.3 requires knowledge of the critical surface tension of these mixtures. In the previous chapter it was shown already that γ_c depends on the nature of the liquid. As these values are not available, simple calculations as given above cannot be made. Nevertheless, it can be observed from table 3.3 that Accurel membranes are more liquid-repellent than Celgard membranes: γ_L^p for Accurel membranes is about 2 . 10^{-3} N/m lower than the comparable value for Celgard membranes and this tendency holds for all solute types.

The results from table 3.4 are more difficult to interpret. In the first place, the number of organic substances that does not wet the membrane at all is larger, so less information is available. In the second place, the experiments with the alcoholic mixtures do not give a constant value of γ_L^p for a certain membrane. An explanation for this phenomenon cannot be given on the basis of the formulated theory.

The phenomenon that γ_L^p slightly increases when the average pore size increases, can be observed for the three Fluoropore membranes. From the photographs, it can be observed that the ratio r/R is increasing as well. As follows from equation 3.2 a change of this variable only has an effect on the height of the pressure difference, but it does not have any effect on the intrinsic contact angle. On the other hand, it can be understood that an increase of r/R also enlarges the possibility that a liquid front gets into contact with a neighbouring liquid front or the next pore. As is stated earlier, it is not possible to quantify this effect.

The observation that the Mitex LC 10.0 membrane is more liquid-repellent than the Fluoropore membranes, is another proof for the fact that type II constrictions are more liquid-repellent. The results on these PTFE membranes can certainly not be explained by the theory of Cassie and Baxter, because the surface porosity of the Fluorpore membranes is higher than those of the Mitex membrane (1,11).

To explain the results of table 3.4 in terms of contact angles is also very difficult. In the first place, the results using the alcohol/water mixtures do not give a constant value of γ_L^p for a certain membrane and in the second place the value of γ_c, given in table 3.2, is the value obtained for a homologous series of aliphatic hydrocarbons in contact with PTFE. Therefore, no direct comparison between the values in the tables 3.2 and 3.4 can be made.

An estimation of a critical surface tension can be made on the basis of knowledge of γ_L^p and θ_{int} of a penetrating liquid mixture for the LC 10.0 membrane (the latter being about 25°). For the carboxylic acids γ_L^p is about $27.7 \cdot 10^{-3}$ N/m, thus giving a value of γ_c of about $26.4 \cdot 10^{-3}$ N/m. Using this value for a calculation of θ_{int} of a penetrating liquid mixture for the Fluoropore membranes produces values varying from 31 to 35°. These values are in the same order of magnitude as the values found for Celgard membranes.

3.6: Conclusions

The penetration of a liquid into a membrane with 'sharp-edged' constrictions (type II pores) is described very well by the model developed. If the same theory is applied to 'rounded' constrictions (type I pores), no agreement between theory and experiment is found. The reason for this effect is that an interference with neighbouring liquid fronts and other pores takes place; in other words the one-pore description cannot be applied to membranes in that case.

Both penetrating drop experiments and calculations show that 'sharp-edged' pores are more liquid-repellent than 'rounded' pores, especially if the 'sharp-edged' structure is regular and the ratio of r/R is low. Therefore, membranes with 'rounded' pores are prefered when a good wetting is needed (for instance in a filtration process) whereas the 'sharp-edged' structure is favourable in membrane distillation where a liquid-repellent membrane is needed.

It is possible to predict whether type I or type II pores are obtained on the basis of the membrane formation mechanism.

3.7: Symbols

The symbols that are used in this chapter are conform the terminology of membrane distillation (13). Additional symbols or symbols which are defined a different way are marked with the *-symbol.

Latin symbols

B	pore geometry coefficient	-	*
P	pressure	N/m^2	
R	radius (defined in figure 3.4 resp. figure 3.5)	m	*
r	pore radius	m	*

Greek symbols

α	correction angle for pore shape (see figure 3.4 resp. figure 3.5 for its definition)	°	*
γ	surface tension	N/m	
γ_c	critical surface tension of wetting	N/m	*

$\gamma_L^{s\,o}$	surface tension of a liquid (mixture) which has a contact angle of 90° when brought in contact with a homogeneous smooth solid material	N/m	*
γ_L^p	surface tension of a liquid (mixture) that is on the verge of penetration into the pores of a (micro)porous membrane	N/m	*
Δ	difference		
θ	contact angle	°	*
θ'	(eq. 8) contact angle on a rough surface	°	*
θ_{app}	apparent contact angle (measured on a porous surface)	°	*
θ_{int}	intrinsic contact angle (measured on a homogeneous surface)	°	*

Subscripts

L	liquid	*
max	maximum	*
min	minimum	*
rel	relative	*
1	liquid phase	*
2	air phase	*

3.8: References

1. A.C.M. Franken, J.A.M. Nolten, M.H.V. Mulder, D. Bargeman & C.A. Smolders; Wetting Criteria for the Applicability of Membrane Distillation; Journal of Membrane Science 33 (1987) 315; also: chapter 2 of this thesis.
2. H.W. Fox & W.A. Zisman; The Spreading of Liquids on Low Energy Surfaces. I. Polyfluoroethylene; Journal of Colloid Science 5 (1950) 514.
3. M.K. Bernett & W.A. Zisman; Wetting of Low-Energy Solids by Aqueous Solutions of Highly Fluorinated Acids and Salts; Journal of Physical Chemistry 63 (1959) 1241.
4. J.R. Dann; Forces Involved in the Adhesive Process. I. Critical Surface Tensions of Polymeric Solids as Determined with Polar Liquids; Journal of Colloid & Interface Science 32 (1970) 302.
5. D. Bargeman, Contact Angles on Nonpolar Solids; Journal Colloid & Interface Science 40 (1972) 344.
6. A. Hernandez, F. Martinez-Villa, J.A. Ibanez, J.I. Arribas & A.F. Tejerina; An Experimentally Fitted and Simple Model for the Pores in Nuclepore Membranes; Separation Science and Technology 21 (1986) 665-677.

7. ASTM F 316-70; Standard Test Method for Pore Size Characteristics of Membrane Filters for Use with Aerospace Fluids.
8. R.A. Cotton & C.W. Fifield; Standardization of Membrane Filters; chapter 2, pages 19-39. In: B.J. Dutka (editor); Membrane Filtration - Application, Techniques and Problems; Marcel Dekker Inc., New York.
9. B.-S. Kim & P. Harriott; Critical Entry Pressure for Liquids in Hydrophobic Membranes; Journal of Colloid and Interface Science 115 (1987) 1-8.
10. A.B.D. Cassie & S. Baxter; Transactions Faraday Society 40 (1944) 546.
11. A.B.D. Cassie & S. Baxter; Contact Angles; Discussion Faraday Society 3 (1948) 11-16.
12. H. Strathmann; Trennung von molekularen Mischungen met Hilfe synthetischer Membranen; Steinkopf, Darmstadt, 1979.
13. W. Pusch; Examination Methods for the Physicochemical Properties of Synthetic Membranes; Pure & Applied Chemistry 58 (1986) 1669-1676.
14. S. Hashida, S. Hirikawa & H. Namio; Porous Structure of Biaxially Drawn Polytetrafluoroethylene Film; Journal of Applied Polymer Science 32 (1986) 5685-5689.
15. H.S. Bierenbaum, R.B. Isaacson, M.L. Druin & S.G. Plovan; Microporous Polymeric Films; Industrial & Engineering Chemistry, Product Research & Development 13 (1974) 2-9.
16. T. Sarada, L.C. Sawyer & M.I. Ostler; Three Dimensional Structure of Celgard Microporous Membranes; Journal of Membrane Science 15 (1983) 97-113.
17. Nuclepore GmbH; Nuclepore Membrantechnologie; prospect.
18. F.W. Altena; Phase Separation Phenomena in Cellulose Acetate Solutions in Relation to Asymmetric Membrane Formation; Ph.D. thesis; University of Twente, 1982.
19. J.G. Wijmans; Synthetic Membranes; Ph.D. thesis; University of Twente, 1984.
20. A.J. Reuvers; Membrane Formation; Ph.D. thesis; University of Twente, 1987.
21. G.T. Caneba & D.S. Soong; Polymer Membrane Formation through the Thermal-Inversion Process. 1. Experimental Study of Membrane Structure Formation; Macromolecules 18 (1985) 2538-2545.
22. R.E. Kesting; Synthetic Polymeric Membranes, A Structural Perspective; second edition; John Wiley & Sons, New York, 1985.
23. C. Josefiak & F. Wechs; Verfahren zur Herstellung von porösen Körpern mit einstellbarem Gesamtporenvolumen, einstellbarer Porengrösse und einstellbarer Porenwandung; German Patent DE 3205289.
24. H. Schonhorn; Heterogeneous Nucleation of Polymer Melts on Surfaces. I. Influence of Substrates on Wettability; Polymer Letters 5 (1967) 919-924.
25. W.A. Zisman; Influence of Constitution on Adhesion; Industrial & Engineering Chemistry 55 (1963) nr. 10, 19-38.

Chapter 4:

ETHANOL/WATER SEPARATION BY MEMBRANE DISTILLATION. 1. MODEL

A.C.M. Franken, M.H.V. Mulder & C.A. Smolders

Summary

A model for the separation of ethanol and water by membrane distillation has been developed. In this model VLE (Vapour-Liquid Equilibrium) data are combined with the effect of temperature polarization and concentration polarization.

4.1: Introduction

Membrane distillation is a distillation process, in which two aqueous liquids with different temperatures are separated by a hydrophobic microporous membrane. In this process the pores of the non-wettable membrane contain the vapour phase.

The vapour pressure difference ΔP_v across the membrane, resulting from the temperature difference ΔT, causes vapour molecules to be transported from the warm side (feed) through the pores to the cold side (permeate) of the membrane.

The advantages of membrane distillation are that the distillation process takes place at moderate temperatures and that a relatively small temperature difference between the two liquids separated by the membrane results in relatively high fluxes (1-3). Because entrainment of dissolved particles is avoided, the permeate is of a better quality than the product of conventional distillation, especially with the separation of dissolved solid/liquid mixtures, such as salt/water (3).

4.2: Theory

4.2.1: Vapour-liquid equilibrium

To describe the membrane distillation process for the separation of a

mixture of an organic liquid and water (i.e. ethanol and water) vapour-liquid equilibrium (VLE) equations have to be used. In analogy to conventional distillation, membrane distillation can be described as the result of:

- evaporation at the feed side of the membrane;
- transport of the vapour through the pores of the microporous membrane;
- condensation of the vapour at the permeate side of the membrane.

In case of membrane distillation, the following assumptions are made:

- VLE exists at both sides of the membrane;
- no coupling of the flux of ethanol vapour and water vapour occurs;
- the membrane itself has no selectivity towards any component (this means that an effect of Knudsen flow (if present) is not included in the calculations (4));
- no transport through the dense polymer membrane matrix occurs.

For the separation of ethanol/water mixtures it can be derived that the component flux, J_j, through the membrane is proportional to the difference in vapour pressure which exists across the membrane, ΔP_j. Using VLE equations in a steady-state situation, the permeate composition is given by the difference in partial vapour pressures of the components:

$$J_j \sim \Delta P_{mj} \rightarrow \text{steady-state: } \frac{x_{pme}}{x_{pmw}} = \frac{\Delta P_{me}}{\Delta P_{mw}} \qquad (4.1)$$

In appendix 1 (section 4.8) it is shown in which way the values of ΔP_e and ΔP_w have been calculated.

4.2.2.: Temperature polarization

For the calculation of the permeate composition by means of VLE equations it is essential that the temperatures of the feed and the permeate at the liquid-membrane interface should be known. Figure 4.1 shows that the experimentally determined values of the bulk temperatures, T_{fb} and T_{pb}, differ from the temperatures at the membrane interface, T_{fm} and T_{pm}. This effect is known as temperature polarization (6,7).

Although it is not possible to measure the temperatures at the membrane surfaces, it is possible to calculate the values of T_{fm} and T_{pm}. If

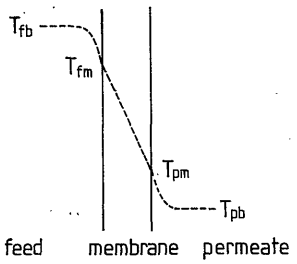

FIGURE 4.1: Temperature profile across a membrane (effect of temperature polarization).

the hydrodynamic conditions at both sides of the membrane are fixed, the heat transfer coefficients, h_f and h_p, can be calculated. If also the values of the bulk temperatures, T_{fb} and T_{pb}, are known, the temperatures at the membrane surfaces can be calculated using the following set of heat transport equations:

$$Q''_f = h_f.(T_{fb}-T_{fm}) - Q''_{vap} = h_f.\Delta T_f - Q''_{vap} \qquad (4.2)$$

$$Q''_m = h_m.(T_{fm}-T_{pm}) = h_m.\Delta T_m \qquad (4.3)$$

$$Q''_p = h_p.(T_{pm}-T_{pb}) + Q''_c = h_p.\Delta T_p + Q''_c \qquad (4.4)$$

$$\Delta T_b = \Delta T_f + \Delta T_m + \Delta T_p \qquad (4.5)$$

In a steady-state situation the heat flux through each thermal boundary layer has the same value, in other words $Q''_f = Q''_m = Q''_p$. If the above equations are combined, the following expressions for ΔT_f and ΔT_m are found:

$$\Delta T_f = (\Delta T_b + \frac{Q''_{vap}}{h_m} + \frac{Q''_{vap}}{h_p} + \frac{Q''_c}{h_p}) \;/\; (1+ \frac{h_f}{h_m} + \frac{h_f}{h_p}) \qquad (4.6)$$

$$\Delta T_m = (\Delta T_b - \frac{Q''_{vap}}{h_f} + \frac{Q''_c}{h_p}) \;/\; (1 + \frac{h_m}{h_f} + \frac{h_m}{h_p}) \qquad (4.7)$$

$$\Delta T_p = (\Delta T_b - \frac{Q''_{vap}}{h_f} - \frac{Q''_c}{h_f} - \frac{Q''_c}{h_m}) \;/\; (1 + \frac{h_p}{h_f} + \frac{h_p}{h_m}) \qquad (4.8)$$

The values of the different variables in equation 4.6 till 4.8 can be

measured or calculated. The values, which can be measured directly, are the bulk temperatures, T_{fb} and T_{pb}.

The value of the heat transfer coefficient of the membrane, h_m, is determined by two heat transfer processes, being conduction through the polymeric matrix and the stagnant vapour/air mixture, and convection by the permeating vapour. In our case the convection term is negligible small compared to the conduction term. From calculations it can be shown that the heat transfer through convection is always less than 4% of the total heat transfer through the membrane. Therefore, this effect was not taken into account. For the calculation of the conduction term it is assumed that the vapour/air mixture in the pores of the membrane is stagnant. This assumption is reasonable, because the flux through the membrane is relatively low. It can be calculated that, if the flux through the membrane is about $3 \cdot 10^{-3}$ kg/m²s, the radial velocity of the vapour is about $4 \cdot 10^{-3}$ m/s. Using the above assumptions, the average heat transfer coefficient of the membrane, h_m, for capillary membranes is given by the following formula:

$$\langle h_m \rangle = k_m / \delta_m \qquad (4.9)$$

In this equation k_m represents the heat conductivity of the membrane-permeant system and δ_m the thickness of the membrane.

The values of the heat transfer coefficients, h_f and h_p, can be calculated from the hydrodynamic conditions. An experimentally checked relation for the heat transfer during laminar flow of Newtonian liquids is given by Sieder and Tate (8):

$$\langle Nu \rangle = \frac{\langle h \rangle . Dh}{k} = 1.86 \; Re^{0.33} \; Pr^{0.33} \; (\frac{Dh}{L})^{-0.33} \; (\frac{\mu_b}{\mu_m})^{0.14} \qquad (4.10)$$

with the boundary condition that $\langle Nu \rangle_{min} = 3.66$.

The best-known empirical correlation for heat transfer during turbulent flow in circular pipes is (8):

$$Nu = \frac{h . Dh}{k} = 0.027 \; Re^{0.8} \; Pr^{0.33} \; (\frac{\mu_b}{\mu_m})^{0.14} \qquad (4.11)$$

which is valid in the region $2000 < Re < 10^5$ and $Pr > 0.7$.

The values of the heat flow as a result of vaporization, Q''_{vap}, and of condensation, Q''_c, are proportional to the flux J through the membrane:

$$Q''_{vap} = J.\Delta H_{vap} \qquad (4.12)$$

$$Q''_c = J.\Delta H_c \qquad (4.13)$$

The heat of vaporization, ΔH_{vap}, and the heat of condensation, ΔH_c, were obtained from literature. The value of the flux J has to be measured or calculated. Calculation of the flux can be done using equations for the diffusion of a vapour through a stagnant gas. From other investigations it appeared that calculation of the flux in this way is very difficult even for relatively simple systems which contain only water (7).

Therefore the flux was calculated by means of a semi-empirical relation in which all membrane parameters were reduced to one membrane constant, which is specific for a certain membrane. The membrane constant C_m is calculated using the experiments of chapter 5 in which the flux J was determined experimentally and the partial vapour pressures, P_{fm} and P_{pm}, were calculated. The constant, C_m, obtained from the quotient of the flux and the difference in partial vapour pressures is used in this chapter in the following semi-empirical relation:

$$J = C_m.(P_{fm}-P_{pm}) \qquad (4.14)$$

According to Schofield et al. (7) the constant C_m is slightly temperature dependent, decreasing by about 3% with a 10°C increase in mean temperature. In our investigations this effect was not found and C_m was kept constant.

4.2.3: Concentration polarization

The effect of concentration polarization has been described by many authors, most of them working in the field of ultrafiltration (9-10). In the field of pervaporation and membrane distillation the effect of concentration polarization either was not supposed to be important or was neglected. Only a few authors, among them Rautenbach (11) and Nakao (12), took this effect into account.

The description of the effect of concentration polarization for mem-

brane distillation does not differ from the description for any other membrane process. In direct-contact membrane distillation it is in principle possible that concentration polarization occurs at the feed side as well as at the permeate side of the membrane. Concentration polarization at the permeate side of the membrane can occur when the composition of the liquid at the permeate side is different from the composition of the permeating vapour. This situation occurs in non-steady state operation and/or in process operation in which the composition changes as a function of the place in the module.

In our calculations only steady-state situations and fixed bulk compositions are considered. In this case the assumption stated in equation 4.1 is valid. From this equation it can be seen that the permeate composition is determined by the component fluxes. Therefore, concentration polarization only occurs at the feed side of the membrane. This situation is shown in figure 4.2.

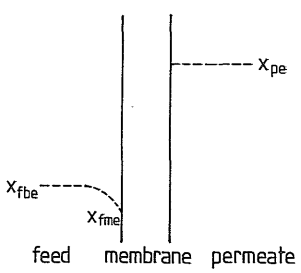

FIGURE 4.2: Concentration polarization in direct-contact membrane distillation in steady-state operation.

Note that in this figure the concentration profile (expressed in molar fractions) of the preferentially permeating component (ethanol) is given.

The equation generally used to describe concentration polarization (10), specified for our case, is:

$$\frac{J_V}{k_{Mf}} = \ln \left(\frac{C_{fmw} - C_{pmw}}{C_{fbw} - C_{pmw}}\right) \qquad (4.15)$$

in which J_V is the volume flux through the membrane and k_{Mf} is the mass transfer coefficient at the feed side of the membrane.

Equation 4.15 is valid for volume related dimensions for flux and con-

centration. In membrane distillation fluxes are given in kg/m²s and compositions in weight fractions. Therefore the above formula is rewritten in the following form:

$$\frac{J}{\rho_{pm} \cdot k_{Mf}} = \ln \left(\frac{\rho_{fm} \cdot w_{fmw} - \rho_{pm} \cdot w_{pmw}}{\rho_{fb} \cdot w_{fbw} - \rho_{pm} \cdot w_{pmw}} \right) \qquad (4.16)$$

Because the density is a function of the weight fraction of water, the number of unknown parameters in the above equation can be reduced. As the weight fraction of ethanol in the experimental system does not exceed 20% by weight, the density in this region can be described very well by a linear function:

$$\rho_{ij} = A + B.w_{ijw} \qquad (4.17)$$

For every temperature the values of A and B have to be determined separately. These values were determined for temperatures ranging from 30 till 80°C at intervals of 10°C. Intermediate values were determined by interpolation.

Combination of equation 4.16 and 4.17 gives the following equation for the concentration polarization:

$$\frac{J}{(A+B.w_{pmw}).k_{Mf}} = \ln \left(\frac{w_{fmw} - w_{pmw}}{w_{fbw} - w_{pmw}} \right) + \ln \left[\frac{1+(B/A).(w_{fmw}+w_{pmw})}{1+(B/A).(w_{fbw}+w_{pmw})} \right] \qquad (4.18)$$

Thus using a linear function for the density the number of parameters in the equation for concentration polarization has been limited to five. Two of these parameters (the flux, J, and the weight fraction of water in the bulk at the feed side, w_{fbw}) can be measured directly. Also the weight fraction of water at the membrane interface at the permeate side, w_{pmw}, can be measured directly as this value is equal to the bulk concentration, w_{pbw}. The weight fraction of water at the membrane interface at the feed side, w_{fmw}, has to be calculated by means of equation 4.18.

The mass transfer coefficient, k_{Mf}, can be calculated if the hydrodynamic conditions at the feed side of the membrane are known. The mass transfer coefficient in the laminar flow region can be calculated by the Leveque equation (8):

$$\langle k_M \rangle = 1.62 \cdot \left(\frac{\langle u \rangle . D^2}{L . Dh} \right)^{0.33} \qquad (4.19)$$

with the condition that the Graetz number ($Gz = D.L/(Dh^2.\langle u\rangle)$) is smaller than 0.05.

For very long channels, when $Gz > 0.1$, the Sherwood number Sh becomes constant. In this case the equation for the mass transfer coefficient is simplified to:

$$\langle k_M\rangle = 3.66\ (D/Dh) \qquad (4.20)$$

The mass transfer in the turbulent flow region is best described by the following equation (8):

$$\langle k_M\rangle = 0.027\ Re^{0.8}\ Sc^{0.33}\ (D/Dh) \qquad (4.21)$$

with the condition that the Reynolds number, Re, is higher than 2000 and that the Schmidt number, Sc, is lower than 0.7.

If the average value of the mass transfer coefficient at the feed side, $\langle k_M\rangle_f$, is known, the effect of concentration polarization can be calculated by means of equation 4.18.

4.2.4: Combined effect of temperature and concentration polarization

Although temperature polarization and concentration polarization are described separately in the above description, there is a combined effect. This effect is limited to the variation of the properties of the feed at the membrane surface. In the heat and mass transfer relations that were used only the viscosity μ_{fm} and the density ρ_{fm} are influenced by this combined effect.

The combined effect of temperature polarization and concentration polarization is calculated iteratively.

4.3: Calculation parameters

4.3.1: Liquid properties

Both feed and permeate consist of a mixture of ethanol and water at different temperatures. The properties of the liquids needed to calculate the dimensionless numbers (Gz, Nu, Re, Pr, Sc and Sh) are density (ρ), diffusion coefficient (D), heat conductivity (k), heat capacity (C_p) and

liquid viscosity (μ). All liquid properties are described as a function of the composition and the temperature and are calculated iteratively.

4.3.2: Membrane modules

Although the calculations with the model can be carried out for any kind of module, we restricted our calculations to existing membrane modules with which the experiments, described in chapter 5, were carried out.

In our investigations two types of capillary modules were used. The module characteristics are listed in table 4.1.

Table 4.1: Characteristics of modules used, with capillary membranes

Parameter	module I	module II
Module length (L) (mm)	497	348
Module diameter (mm)	14.0	11.0
Membrane diameter outside (mm)	8.50	2.40
inside (mm)	5.50	1.70
Membrane thickness (δ_m) (mm)	1.50	0.35
Membrane conductivity k_m (W/mK)	0.048	0.048
Membrane constant C_m (g/(m².s.mmHg))	0.00589	0.0212
Number of membranes in module	1	4
Feed flow	inside	inside
Permeate flow	outside	outside
Hydraulic diameter inside (Dh_f) (mm)	5.50	1.70
outside (Dh_p) (mm)	5.50	4.75

4.3.3: Fixed variables

In all the calculations the bulk feed concentration was kept constant at a level of 5 wt% ethanol; the other parameters were varied.

During the investigations of the hydrodynamic conditions, the bulk temperatures of both feed and permeate were kept constant at a level of 70°C and 30°C respectively.

When the effect of the temperature difference was investigated the Reynolds numbers of feed and permeate were kept constant. The temperature effect was calculated for two sets of Reynolds numbers. In the first set Re_f and Re_p both have a value of 4000; in the second set Re_f = 4000 and Re_p = 1000. The second set corresponds with the experimental conditions to be described in the next chapter.

4.4: Results and discussion of calculations

4.4.1: Influence of hydrodynamic conditions

The calculated flux and selectivity as a function of the hydrodynamic conditions are given in figures 4.3 till 4.6 and in tables 4.2 and 4.3. These tables and tables 4.4 and 4.5 are given in appendix 2.

The selectivity is defined as:

$$\alpha = \left(\frac{w_{pe}}{1-w_{pe}}\right) / \left(\frac{w_{fme}}{1-w_{fme}}\right) \qquad (4.22)$$

Note that the selectivity is defined as an intrinsic property, using the concentrations at the membrane surface.

In figures 4.3 till 4.6 it can be seen that the calculated curves show a discontinuity at Re = 2000, corresponding to a change from laminar flow to turbulent flow. For both regimes different equations for heat and mass transfer were used. Nevertheless the transition is not as sharp as shown in these figures. In literature on heat and mass transfer it can be found that a transition region exists in which the flow cannot be described as fully laminar nor fully turbulent. The width of this transition region depends on several factors, among others the surface roughness of the tubes. In general the transition region extends from a Re number of 2000 till 4000. It is very difficult to describe this transition region mathematically and in most cases heat and mass tranfer relations are given for the laminar and the turbulent region only. In figures 4.3 till 4.6 the dashed line is used to represent the selectivities according to the vapour-liquid equilibrium. These lines show the situation in which no temperature or concentration polarization occurs; in fact these are the lines were the Re numbers at both feed and permeate side become infinite.

The calculated selectivity as a function of the hydrodynamic conditions for module I is given in figures 4.3a and 4.3b and in table 4.2.

Both figures show that the selectivity does not change much once the flow at both sides of the membrane is turbulent. If curves a and b are compared, it can be seen that an increase of the Re number in the turbulent region only has a minor effect on the decrease of temperature and concentration polarization. Therefore the selectivity is only slightly changed.

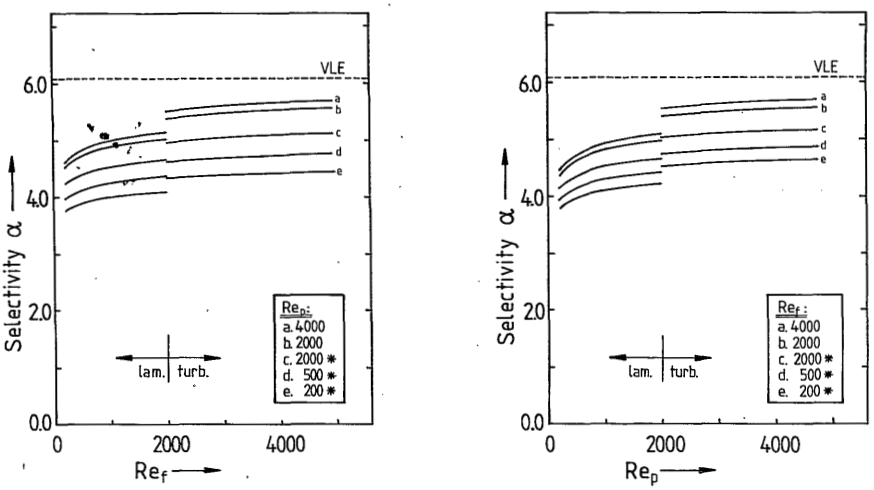

FIGURE 4.3: Selectivity as a function of the Reynolds number at the feed (a) and the permeate (b) side in module I.

On the other hand, if the calculation is carried out with the same Re number of 2000 but with equations for laminar flow instead of turbulent flow, a relatively large decrease in selectivity is found. A further decrease of the Re number at feed and/or permeate side of the membrane results in the (expected) decrease in selectivity.

The calculated selectivity as a function of the hydrodynamic conditions for module II is given in figures 4.4a and 4.4b and in table 4.3.

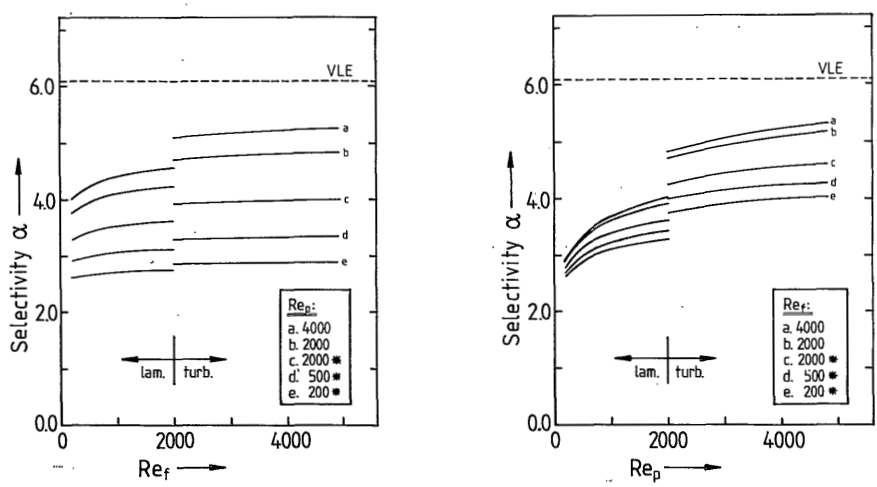

FIGURE 4.4: Selectivity as a function of the Reynolds number at the feed (a) and the permeate (b) side in module II.

The only difference between the results in figures 4.3 and 4.4 is the use of a different module. Figures 4.4a and 4.4b clearly show that the selectivities are lower and that the effect of hydrodynamic conditions on the selectivities are much more pronounced. The explanation for this phenomenon is that the wall thickness of the membranes in module II (δ = 0.35 mm) is less than in module I (δ = 1.50 mm). This means that the insulating capacity of the membranes in module II is about four times lower, resulting in a heat transfer coefficient which is about four times higher. From equations 4.6 till 4.8 it can be seen that if h_m becomes larger the effect of temperature polarization becomes more pronounced.

Another effect which contributes to temperature polarization is the flux through the membrane. If the flux is higher then the heat of vaporization Q''_{vap}, and condensation Q''_c, becomes higher. Because this heat is withdrawn from the feed, respectively added to the permeate, a higher flux gives a more pronounced effect of temperature polarization. Since the flux in module II is higher than in module I by a factor of about 3.5, the effect of the lower insulating capacity is augmented by that of the higher flux value.

As can be seen in these figures as well, the selectivity is not changed very much once the flow becomes turbulent. Comparable to figures 4.3a and 4.3b, a relatively large decrease in selectivity is found if the calculations are carried out with the same Re number of 2000, but with equations for laminar flow instead of turbulent flow.

The phenomenon that the selectivity is more strongly influenced by the Re number at the permeate side than the Re number at the feed side is very pronounced in the case of module II. For instance, comparing point 30 and point 46 from table 4.3, it is demonstated that the selectivity is higher when the Re number at the permeate side is higher. This applies for other sets of calculations as well. The reason for this phenomenon can be found in the fact that the temperature dependence of the partial vapour pressure is very large and that the activity coefficient changes very much at lower temperatures (see appendix 1).

The calculated flux as a function of the hydrodynamic conditions are given in figures 4.5a and 4.5b and in tables 4.2 and 4.3.

The same phenomena that were found for the selectivity as a function of the Re number are also found for the flux. If the flow becomes turbulent the flux does not change very much and if the calculations are carried out with the same Re number but with equations for laminar flow instead of tur-

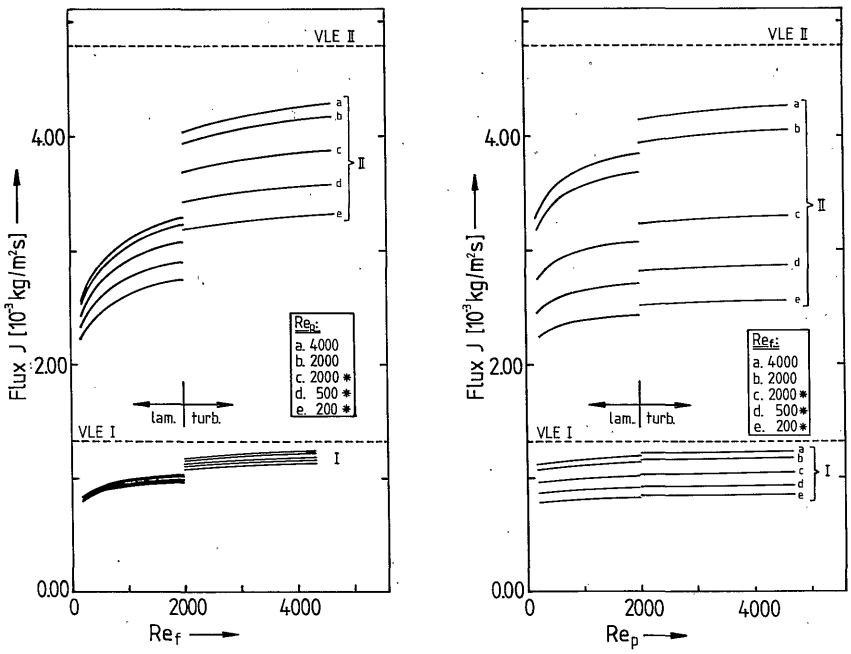

FIGURE 4.5: Flux as a function of the Reynolds number at the feed (a) and the permeate (b) side.

bulent flow, a relatively large decrease in flux is found.

From figures 4.3 and 4.4 it appeared that the selectivity is more strongly influenced by the Re number at the permeate side than the Re number at the feed side. For the flux, however, the opposite relation is found. It appears that the flux is strongly influenced by the Re number at the feed side. If figure 4.5b is observed, it can be seen that it hardly makes any difference whether the Re number at the permeate side is high or low. Even the discontinuity at Re = 2000 is hardly present, especially in the case of module I. On the other hand, in figure 4.5a the discontinuity at Re = 2000 is distinctly present. This phenomenon can be explained by means of equation 4.14 and the Antoine relation (equation 4.A.6). From equation 4.14 it can be seen that the flux is directly proportional to the vapour pressure difference between feed and permeate and from the Antoine relation it can be seen that the vapour pressure is increasing with temperature through an exponential relation. This means that a small temperature change at a high temperature level gives a larger change in partial vapour pressure than the same temperature change at a low temperature. For instance, at 30°C the vapour pressure of water changes 1.9 mmHg/°C whereas at 70°C the vapour pressure changes 10.2 mmHg/°C.

The effect of the hydrodynamic conditions on the concentration polarization at the feed side of the membrane is given in figures 4.6a and 4.6b. In figure 4.6a the weight percentage ethanol at the membrane surface in the feed as a function of the Reynolds number at the feed side for module I is given. In figure 4.6b the same variables are plotted for module II.

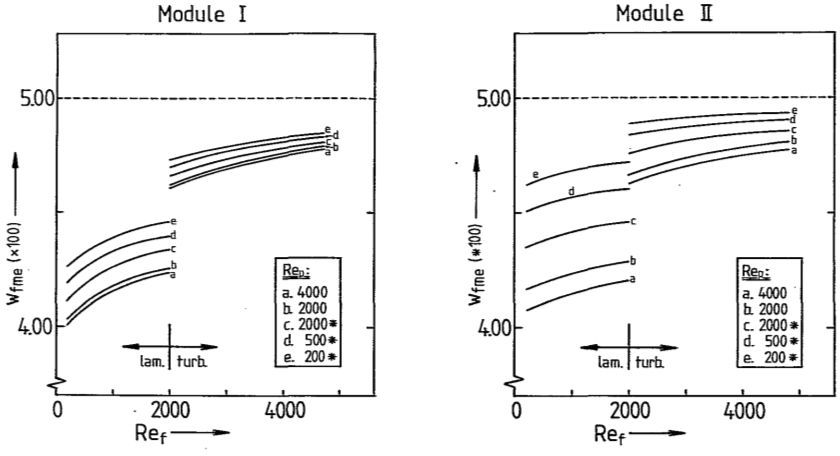

FIGURE 4.6: Weight percentage ethanol at the membrane surface in the feed as a function of the Reynolds number at the feed side for module I (a) and for module II (b).

As can be seen from equation 4.15, the weight fraction of ethanol at the membrane surface at the feed side, w_{fme}, is influenced by the flux, the selectivity and the mass transfer coefficient k_{Mf}.

As expected the hydrodynamic conditions at the feed side have a large influence on the concentration polarization. In both figures it can be observed that the concentration decreases when the Reynolds number decreases and again a discontinuity is observed at Re = 2000. This is due to a decrease of the mass transfer coefficient with decreasing Re numbers. For module I the mass transfer coefficient decreases from 59 x 10^{-6} m/s at Re = 4000 to 6.1 . 10^{-6} m/s for Re = 200 and for module II the mass transfer coefficient decreases from 190 . 10^{-6} m/s at Re = 4000 to 15 . 10^{-6} m/s for Re = 200. If on the other hand it is considered that the flux through the membranes in module II is about three times higher than in module I, roughly the same effect of concentration polarization might be expected for both modules. For higher Re numbers (especially in the turbulent region) this effect is found indeed.

Although concentration polarization is limited to the feed side, the hydrodynamic conditions at the permeate side have an influence on this effect as well. As can be seen from the figures concentration polarization (for a fixed Re number at the feed side) is decreasing if the Re number at the permeate side is decreasing. This phenomenon can be explained as follows. When the Re number at the permeate side is decreasing, the effect of temperature polarization is increasing and as a consequence the selectivity and the flux are lowered. Using equation 4.15, it can be demonstrated that both effects contribute to the decrease of the effect of concentration polarization.

4.4.2: Influence of temperature difference

The calculated flux and selectivity as a function of the temperature difference at two different sets of hydrodynamic conditions are given in figures 4.7 and 4.8 and in tables 4.4 and 4.5.

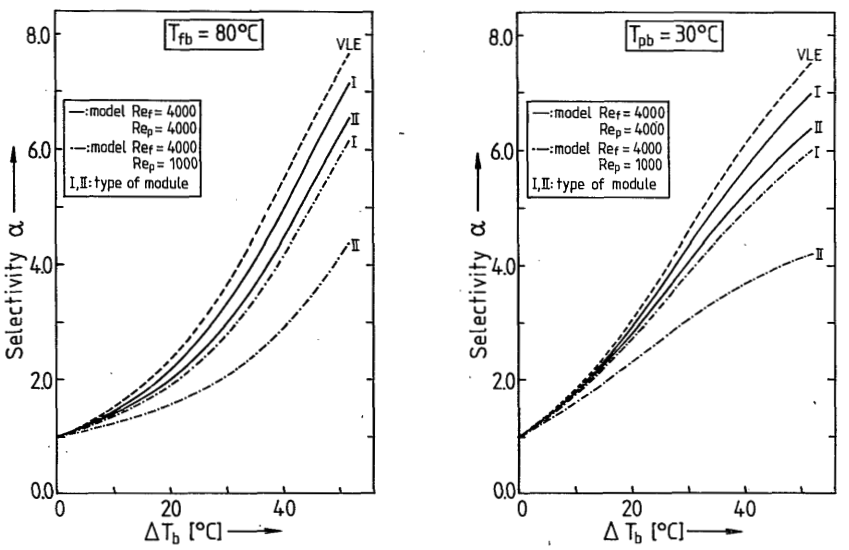

FIGURE 4.7: Selectivity as a function of the temperature difference:
a. fixed feed temperature (80°C);
b. fixed permeate temperature (30°C).

For the investigation of the influence of the temperature difference two different sets of hydrodynamic conditions were considered. In the first set the Reynolds number of feed and permeate were chosen in the turbulent

region at a value of 4000. This value was chosen, because it is about the minimum level at which the flow can be assumed to be fully turbulent. The second set of hydrodynamic conditions consists of Re = 4000 at the feed side and Re = 1000 at the permeate side. These are the Re numbers at which the experiments, discussed in the next chapter, were carried out.

In figure 4.7a the calculated selectivity is given as a function of the bulk temperature difference. In this figure the bulk temperature of the feed is fixed at 80°C and the permeate temperature has been varied. In figure 4.7b the bulk temperature of the permeate is fixed at 30°C and the feed temperature has been varied. (N.B. Not all the calculations which are listed in table 4.4 and 4.5 are given in figure 4.7a and 4.7b). The dashed lines in the figures represent the vapour-liquid equilibria. The full lines are calculated with the first set of hydrodynamic conditions (Re_f = 4000; Re_p = 4000) and the broken lines are calculated making use of the second set (Re_f = 4000; Re_p = 1000). The roman numbers indicate the module on which the calculation applies.

From both figures it is clear that the selectivity increases strongly when the temperature difference increases. This strong increase might be expected, because the vapour pressure difference increases exponentially with the temperature.

Another observation is that the selectivities calculated with the first set of hydrodynamic conditions lie close to the selectivities according to the vapour-liquid equilibrium. This means that once the flow becomes turbulent the selectivity hardly changes any more. Therefore, in applications of membrane distillation the flow conditions should be fully turbulent; this means that a Reynolds number of about 4000 at **both** sides of the membrane is sufficient to achieve a good separation. When making these statements, the insulating properties of the membrane should be considered. In our calculations the thinner membrane has a thickness of 0.35 mm. If membranes with a lower thickness or, in general, membranes with a lower insulating capacity are used, a further increase of the Re number in the turbulent region might be necessary to produce optimal separation results.

The results obtained with the second set of hydrodynamic conditions clearly show why a laminar flow at one side of the membrane gives rather poor separation results. For instance, at a bulk temperature difference of 50°C the selectivity for module II at this flow condition is 4.13 while the maximum selectivity is 7.33. When the Re number at the permeate side is increased to 4000 the selectivity becomes 6.22, which is a considerable

improvement.

Comparing figure 4.7a and 4.7b, it can be seen that the selectivities in the latter figure are slightly better. For instance at a temperature difference of 30°C the VLE-selectivity in figure 4.7a (T_{fb} = 80°C and T_{pb} = 50°C) is 3.64, whereas the selectivity in figure 4.7b (T_{fb} = 60°C and T_{pb} = 30°C) is 4.57. Again the reason for this difference has to be found in the partial vapour pressure difference and the temperature dependency of the activity coefficient.

In figure 4.8a the calculated flux as a function of the bulk temperature difference is given; in this figure the bulk temperature of the feed is fixed at 80°C and the permeate temperature is varied. In figure 4.8b the bulk temperature of the permeate is fixed at 30°C and the feed temperature is varied. The representation of the hydrodynamic conditions is carried out in the same way as for figure 4.7a and 4.7b.

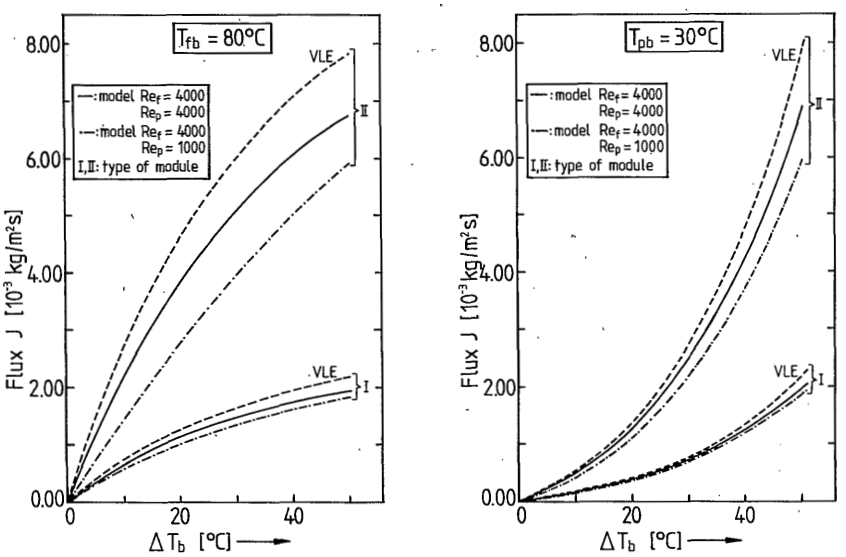

FIGURE 4.8: Flux as a function of the temperature difference:
a. fixed feed temperature (80°C);
b. fixed permeate temperature (30°C).

The most remarkable observation that can be made from these figures is that the different sets of hydrodynamic conditions do not have a large impact on the flux, the Re number at the feed side being 4000 in all cases. As it has already been shown in figure 4.5 that the flux is mainly deter-

mined by the highest temperature, it is not surprising that the fluxes for both sets of hydrodynamic conditions do not change very much. If on the other hand the Re number at the feed side would be lowered, the impact on the flux would be much more severe.

4.5: Conclusions

Provided the flow in the module at the feed and permeate side is turbulent, the selectivity and the flux hardly change any more for changing hydrodynamic conditions. For the application of membrane distillation a Reynolds number of about 4000 is necessary but sufficient to achieve a good separation. The insulating properties of the membrane and other module characteristics should be taken into account before this statement can be generalized.

Both flux and selectivity increase if the temperature difference increases. From our calculations it can be concluded that a minimum temperature difference of at least 30 to 40°C is necessary for an efficient separation.

4.6: Symbols

The symbols that are used in this chapter are conform the terminology of membrane distillation (13). Additional symbols or symbols which are defined in a different way are marked with the *-symbol.

Latin symbols

A,B,C	constants (eq. 4.A.6)	-	*
A_{ij}	Margules constant (eq. 4.A.7, 4.A.8)	-	*
A,B	constants (eq. 4.17, 4.18)	-	*
C	concentration	kg/m^3	
C_m	membrane constant	$g/(m^2.s.mmHg)$	*
C_p	heat capacity	J/kg.K	
D	diffusion coefficient	m^2/s	
Dh	hydraulic diameter	m	
Gz	Graetz number (= $D.L/(Dh^2.\langle u \rangle)$)	-	
ΔH_c	latent heat of condensation	J/kg	

ΔH_{vap}	latent heat of vaporization	J/kg	
h	heat transfer coefficient	W/m^2K	
J	mass flux	kg/m^2s	
J_V	volume flux	m^3/m^2s	
k	thermal conductivity	W/m.K	
k_M	mass transfer coefficient	m^3/m^2s	*
L	length of the module	m	*
Nu	Nusselt number (= h.Dh/k)	-	*
P	pressure	Pa	
Q"	heat flux	W/m^2	
Pr	Prandtl number (= $(\mu.C_p)/k$)	-	*
Re	Reynolds number (= $(\rho.\langle u\rangle.Dh)/\mu$)	-	*
Sc	Schmidt number (= $\mu/(\rho.D)$)	-	*
Sh	Sherwood number (= $(k_M.Dh)/D$)	-	*
T	temperature	K	
TPC	Temperature Polarization Coefficient	-	
u	tangential velocity	m/s	
w	weight fraction	-	
x	molar fraction	-	

Greek symbols

α	selectivity	-	
γ	activity coefficient	N/m	*
Δ	difference	-	
δ	membrane thickness	m	
μ	liquid viscosity	Pa.s	
ρ	density	kg/m^3	

Subscripts

b	bulk	
c	condensation	
e	ethanol	*
f	feed	
i,j	index	
m	membrane	
p	permeate	
vap	vaporization	
w	water	

Superscripts

o	pure component	*
∞	infinite dilution	*

4.7: References

1. S.-I. Andersson, N. Kjellander & B. Rodesjö; Design and Field Tests of a New Membrane Distillation Desalination; Desalination 56 (1985) 345-354.
2. P.K. Weyl; Recovery of Demineralized Water from Saline Waters; US patent 3,340,186.
3. K. Schneider and T.J. van Gassel; Membrandestillation; Chemie Ingenieur Technik 56 (1984) 514.
4. R. Marcel; Gas and Vapour Transport through Porous Media; lecture presented at "Summer school on membrane processes" at Cadarache, France, 3 - 7 September 1984.
5. J. Gmehling & U. Onken; Vapour-liquid equilibrium data collection (aqueous-organic systems), volume I, part 1; Dechema, Frankfurt, 1977.
6. F. Bellucci; Temperature Polarization Effects in Thermo-osmosis; Journal of Membrane Science 9 (1981) 285.
7. R.W. Schofield, A.G. Fane & C.J.D. Fell; Heat and Mass Transfer in Membrane Distillation; Journal of Membrane Science 33 (1987) 299-313.
8. W.J. Beek and K.M.K. Muttzall; Transport Phenomena; John Wiley, London - New York (1975).
9. W.F. Blatt, A. Dravid, A.S. Michaels & L. Nelsen; Solute Polarization and Cake Formation in Membrane Ultrafiltration: Causes, Consequences, and Control Techniques; pages 47-97. In: J.E. Flinn (editor); Membrane Science and Technology; Plenum, New York, 1970.
10. H. Strathmann; Trennung von molekularen Mischungen mit Hilfe synthetischer Membranen; pages 145-170; Steinkopf, Darmstadt, 1979.
11. R. Rautenbach & R. Albrecht; On the Behaviour of Asymmetric Membranes in Pervaporation; Journal of Membrane Science 19 (1984) 1-22.
12. S. Nakao, F. Saitoh, T. Asakura, K. Toda & S. Kimura; Continuous Ethanol Extraction by Pervaporation from a Membrane Bioreactor; Journal of Membrane Science 30 (1987) 273-287.
13. A.C.M. Franken & S. Ripperger; Terminology for Membrane Distillation; European Society of Membrane Science and Technology, January 1988 (given as an appendix to this thesis).

4.8: Appendix 1

For the separation of ethanol(e)/water(w) mixtures the following equations are derived from the VLE theory:

$$J_j \sim \Delta P_{mj} \rightarrow \text{steady state: } \frac{x_{pme}}{x_{pmw}} = \frac{\Delta P_{me}}{\Delta P_{mw}} \qquad (4.A.1)$$

$$\Delta P_{me} = P_{fme} - P_{pme} = x_{fme} \cdot \gamma_{fme} \cdot P^{o}_{fme} + x_{pme} \cdot \gamma_{pme} \cdot P^{o}_{pme} \qquad (4.A.2)$$

$$\Delta P_{mw} = P_{fmw} - P_{pmw} = x_{fmw} \cdot \gamma_{fmw} \cdot P^{o}_{fmw} - x_{pmw} \cdot \gamma_{pmw} \cdot P^{o}_{pmw} \qquad (4.A.3)$$

$$x_{fme} = 1 - x_{fmw} \qquad (4.A.4)$$

$$x_{pme} = 1 - x_{pmw} \qquad (4.A.5)$$

The partial pressures P^{o}_{imj} can be calculated from the temperatures of the feed and the permeate by means of the Antoine relation:

$$\log \left(P^{o}_{imj}\right) = A - \frac{B}{(T_{im} + C)} \qquad (4.A.6)$$

where P^{o}_{imj} is the vapour pressure of the pure component j in mmHg and T_{im} is the temperature in °C.

The values A, B and C are constants which were derived from VLE data (5). The values that are used for the calculation of the partial vapour pressure by means of equation 4.A.6 are listed in table 4.A.1.

Table 4.A.1: Antoine-constants for ethanol and water

	A	B	C
ethanol	8.11220	1592.864	226.184
water	8.07131	1730.630	233.426

The values of the activity coefficients γ_{imj} were abstracted from the same VLE data (5).

In our calculations the Margules equation was used for the determination of the values of γ_{imj}:

$$\ln \gamma_{ime} = \left(A_{ew} + 2.(A_{we} - A_{ew}).x_{ime}\right).x_{imw}^{2} \qquad (4.A.7)$$

$$\ln \gamma_{imw} = \left(A_{we} + 2.(A_{ew} - A_{we}).x_{imw}\right).x_{ime}^{2} \qquad (4.A.8)$$

The Margules equation was chosen, because it gave the best fit for the calculation of experimental data on mixtures of ethanol and water (5). The disadvantage of the Margules equation is, however, that the constants A_{ew} and A_{we} are temperature-dependent. It appeares that the constants A_{ew} and A_{we} are a function of γ_w^∞ and γ_e^∞ respectively. By plotting γ_e^∞ and γ_e^∞ as a function of the temperature, the values of A_{ew} and A_{we} can be obtained graphically. All the data, that were used to construct figures 4.A.1 and 4.A.2 were obtained from the Dechema series (5).

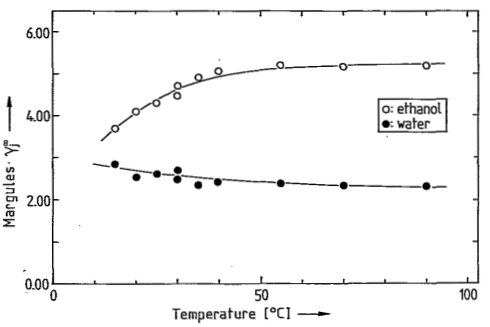

FIGURE 4.A.1: γ_e^∞ and γ_w^∞ as a function of the temperature.

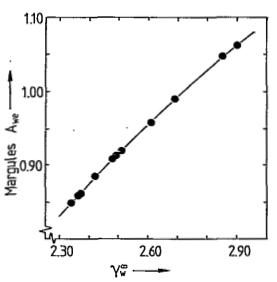

FIGURE 4.A.2a:
A_{we} as a function of γ_w^∞.

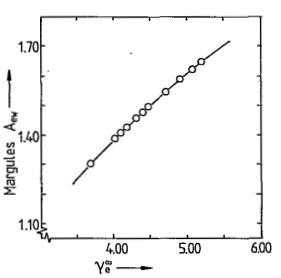

FIGURE 4.A.2b:
A_{ew} as a function of γ_e^∞.

If the temperature of the feed and the permeate are known, the values of γ_{imj} and P^o_{imj} can be calculated. Substituting these values in equation tion 4.A.1 till 4.A.5, reduces the number of variables to 6. If one of the composition parameters is known, the other parameters can be calculated.

4.9: Appendix 2

Table 4.2:
Calculated flux and selectivity as a function of hydrodynamic conditions for module I (w_{fbe} = 0.05)

nr.	Re_f [-]	Re_p [-]	T_{fb} [°C]	T_{fm} [°C]	T_{pm} [°C]	T_{pb} [°C]	TPC+ [-]	w_{fme} [%]	w_{pe} [%]	flux [g/m²s]	selectivity model [-]	selectivity VLE [-]
1	4000	4000	70.0	68.80	30.91	30.0	.947	4.75	22.0	1.220	5.67	6.09
2		2000	70.0	68.82	31.56	30.0	.931	4.75	21.6	1.210	5.53	6.09
3		2000*	70.0	68.86	33.52	30.0	.883	4.78	20.4	1.179	5.09	6.09
4		500*	70.0	68.89	35.35	30.0	.839	4.81	19.3	1.148	4.74	6.09
5		200*	70.0	68.93	36.99	30.0	.799	4.83	18.3	1.119	4.42	6.09
6	2000	4000	70.0	67.99	30.87	30.0	.928	4.61	21.1	1.165	5.53	6.09
7		2000	70.0	68.01	31.50	30.0	.913	4.62	20.7	1.156	5.40	6.09
8		2000*	70.0	68.08	33.41	30.0	.867	4.66	19.6	1.128	4.98	6.09
9		500*	70.0	68.14	35.19	30.0	.824	4.70	18.6	1.101	4.64	6.09
10		200*	70.0	68.20	36.78	30.0	.785	4.73	17.7	1.074	4.34	6.09
11	2000*	4000	70.0	65.85	30.79	30.0	.876	4.24	18.6	1.028	5.15	6.09
12	*	2000	70.0	65.88	31.37	30.0	.863	4.26	18.3	1.021	5.04	6.09
13	*	2000*	70.0	66.00	33.12	30.0	.822	4.34	17.5	1.001	4.66	6.09
14	*	500*	70.0	66.12	34.76	30.0	.784	4.40	16.8	0.981	4.37	6.09
15	*	200*	70.0	66.22	36.24	30.0	.749	4.46	16.1	0.961	4.11	6.09
16	500*	4000	70.0	63.98	30.73	30.0	.831	4.08	17.1	0.922	4.85	6.09
17	*	2000	70.0	64.03	31.26	30.0	.819	4.11	16.9	0.917	4.75	6.09
18	*	2000*	70.0	64.18	32.88	30.0	.783	4.19	16.3	0.902	4.45	6.09
19	*	500*	70.0	64.34	34.41	30.0	.748	4.27	15.6	0.886	4.16	6.09
20	*	200*	70.0	64.48	35.79	30.0	.717	4.33	15.1	0.871	3.93	6.09
21	200*	4000	70.0	62.42	30.68	30.0	.794	4.00	16.1	0.842	4.62	6.09
22	*	2000	70.0	62.48	31.17	30.0	.783	4.03	16.0	0.838	4.53	6.09
23	*	2000*	70.0	62.66	32.69	30.0	.749	4.11	15.4	0.826	4.25	6.09
24	*	500*	70.0	62.85	34.12	30.0	.718	4.19	14.8	0.813	3.98	6.09
25	*	200*	70.0	63.01	35.43	30.0	.690	4.26	14.4	0.800	3.78	6.09

*: calculations carried out with equations for laminar flow

+: Temperature Polarization Coefficient; TPC = $(T_{fm}-T_{pm})/(T_{fb}-T_{pb})$

Table 4.3:
Calculated flux and selectivity as a function of hydrodynamic conditions for module II (w_{fbe} = 0.05)

nr.	Re_f [-]	Re_p [-]	T_{fb} [°C]	T_{fm} [°C]	T_{pm} [°C]	T_{pb} [°C]	TPC$^+$ [-]	w_{fme} [%]	w_{pe} [%]	flux [g/m²s]	selectivity model [-]	selectivity VLE [-]
26	4000	4000	70.0	68.65	32.85	30.0	.895	4.76	20.7	4.251	5.23	6.09
27		2000	70.0	68.70	34.77	30.0	.848	4.79	19.5	4.138	4.82	6.09
28		2000*	70.0	68.81	39.17	30.0	.741	4.85	16.9	3.853	4.00	6.09
29		500*	70.0	68.92	43.09	30.0	.646	4.90	14.7	3.561	3.34	6.09
30		200*	70.0	69.01	46.18	30.0	.571	4.93	13.0	3.303	2.89	6.09
31	2000	4000	70.0	67.74	32.75	30.0	.875	4.63	19.8	4.037	5.09	6.09
32		2000	70.0	67.81	34.59	30.0	.831	4.67	18.7	3.938	4.70	6.09
33		2000*	70.0	68.00	38.88	30.0	.728	4.76	16.4	3.686	3.92	6.09
34		500*	70.0	68.18	42.72	30.0	.636	4.84	14.4	3.423	3.30	6.09
35		200*	70.0	68.33	45.77	30.0	.564	4.89	12.8	3.187	2.86	6.09
36	2000*	4000	70.0	64.22	32.36	30.0	.796	4.21	16.7	3.296	4.57	6.09
37	*	2000	70.0	64.38	33.97	30.0	.760	4.29	16.0	3.236	4.25	6.09
38	*	2000*	70.0	64.78	37.79	30.0	.675	4.46	14.5	3.079	3.63	6.09
39	*	500*	70.0	65.19	41.31	30.0	.597	4.61	13.1	2.907	3.12	6.09
40	*	200*	70.0	65.53	44.16	30.0	.534	4.72	12.0	2.746	2.75	6.09
41	500*	4000	70.0	61.81	32.12	30.0	.742	4.11	15.4	2.862	4.25	6.09
42	*	2000	70.0	62.02	33.58	30.0	.711	4.20	14.8	2.820	3.97	6.09
43	*	2000*	70.0	62.54	37.08	30.0	.636	4.38	13.6	2.706	3.44	6.09
44	*	500*	70.0	63.06	40.35	30.0	.568	4.54	12.5	2.579	3.00	6.09
45	*	200*	70.0	63.52	43.05	30.0	.512	4.66	11.6	2.457	2.68	6.09
46	200*	4000	70.0	59.88	31.94	30.0	.698	4.08	14.5	2.548	3.99	6.09
47	*	2000	70.0	60.12	33.28	30.0	.671	4.17	14.0	2.516	3.75	6.09
48	*	2000*	70.0	60.71	36.53	30.0	.605	4.35	13.0	2.429	3.29	6.09
49	*	500*	70.0	61.31	39.60	30.0	.543	4.51	12.0	2.330	2.90	6.09
50	*	200*	70.0	61.84	42.16	30.0	.492	4.63	11.2	2.233	2.61	6.09

*: calculations carried out with equations for laminar flow

$^+$: Temperature Polarization Coefficient; TPC = $(T_{fm}-T_{pm})/(T_{fb}-T_{pb})$

Table 4.4:
Calculated flux and selectivity as a function of hydrodynamic conditions and temperature difference for module I (w_{fbe} = 0.05)

nr.	Re_f [-]	Re_p [-]	T_{fb} [°C]	T_{fm} [°C]	T_{pm} [°C]	T_{pb} [°C]	TPC$^+$ [-]	w_{fme} [%]	w_{pe} [%]	flux [g/m²s]	selectivity model [-]	selectivity VLE [-]
51	4000	4000	80.0	79.45	70.53	70.0	.893	5.00	7.1	0.655	1.45	1.51
52			80.0	79.02	60.90	60.0	.906	4.99	10.2	1.137	2.16	2.34
53			80.0	78.68	51.13	50.0	.918	4.90	14.5	1.490	3.30	3.64
54			80.0	78.40	41.27	40.0	.928	4.75	19.7	1.751	4.93	5.44
55			80.0	78.17	31.33	30.0	.937	4.58	24.6	1.940	6.81	7.33
56	4000	4000	70.0	69.59	60.39	60.0	.920	5.00	7.3	0.469	1.50	1.56
57			70.0	69.27	50.65	50.0	.931	4.97	10.9	0.804	2.35	2.50
58			70.0	69.02	40.81	40.0	.940	4.88	16.1	1.045	3.73	4.04
59			70.0	68.80	30.91	30.0	.947	4.75	22.0	1.220	5.67	6.09
60	4000	4000	60.0	59.70	50.28	50.0	.941	5.00	7.7	0.324	1.58	1.62
61			60.0	59.46	40.47	40.0	.949	4.96	11.9	0.549	2.60	2.73
62			60.0	59.26	30.58	30.0	.956	4.88	18.1	0.708	4.31	4.57
63	4000	4000	50.0	49.78	40.21	40.0	.957	5.00	8.1	0.216	1.67	1.71
64			50.0	49.60	30.34	30.0	.963	4.96	13.3	0.362	2.93	3.05
65	4000	4000	40.0	39.84	30.15	30.0	.968	5.00	8.6	0.139	1.79	1.83
66	4000	1000*	80.0	79.54	72.26	70.0	.728	5.00	6.7	0.550	1.35	1.51
67		*	80.0	79.15	64.01	60.0	.757	5.00	9.1	0.998	1.90	2.34
68		*	80.0	78.81	55.20	50.0	.787	4.94	12.6	1.356	2.77	3.64
69		*	80.0	78.53	45.96	40.0	.814	4.82	17.2	1.637	4.10	5.44
70		*	80.0	78.28	36.33	30.0	.839	4.67	22.2	1.853	5.85	7.33
71	4000	1000*	70.0	69.64	61.76	60.0	.788	5.00	6.9	0.411	1.42	1.56
72		*	70.0	69.34	53.03	50.0	.816	4.98	9.9	0.732	2.10	2.50
73		*	70.0	69.09	43.87	40.0	.841	4.91	14.3	0.978	3.23	4.04
74		*	70.0	68.87	34.35	30.0	.863	4.79	19.9	1.165	4.93	6.09
75	4000	1000*	60.0	59.73	51.33	50.0	.840	5.00	7.3	0.295	1.50	1.62
76		*	60.0	59.50	42.25	40.0	.862	4.97	11.0	0.514	2.37	2.73
77		*	60.0	59.30	32.82	30.0	.883	4.90	16.6	0.677	3.85	4.57
78	4000	1000*	50.0	49.79	40.99	40.0	.880	5.00	7.8	0.202	1.60	1.71
79		*	50.0	49.62	31.65	30.0	.898	4.97	12.4	0.346	2.72	3.05
80	4000	1000*	40.0	39.84	30.74	30.0	.910	5.00	8.3	0.132	1.73	1.83

*: calculations carried out with equations for laminar flow

$^+$: Temperature Polarization Coefficient; TPC = $(T_{fm}-T_{pm})/(T_{fb}-T_{pb})$

Table 4.5:
Calculated flux and selectivity as a function of hydrodynamic conditions and temperature difference for module II (w_{fbe} = 0.05)

nr.	Re_f [-]	Re_p [-]	T_{fb} [°C]	T_{fm} [°C]	T_{pm} [°C]	T_{pb} [°C]	TPC+ [-]	w_{fme} [%]	w_{pe} [%]	flux [g/m²s]	selectivity model [-]	selectivity VLE [-]
81	4000	4000	80.0	79.43	71.52	70.0	.792	5.00	6.8	2.130	1.39	1.52
82			80.0	78.96	62.65	60.0	.816	5.00	9.5	3.788	2.00	2.34
83			80.0	78.57	53.41	50.0	.839	4.92	13.3	5.061	2.97	3.64
84			80.0	78.24	43.89	40.0	.859	4.78	18.1	6.025	4.42	5.44
85			80.0	77.96	34.12	30.0	.877	4.61	23.1	6.741	6.22	7.33
86	4000	4000	70.0	69.56	61.17	60.0	.839	5.00	7.1	1.563	1.45	1.56
87			70.0	69.20	51.99	50.0	.861	4.98	10.3	2.736	2.20	2.50
88			70.0	68.91	42.54	40.0	.879	4.89	15.0	3.605	3.43	4.04
89			70.0	68.65	32.85	30.0	.895	4.76	20.7	4.251	5.23	6.09
90	4000	4000	60.0	59.66	50.88	50.0	.879	5.00	7.4	1.102	1.53	1.62
91			60.0	59.39	41.48	40.0	.895	4.96	11.4	1.897	2.46	2.73
92			60.0	59.16	31.86	30.0	.910	4.88	17.1	2.473	4.02	4.57
93	4000	4000	50.0	49.75	40.66	40.0	.909	5.00	7.9	0.746	1.63	1.71
94			50.0	49.54	31.10	30.0	.922	4.96	12.7	1.266	2.79	3.05
95	4000	4000	40.0	39.81	30.50	30.0	.931	5.00	8.4	0.484	1.75	1.83
96	4000	1000*	80.0	79.63	74.64	70.0	.499	5.00	6.1	1.416	1.23	1.51
97		*	80.0	79.27	68.66	60.0	.530	5.00	7.6	2.720	1.56	2.34
98		*	80.0	78.93	61.84	50.0	.570	4.99	9.8	3.917	2.07	3.64
99		*	80.0	78.60	54.18	40.0	.611	4.93	13.0	4.969	2.87	5.44
100		*	80.0	78.29	45.57	30.0	.654	4.81	17.3	5.875	4.13	7.33
101	4000	1000*	70.0	69.69	63.90	60.0	.579	5.00	6.4	1.133	1.29	1.56
102		*	70.0	69.39	57.05	50.0	.617	5.00	8.4	2.137	1.74	2.50
103		*	70.0	69.12	49.45	40.0	.656	4.96	11.4	2.998	2.48	4.04
104		*	70.0	68.86	41.00	30.0	.696	4.87	15.9	3.721	3.68	6.09
105	4000	1000*	60.0	59.74	53.15	50.0	.659	5.00	6.7	0.863	1.37	1.62
106		*	60.0	59.50	45.61	40.0	.695	4.99	9.4	1.583	1.98	2.73
107		*	60.0	59.28	37.32	30.0	.732	4.93	13.6	2.170	3.04	4.57
108	4000	1000*	50.0	49.79	42.51	40.0	.728	5.00	7.2	0.620	1.47	1.71
109		*	50.0	49.60	34.38	30.0	.761	4.98	10.7	1.108	2.30	3.05
110	4000	1000*	40.0	39.83	31.99	30.0	.784	5.00	7.8	0.421	1.60	1.83

*: calculations carried out with equations for laminar flow

+: Temperature Polarization Coefficient; TPC = $(T_{fm}-T_{pm})/(T_{fb}-T_{pb})$

Chapter 5:

ETHANOL/WATER SEPARATION BY MEMBRANE DISTILLATION. 2. EXPERIMENTAL RESULTS

A.C.M. Franken, J.A.M. Nolten, M.H.V. Mulder & C.A. Smolders

Summary

In chapter 4 a model for the separation of ethanol and water by membrane distillation has been developed. In this model VLE (Vapour-Liquid Equilibrium) data are combined with the effect of temperature polarization and concentration polarization.

In this chapter membrane distillation experiments with ethanol/water mixtures are described and the experimental selectivities and fluxes are compared with the calculated values. A good agreement between model and experiments was found.

5.1: Introduction

As explained in chapter 4, membrane distillation is a distillation process, in which the vapour pressure difference across the membrane causes vapour molecules to be transported through the pores of the membrane from the warm side (feed) to the cold side (permeate) of the membrane.

The applications of membrane distillation are mainly found in the separation of inorganic components in aqueous solutions and especially in those separations in which a high purity of the permeate (water) is desired (1-3).

As far as separation of aqueous mixtures of volatile organic components is concerned, membrane distillation is not a real alternative to conventional distillation. Therefore, applications of membrane distillation must be found in mixtures in which the feed cannot be heated to high temperatures (e.g. fermentation broths (4)). Also (small-scale) applications in which use can be made of waste heat or solar heat can be attractive.

In this chapter experiments with an ethanol/water mixture containing about 5 wt% ethanol (a typical composition for a fermentation broth) are described. The effect of hydrodynamic conditions and temperature difference

on flux and selectivity are measured. The experimental results are compared with the model calculations from the previous chapter (5).

5.2: Theory

The model that was developed to describe the transport mechanism of membrane distillation has been described in detail in chapter 4 (5). In this chapter only a brief qualitative description will be given.

As membrane distillation is in fact a special form of distillation, the basis for our model is formed by the vapour-liquid equilibria existing at the feed/membrane interface and at the permeate/membrane interface.

In order to describe the transport mechanism in membrane distillation it is not enough to know the temperatures of feed and permeate only. For the calculation of the permeate composition by means of VLE equations it is essential that the temperatures of the feed and the permeate at the liquid/membrane interfaces are known. Because of the occurence of temperature polarization the bulk temperatures, T_{fb} and T_{pb}, differ from the temperatures at the membrane interfaces T_{fm} and T_{pm}. T_{fm} and T_{pm} cannot be measured directly, but they can be calculated if the hydrodynamic conditions at both sides of the membrane are known.

The same hydrodynamic conditions are also used to calculate the effect of concentration polarization at the feed side of the membrane. As a result of the preferential permeation of ethanol through the membrane, its concentration at the liquid/membrane interface is decreased and consequently the concentration of the less permeable component (water) is increased.

As a result of both temperature and concentration polarization, the flux and the selectivity of the membrane distillation operation will be lower than expected on the basis of the applied driving forces.

5.3: Experimental

5.3.1: Apparatus

The apparatus on which the membrane distillation experiments were performed has been drawn schematically in figure 5.1.

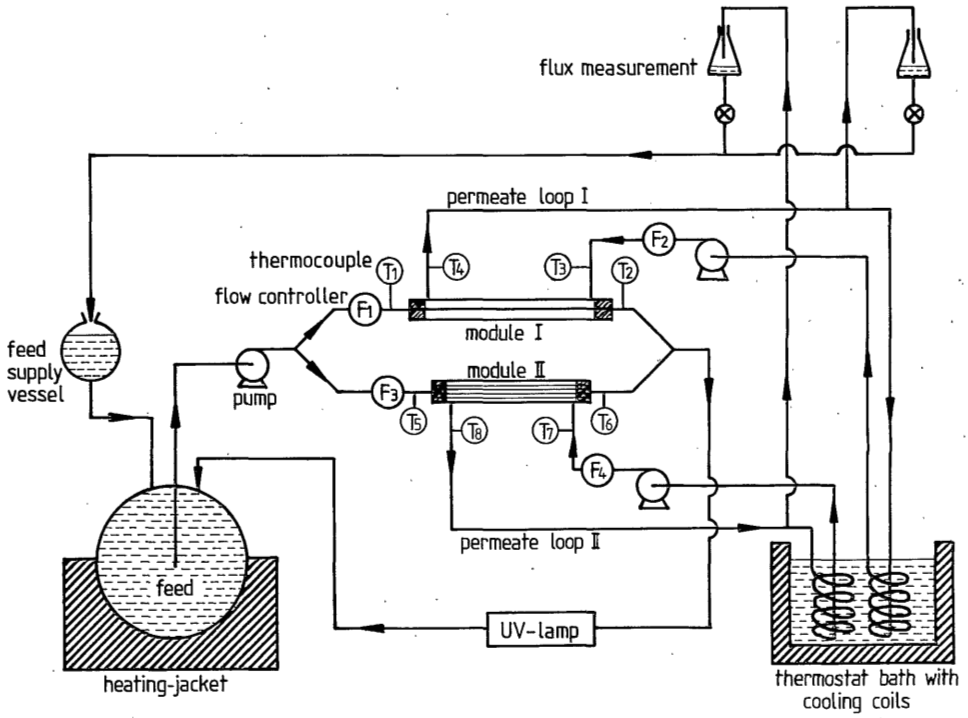

FIGURE 5.1: Membrane distillation set-up.

The feed mixture in the feed reservoir (containing about 5 wt% of ethanol in water) is heated by a heating-jacket and the temperature is kept constant by an Eurotherm temperature controller fitted with a proportional band. The feed is pumped from the vessel by an Iwaki MD 30-RZ magnet pump. At the outlet of the pump the feed stream is split into two streams: one stream being the feed for module I and the other the feed for module II. The flow of the feed through module I and module II is measured and controlled by Brooks flowmeters (F1 respectively F3). The feed mixture flows through the bore of the tubular membranes. The temperatures of the inlet and the outlet streams of the modules are measured with thermocouples (T1, T2, T5 and T6). The outlet streams of the modules are combined again and this stream flows along an UV-lamp to prevent growth of algae. From earlier measurements it is known that due to growth of algae a decline of flux and selectivity occurs (6). In this experimental set-up no decline of flux and selectivity was observed even after three months of operation. The feed stream is returned to the feed reservoir. As a result of permeation through the membranes the amount of feed is reduced. This reduction is supplied from the feed supply vessel. To avoid depletion of ethanol from the feed,

the feed supply vessel is filled with a mixture having about the same composition as obtained at the flux measurement points. The total volume of the feed side, including the feed reservoir, tubes and feed compartments of the modules, is about 3000 ml.

The permeate is pumped through Brooks flowmeters (F2 and F4) into the modules by Iwaki MD 30-RZ magnet pumps. The liquid at the permeate side flows at the outside of the tubular membranes. The temperatures of inlet and outlet streams are measured with thermocouples (T3, T4, T7 and T8). The permeate streams are circulated through cooling coils, which are placed in a thermostat-bath. The temperature at the permeate side is controlled by this thermostat-bath. The flux through the membranes is measured at two flux measurement points. When the flux is not measured, these points are connected to the feed supply vessel. In this way the depleted feed is returned directly. The total volume at the permeate side for both module I and module II is about 250 ml.

In contrast to the feed stream, the permeate streams of module I and module II are separate. In this way the permeate concentration of both modules can be determined individually. During the measurements the concentration at the feed side is kept as constant as possible (about 5 wt% ethanol in water) and changes in the permeate concentration are measured as a function of the temperature difference and the hydrodynamic conditions.

5.3.2: Cross-flow modules

Table 5.1: Characteristics of modules used, with capillary membranes.

Parameter	module I	module II
Type of membrane	V 8/2	S 6/1
Module length (L) (mm)	497	348
Module diameter (mm)	14.0	11.0
Membrane diameter outside (mm)	8.50	2.40
inside (mm)	5.50	1.70
Membrane thickness (δ_m) (mm)	1.50	0.35
Membrane conductivity k_m (W/mK)	0.048	0.048
Membrane constant C_m ($g/(m^2.s.mmHg)$)	0.00589	0.02127
Number of membranes in module	1	4
Feed flow	inside	inside
Permeate flow	outside	outside
Hydraulic diameter inside (Dh_f) (mm)	5.50	1.70
outside (Dh_p) (mm))	5.50	4.75

The experiments were carried out on two different crossflow-modules with capillary membranes in counter-current flow.

Microporous hydrophobic polypropylene membranes (Accurel obtained from Enka) were used in the membrane distillation experiments. The characteristics of the modules are listed in table 5.1.

5.3.3: Product analysis

Analysis of the binary solutions (consisting of ethanol of analytical grade and ultrafiltrated water) was conducted with a Carl-Zeiss refractometer. The samples were directly taken from the feed line and the permeate line.

5.3.4: Calculation parameters

The model calculations were carried out with mixtures of ethanol and water at different temperatures. The physical properties needed for the calculations are density (ρ), diffusion coefficient (D), thermal conductivity (k), heat capacity (C_p) and dynamic viscosity (μ). All these properties are described as a function of the composition and the temperature and are calculated iteratively.

The VLE data of the ethanol/water mixtures were obtained from the Dechema series (7).

5.4: Results and discussion

5.4.1: Experimental conditions

The experiments were carried out on cross-flow modules in counter-current flow and no additional heating or cooling is applied to the modules. This means that the temperature of an inlet stream differs from the temperature of its outlet stream and that the temperature is a function of the place in the module. In the model, however, the bulk temperatures of feed and permeate are considered constant, being the average temperatures. If the temperature difference between inlet and outlet stream is small in relation to the temperature difference between feed and permeate, this assumption is quite reasonable. On the other hand in cases in which low

Reynolds numbers are considered the use of average temperatures might not be correct and the experimental results might differ considerably from the calculated values.

In our model the effect of Knudsen flow was not considered. The maximum effect of Knudsen flow that theoretically can be expected for the separation of a mixture of ethanol and water is α_w of about 1.60. Since ethanol is the preferentially permeating component, an effect of Knudsen flow would decrease the calculated selectivity. Knowing that the pores of the microporous membranes used have an hydraulic radius of about 2 μm, it can be calculated that a separating effect of Knudsen flow is within the experimental error ($\alpha_w < 1.05$) [8].

Another effect which was not taken into account is the surface roughness of the membranes. The effect of a rough surface is that it works as a turbulence promotor. Therefore, the effect only exists for Re > 2000, which values only occur on the inside of the membranes (feed side) in our practical situation. As the mean height of the irregularities is in the order of magnitude of 2 μm for both membrane types and the Re number is less than 5000, the effect on the friction factor is within 5% as compared with smooth tubes [9]. This effect can be interpreted as an increase of the Re number with 5%. As it is shown in the previous chapter that an increase of the Re number in the turbulent region hardly has any effect on the selectivity (doubling of the Re number results in an increase of the selectivity with less than 5%), the effect of the surface roughness is negligible small.

Comparing the experimental results with the calculated ones, the error in the measurement of the liquid compositions should be considered. The error in the experimentally determined weight percentage ethanol for both feed and permeate is about 0.1 to 0.2 wt%. Especially the error in the feed concentration might lead to a considerable variation in selectivity. Because the feed concentration is also used in the model for the calculation of the weight percentage of ethanol at the permeate side, the latter value is also affected by the error in the experimental results.

As a result of the difference between inlet and outlet temperature the viscosity of the liquid changes also. This results in a change of the values of Reynolds, Prandtl and Schmidt numbers. These changes again affect the heat and mass transfer coefficients. Therefore, the effect of temperature and concentration polarization is a function of the place in the module, which has not been taken into account in the model.

Another point which was not taken into account is the effect of the flow at the outside of the capillary membranes. The hydraulic diameters are calculated for an ideal situation, in which the capillaries are considered to be rigid tubes at equal distances from each other. In the practical situation, however, the membranes are flexible and their positioning in the module is not as ideal as described above. Due to these experimental limitations, an effect of 'channeling' at the outside of the capillary membranes (permeate side) might not be excluded.

5.4.2: Normalized flux and selectivity

The experimental fluxes and selectivities are given in tables 5.2 to 5.5. These tables, as well as tables 5.6 to 5.9, are given as an appendix to this chapter.

All selectivities are defined as intrinsic selectivities. The calculation of this value proceeds according to the following formula:

$$\alpha = \left(\frac{w_{pe}}{1-w_{pe}}\right) / \left(\frac{w_{fme}}{1-w_{fme}}\right) \qquad (5.1)$$

In our experiments we have tried to keep the bulk temperatures of feed and permeate and the feed concentration as constant as possible. For the hydrodynamic conditions used, the target values were T_{fb} = 70°C, T_{pb} = 30°C and w_{fbe} = 0.05. As can be seen from tables 5.1 and 5.2 the experimental values differ sometimes quite a lot from the target values. This makes it very difficult to compare the results of the experiments with each other.

Therefore, all the experimental values of flux and selectivity are normalized to standard conditions. The normalization to standard conditions has been carried out on the basis of calculations with the developed model. The calculations were carried out for the actual experimental conditions and for the normalized conditions.

$$J_{norm} = J_{exp} \cdot \frac{J_{model,norm}}{J_{model,exp}} \qquad (5.2)$$

$$\alpha_{norm} = \alpha_{exp} \cdot \frac{\alpha_{model,norm}}{\alpha_{model,exp}} \qquad (5.3)$$

The reason why this procedure was prefered over changing the experi-

mental conditions after each experiment to the standard conditions is two-fold. In the first place the feed for both modules is supplied from the same vessel. This makes it difficult to control the temperature and the feed concentration very precisely.

The second reason is the fact that it takes quite a long time before the concentration at the permeate side becomes constant. Because the permeating vapour is directly condensed against the liquid at the permeate side, the composition of the permeating vapour cannot be determined unless steady-state conditions are reached. The time to achieve steady-state conditions can be calculated if the permeate side of the membrane is considered as a 'continuous stirred-tank vessel'. If it is assumed that the composition and the flux of the permeating vapour through the membrane are constant, the concentration as a function of time can be described by equation 5.4.

$$C_t = C^{\infty} \cdot \left(1 - \exp^{-(J.A.t/V)}\right) \qquad (5.4)$$

An equilibrium value is assumed to be reached when C_t is within 1% of the value C^{∞}. In this case the numerical value of the exponent should be about 5. The time, necessary to reach steady-state, can then be estimated from,

$$t = \frac{5.V}{J.A} \qquad (5.5)$$

In case of module I when a flux is assumed of 1 g/m^2s, it takes about 40 hours to reach the equilibrium value. Of course it must be remembered that equation 5.4 and 5.5 are only valid if the concentration of ethanol at the permeate side starts from zero. This was only the case when the first experiment was performed. If the concentration of ethanol at the permeate side already has a certain value (which is the steady-state value of the experiment that has just been performed), the time needed to reach the new steady-state value is much shorter.

Equations 5.4 and 5.5 were experimentally checked by performing an experiment of 15 days. It appeared that after 24 hours, no significant differences in the permeate composition could be determined.

Nevertheless, to be sure that the equilibrium value is actually reached, at least the time as calculated by equation 5.5 was taken. This calculation shows that the permeation experiment has to be continued during a few days after each variation of a parameter before measurements were performed.

Thus, the fact that it is very difficult to achieve the same feed concentration and the fact that the experiments are time-consuming are the reasons why the feed concentration and the temperatures were not changed to standard conditions for each new experiment.

5.4.3: Influence of hydrodynamic conditions

The experimental fluxes and selectivities for the two modules as a function of the hydrodynamic conditions are given in tables 5.2 and 5.3. The normalized values are given in tables 5.6 and 5.7 respectively. The normalized selectivities (both the experimental and the calculated ones) as a function of the Reynolds number at the feed side and permeate side are given in figures 5.2 and 5.3 respectively.

Comparing the experimental selectivities of tables 5.2 and 5.3 with the calculated selectivities, it can be seen that the agreement between model and experiment is good. Especially when it is taken into account that the model is not corrected for the actual experimental conditions (see paragraph 5.4.1) and that the model makes use of equations for laminar flow and turbulent flow which show a discontinuity at a Reynolds number of 2000. Also the fact that it is very difficult to determine the exact Re number at which the flow changes from laminar to turbulent makes it very difficult to choose the right flow regime. Therefore all the model calculations with Re numbers between 2000 and 3000 are carried out with equations for both turbulent flow and laminar flow.

The agreement between the experimental flux and the calculated flux is very good, especially if the feed temperature is 70°C and if the Re numbers at both feed and permeate side are maximal. This is not surprising because these measurements are used to determine the constant C_m, which is necessary to calculate the model flux (5).

The normalized selectivities as a function of the Re number at the feed side are given in figure 5.2 and the normalized selectivities as a function of the Re number at the permeate side are given in figure 5.3.

From both figures it can be seen that the agreement between model and normalized experiments is good, especially if high Re numbers are considered. From both figures and for both modules one sees that the deviation between model and experiment is largest if the lowest Re numbers at both feed and permeate side are considered.

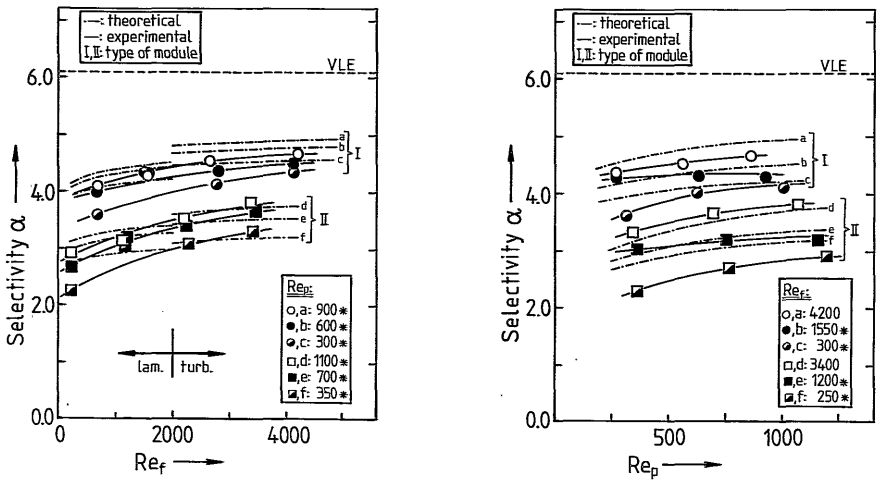

FIGURE 5.2: Normalized selectivity as a function of the Reynolds number at the feed side.

FIGURE 5.3: Normalized selectivity as a function of the Reynolds number at the permeate side.

These deviations can be caused by the fact that the accuracy of the experiments at these low Re numbers is insufficient. For instance, if the value of the Re number at the feed side is higher than 1000, then the temperature difference between inlet and outlet is lower than 5°C. But if the lowest Re_f numbers for module I are considered a temperature difference between inlet and outlet of about 10°C is found. The situation for module II is even worse since the temperature difference for those conditions is about 18°C. For the permeate side this temperature difference is 3°C maximally. This means that a comparison between model and experiment at low Re numbers (especially those at the feed side) should be considered very carefully.

It is not possible to calculate the concentration of ethanol at the permeate side, w_{pe}, directly from the intrinsic selectivity value and the bulk feed concentration of ethanol (equation 5.1). The fact that seemingly the selectivity is increased due to a decrease of w_{fme}, gives a false view into the separation potential of membrane distillation. To get a better insight into this separation potential at different hydrodynamic conditions, the weight fraction of ethanol obtained at the permeate side should

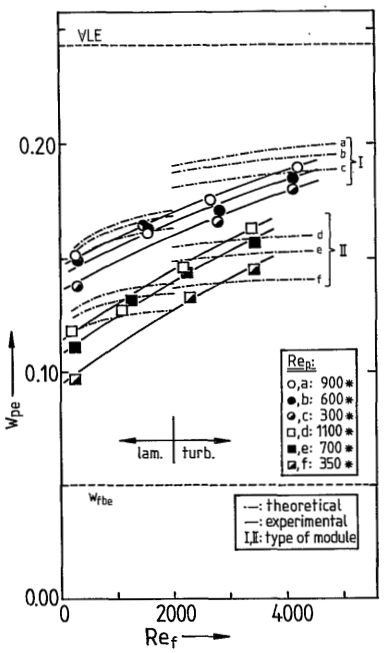

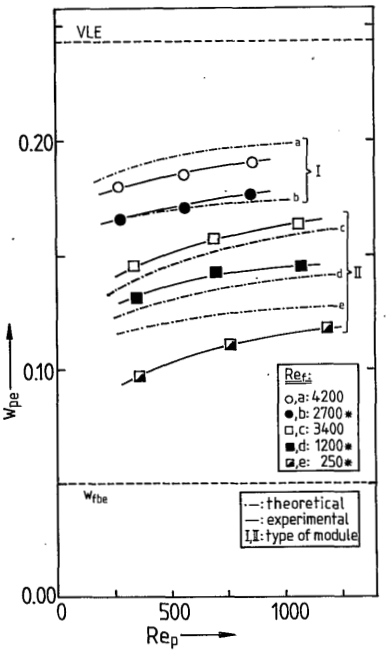

FIGURE 5.4: Weight fraction of ethanol at the permeate side (w_{pe}) as a function of the Reynolds number at the feed side.

FIGURE 5.5: Weight fraction of ethanol at the permeate side (w_{pe}) as a function of the Reynolds number at the permeate side.

be considered independently. In figure 5.4 and 5.5 values of w_{pe} (normalized to standard conditions) are given as a function of the Reynolds number.

Figure 5.4 shows that the discontinuity at Re = 2000 for the calculated curves of w_{pe} is very large compared to the discontinuity in α in figure 5.2. The reason for this effect is that the curves in figure 5.2 are calculated according to the intrinsic selectivity, which takes the effect of concentration polarization into account. The values of w_{pe} in the figures 5.4 and 5.5 are also calculated according to equation 5.1. In this case, however, it must be remembered that due to a decrease of the Re number both the intrinsic selectivity and w_{fme} decrease, thus intensifying the decrease of w_{pe}.

5.4.4: Influence of temperature difference

The experimental flux and selectivity as a function of the temperature

difference are given in tables 5.4 and 5.5. The normalized values are given in tables 5.8 and 5.9 respectively. In figures 5.6 and 5.7 the normalized weight fraction at the permeate side is given as a function of the bulk temperature difference between the feed side and permeate side.

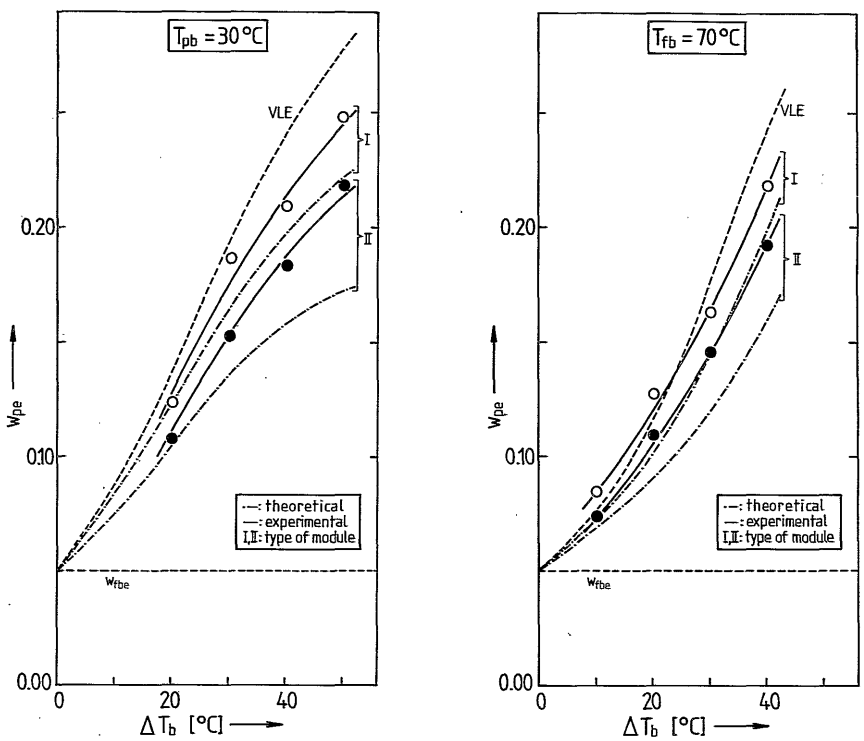

FIGURE 5.6: Weight fraction of ethanol at the permeate side (w_{pe}) as a function of the bulk temperature difference between feed and permeate, when T_{pb} is fixed at 30°C.

FIGURE 5.7: Weight fraction of ethanol at the permeate side (w_{pe}) as a function of the bulk temperature difference between feed and permeate, when T_{fb} is fixed at 70°C.

The tables and the figures show that the agreement between model and experiment is less good than in the case where the hydrodynamic conditions were varied. It appears that all the experimental results are higher than predicted by the model. In a rare case (see table 5.4, nr. 31 and 32) a higher selectivity than could be expected from the vapour-liquid equilibrium was obtained.

A possible explanation for the deviation between model and experiment

is found in the fact that the measurements are very sensitive to experimental errors. For instance, if experiment nr. 25 from table 5.4 is considered and if it is assumed that the value of w_{fbe} would be 2.9 instead of 2.8, then the value of the experimental selectivity would be reduced from 5.74 to 5.34. Another indication for the fact that the experimental results are very sensitive to measuring errors is found when for instance the normalized experiments nr. 66 and 69 are compared with each other. In the first case a normalized selectivity of 5.24 is obtained and in the second case a value of 5.53.

From figure 5.6 and 5.7 it is clear that the experimental curves have the same shape as the calculated curves. This phenomenon and the fact that the weight fraction of ethanol at the permeate side in case of module II is lower than for module I are in good agreement with the concepts of temperature and concentration polarization and provide a good indication that the model using vapour-liquid equilibria is correct.

The agreement between the calculated and experimental fluxes is good. This is not surprising as the model flux is calculated on the basis of the experiments in which the feed temperature is 70°C and the permeate temperature is 30°C. Although it was found by Schofield et al. (10) that the constant C_m used to calculate the flux is slightly temperature dependent, decreasing by about 3% with a 10°C increase in mean temperature, in our experiments no experimental evidence was found to support this. In fact, if this temperature dependency would be applied to the experiments listed in table 5.4 and 5.5, then the agreement between calculated and experimental flux would be worse in 75% of the cases and would improve in 25%.

5.5: Conclusions

The main conclusion that can be drawn is that a rather good agreement between theory and experiment was found and that the model can be used to predict fluxes and selectivities of membrane modules on the basis of a few simple experiments in which the membrane constant C_m has to be determined.

As far as the hydrodynamic conditions are concerned, it can be concluded that a higher flow velocity at both feed and permeate side gives higher selectivities and permeation rates. The conclusion, drawn in the previous chapter (5), that the selectivity and the flux hardly change any more once the flow becomes turbulent, is only partially confirmed by the

experimental results. From the experiments it can be concluded that the flux and the selectivity are still increasing even when a Reynolds number of 4000 at the feed side is measured. Therefore, the flow at **both** sides of the membrane should be fully turbulent to achieve an optimal separation. This means that (in most cases) a Reynolds number of at least 4000 is necessary.

Concerning the effect of temperature difference, it can be concluded that both flux and selectivity increase when the temperature difference increases and that a rather good agreement between the experimental results and the model was found.

5.6: Symbols

The symbols that are used in this chapter are conform the terminology of membrane distillation (11). Additional symbols or symbols which are defined in another way are marked with the *-symbol.

Latin symbols

A	membrane area	m^2	
C	concentration	kg/m^3	
C_m	membrane constant	$g/(m^2.s.mmHg)$	*
J	mass flux	kg/m^2s	
L	module length	mm	*
Re	Reynolds number	-	*
T	temperature	K	
t	time	s	
V	volume	m^3	
w	weight fraction	-	

Greek symbols

α	selectivity	-
δ	membrane thickness	mm
μ	liquid viscosity	Pa.s
ρ	density	kg/m^3

Subscripts

b	bulk

e	ethanol	*
exp	experimental	*
f	feed	
m	membrane	
norm	normalized	*
p	permeate	
t	time	
w	water	

Superscripts

∞	infinite	*

5.7: References

1. S.-I. Andersson, N. Kjellander & B. Rodesjö; Design and Field Tests of a New Membrane Distillation Desalination; Desalination 56 (1985) 345-354.
2. P.K. Weyl; Recovery of Demineralized Water from Saline Waters; US patent 3,340,186.
3. K. Schneider and T.J. van Gassel; Membrandestillation; Chemie Ingenieur Technik 56 (1984) 514.
4. M.H.V. Mulder & C.A. Smolders; Continuous Ethanol Production Controlled by Membrane Processes; Process Biochemistry, April 1986, 35-39.
5. A.C.M. Franken, M.H.V. Mulder & C.A. Smolders; Ethanol/Water Separation by Membrane Distillation. 1. Model; this thesis.
6. A.C.M. Franken, J.A.M. Nolten, M.H.V. Mulder & C.A. Smolders; Ethanol/Water Separation by Membrane Distillation: Effect of Temperature Polarization. In: B. Sedlacek & J. Kahovec (editors); Synthetic Polymeric Membranes, pages 531-540; de Gruyter, Berlin, 1987.
7. J. Gmehling & U. Onken; Vapour-liquid equilibrium data collection (aqueous-organic systems), volume I, part 1; Dechema, Frankfurt, 1977.
8. R. Marcel; Gas and Vapour Transport through Porous Media; lecture presented at "Summer school on membrane processes" at Cadarache, France, September 3 - 7, 1984.
9. W.J. Beek & K.M.K. Muttzall; Transport Phenomena; John Wiley, London - New York (1975).
10. R.W. Schofield, A.G. Fane & C.J.D. Fell; Heat and Mass Transfer in Membrane Distillation; Journal of Membrane Science 33 (1987) 299-313.
11. A.C.M. Franken & S. Ripperger; Terminology for Membrane Distillation; European Society for Membrane Science and Technology, January 1988 (given as an appendix to this thesis).

5.8: Appendix

Table 5.2:
Experimental flux and selectivity as a function of the hydrodynamic conditions for module I.

nr.	Re_f [-]	Re_p [-]	T_{fb} [°C]	T_{fm} [°C]	T_{pm} [°C]	T_{pb} [°C]	TPC+ [-]	w_{fbe} exp [%]	w_{fme} model [%]	w_{pe} model [%]	w_{pe} exp	flux model [g/m²s]	flux exp [g/m²s]	selectivity model [-]	selectivity exp [-]	selectivity VLE [-]
1	4360	890*	71.7	70.57	34.74	29.9	.857	4.5	4.33	18.5	17.7	1.258	1.277	5.01	4.75	6.24
2	4290	590*	71.6	70.47	35.45	30.0	.842	4.4	4.24	17.6	16.8	1.237	1.252	4.83	4.56	6.19
3	4310	290*	72.1	70.99	37.51	30.7	.809	4.4	4.26	16.7	16.1	1.233	1.227	4.51	4.31	6.11
4	2780	920*	71.7	70.12	34.89	30.2	.849	4.2	4.00	16.8	15.3	1.217	1.208	4.84	4.34	6.11
4a	2780*	970*	71.7	67.87	34.41	30.2	.806	4.2	3.72	15.0	15.3	1.077	1.208	4.56	4.68	6.11
5	2950	610*	71.7	70.21	35.71	30.4	.835	4.2	4.02	16.4	14.7	1.208	1.201	4.70	4.12	6.07
5a	2950*	650*	71.7	67.98	35.17	30.4	.794	4.2	3.75	14.7	14.7	1.071	1.201	4.44	4.43	6.07
6	2920	310*	71.6	70.14	37.16	30.7	.807	4.1	3.95	15.3	13.8	1.175	1.170	4.40	3.90	5.97
6a	2920*	330*	71.6	67.98	36.54	30.7	.769	4.1	3.71	13.9	13.8	1.046	1.170	4.18	4.16	5.97
7	1570*	1000*	68.4	64.39	32.94	29.3	.805	4.0	3.51	13.6	13.1	.901	1.070	4.35	4.15	5.80
8	1590*	720*	68.6	64.64	33.85	29.8	.794	3.7	3.29	12.4	12.1	.896	1.030	4.14	4.04	5.65
9	1550*	350*	68.9	64.99	35.56	30.5	.766	3.6	3.25	11.5	11.8	.886	1.014	3.88	3.98	5.52
10	280*	1160*	62.2	57.30	32.09	29.6	.773	3.6	3.26	10.5	10.3	.588	.754	3.50	3.41	4.74
11	300*	710*	61.8	57.10	32.27	29.4	.766	3.8	3.44	11.0	10.7	.579	.736	3.46	3.36	4.76
12	310*	350*	61.6	57.13	33.69	30.2	.747	4.0	3.67	10.9	10.0	.562	.719	3.22	2.91	4.60

*: calculations carried out with equations for laminar flow
+: Temperature Polarization Coefficient; TPC = $(T_{fm}-T_{pm})/(T_{fb}-T_{pb})$

Table 5.3:
Experimental flux and selectivity as a function of the hydrodynamic conditions for module II.

nr.	Re_f [-]	Re_p [-]	T_{fb} [°C]	T_{fm} [°C]	T_{pm} [°C]	T_{pb} [°C]	TPC+ [-]	w_{fbe} exp [%]	w_{fme} model [%]	w_{pe} model [%]	w_{pe} exp	flux model [g/m²s]	flux exp [g/m²s]	selectivity model [-]	selectivity exp [-]	selectivity VLE [-]
13	3470	1200*	70.7	69.43	42.28	31.7	.696	4.4	4.31	13.5	13.8	3.713	3.676	3.46	3.56	5.70
14	3510	780*	70.4	69.20	43.38	31.7	.667	4.4	4.32	12.8	13.3	3.568	3.593	3.26	3.40	5.66
15	3520	390*	71.2	70.05	46.66	32.6	.606	4.4	4.35	11.6	12.1	3.469	3.246	3.47	3.02	5.58
16	2260	1230*	70.1	68.39	41.71	31.6	.693	4.2	4.08	12.6	11.9	3.513	3.394	3.40	3.17	5.59
16a	2260*	1280*	70.1	65.32	40.43	31.6	.647	4.2	3.90	11.5	11.9	2.971	3.394	3.20	3.33	5.59
17	2310	820*	70.2	68.57	43.26	32.0	.663	4.1	4.01	11.7	11.4	3.427	3.271	3.17	3.08	5.50
17a	2310*	840*	70.2	65.60	41.89	32.0	.621	4.1	3.86	10.8	11.4	2.913	3.271	3.01	3.20	5.50
18	2360	410*	70.4	68.89	45.74	32.4	.609	4.0	3.95	10.5	10.1	3.274	2.941	2.84	2.74	5.42
18a	2360*	420*	70.4	66.05	44.23	32.4	.574	4.0	3.84	9.8	10.1	2.812	2.941	2.73	2.82	5.42
19	1160*	1300*	68.5	63.00	38.78	30.7	.641	4.0	3.67	10.7	10.0	2.648	2.592	3.15	2.92	5.51
20	1290*	880*	69.0	63.75	40.63	31.5	.616	3.7	3.47	9.6	9.4	2.646	2.557	2.94	2.89	5.35
21	1210*	440*	69.1	64.11	43.08	32.2	.570	3.6	3.48	8.7	8.9	2.529	2.342	2.65	2.71	5.19
22	200*	1410*	59.6	53.62	35.37	30.3	.623	3.6	3.43	8.2	7.6	1.478	1.288	2.53	2.31	4.21
23	240*	890*	60.5	54.73	36.63	30.6	.606	3.8	3.62	8.6	7.6	1.547	1.402	2.50	2.19	4.31
24	240*	420*	60.6	55.18	38.65	31.4	.566	4.0	3.85	8.5	6.9	1.483	1.314	2.30	1.85	4.20

*: calculations carried out with equations for laminar flow
+: Temperature Polarization Coefficient; TPC = $(T_{fm}-T_{pm})/(T_{fb}-T_{pb})$

Table 5.4:
Experimental flux and selectivity as a function of the temperature difference for module I.

nr.	Re_f [-]	Re_p [-]	T_{fb} [°C]	T_{fm} [°C]	T_{pm} [°C]	T_{pb} [°C]	TPC+ [-]	w_{fbe} exp [%]	w_{fme} model [%]	w_{pe} model [%]	w_{pe} exp	flux model [g/m²s]	flux exp [g/m²s]	selectivity model [-]	selectivity exp [-]	selectivity VLE [-]
25	5090	1150*	81.3	79.87	39.23	32.8	.838	2.8	2.71	12.4	13.8	1.855	2.064	5.07	5.74	6.50
26	4600	1140*	72.0	70.93	35.49	30.9	.862	2.8	2.74	11.5	12.1	1.230	1.228	4.59	4.89	5.69
27	4070	1140*	61.4	60.66	32.57	29.6	.883	3.0	2.96	10.4	11.8	.718	.696	3.82	4.39	4.51
28	3270	1100*	50.7	50.23	31.20	29.5	.897	4.4	4.37	11.4	11.4	.366	.350	2.82	2.82	3.18
29	4650	1110*	72.1	71.02	35.14	30.5	.862	3.0	2.93	12.4	13.7	1.246	1.252	4.71	5.27	5.83
30	4560	1510*	72.1	71.20	44.95	41.2	.850	3.7	3.66	10.8	12.1	1.070	1.099	3.19	3.62	3.90
31	4470	1970*	72.3	71.61	53.70	50.9	.837	3.9	3.90	8.1	10.3	.846	.907	2.18	2.83	2.55
32	4530	2040	72.4	71.94	61.12	60.3	.894	6.8	6.80	10.7	12.5	.593	.618	1.65	1.96	1.75
32a	4530	2040*	72.4	71.97	62.10	60.3	.816	6.8	6.80	10.3	12.5	.550	.613	1.57	1.96	1.75

*: calculations carried out with equations for laminar flow
+: Temperature Polarization Coefficient; TPC = $(T_{fm}-T_{pm})/(T_{fb}-T_{pb})$

Table 5.5:
Experimental flux and selectivity as a function of the temperature difference for module II.

nr.	Re_f [-]	Re_p [-]	T_{fb} [°C]	T_{fm} [°C]	T_{pm} [°C]	T_{pb} [°C]	TPC+ [-]	w_{fbe} exp [%]	w_{fme} model [%]	w_{pe} model [%]	w_{pe} exp	flux model [g/m²s]	flux exp [g/m²s]	selectivity model [-]	selectivity exp [-]	selectivity VLE [-]
33	4120	1520*	79.9	78.37	48.89	35.1	.658	2.8	2.79	8.7	11.0	5.375	5.888	3.32	4.30	5.86
34	3720	1440*	70.8	69.61	42.65	32.4	.702	2.8	2.79	8.5	9.8	3.644	3.638	3.24	3.79	5.21
35	3140	1410*	60.4	59.53	37.60	30.8	.741	3.0	2.98	8.0	9.0	2.136	1.915	2.85	3.22	4.13
36	2570	1310*	50.0	49.43	34.05	30.0	.769	4.4	4.38	9.5	9.5	1.101	.899	2.29	2.29	3.00
36a	2570*	1330*	50.0	48.23	33.74	30.0	.725	4.4	4.32	9.0	9.5	.999	.899	2.19	2.32	3.00
37	3670	1390*	70.9	69.68	42.58	32.2	.700	3.0	2.98	9.2	11.1	3.676	3.680	3.28	4.07	5.31
38	3620	1820*	71.3	70.31	50.58	42.3	.680	3.7	3.70	8.4	10.3	3.105	2.956	2.38	2.99	3.61
39	3620	2230	71.4	70.56	54.64	51.5	.800	3.9	3.90	7.5	8.5	2.695	2.238	2.00	2.29	2.39
39a	3620	2230*	71.4	70.68	57.52	51.5	.661	3.9	3.90	6.7	8.5	2.342	2.238	1.77	2.29	2.39
40	3480	2450	71.7	71.17	62.38	60.5	.785	6.8	6.80	9.9	10.5	1.747	1.297	1.50	1.61	1.68
40a	3480	2450*	71.7	71.26	64.14	60.5	.635	6.8	6.80	9.2	10.5	1.458	1.297	1.38	1.61	1.68

*: calculations carried out with equations for laminar flow
+: Temperature Polarization Coefficient; TPC = $(T_{fm}-T_{pm})/(T_{fb}-T_{pb})$

Table 5.6:
Normalized flux and selectivity as a function of the hydrodynamic conditions for module I.

nr.	Re_f [-]	Re_p [-]	T_{fb} [°C]	T_{fm} [°C]	T_{pm} [°C]	T_{pb} [°C]	TPC+ [-]	w_{fme} model [%]	w_{pe} model [%]	w_{pe} exp [%]	flux model [g/m²s]	flux exp [g/m²s]	selectivity model [-]	selectivity exp [-]	selectivity VLE [-]
41	4210	860*	70.0	68.92	34.57	30.0	.859	4.80	19.8	19.0	1.164	1.182	4.90	4.65	6.09
42	4140	560*	70.0	68.92	35.19	30.0	.843	4.81	19.4	18.5	1.153	1.167	4.77	4.49	6.09
43	4140	270*	70.0	68.95	36.43	30.0	.813	4.83	18.7	18.0	1.131	1.126	4.53	4.33	6.09
44	2660	850*	70.0	68.47	34.49	30.0	.850	4.74	19.4	17.6	1.135	1.127	4.83	4.31	6.09
44a	2660*	850*	70.0	66.37	34.11	30.0	.807	4.41	17.3	17.6	1.007	1.130	4.53	4.65	6.09
45	2830	560*	70.0	68.56	35.10	30.0	.837	4.76	19.1	17.1	1.130	1.123	4.73	4.12	6.09
45a	2830*	560*	70.0	66.47	34.67	30.0	.795	4.43	17.1	17.0	1.003	1.125	4.45	4.43	6.09
46	2790	280*	70.0	68.58	36.27	30.0	.808	4.77	18.4	16.6	1.109	1.104	4.50	3.97	6.09
46a	2790*	280*	70.0	66.53	35.75	30.0	.769	4.47	16.6	16.5	.988	1.106	4.25	4.23	6.09
47	1560*	920*	70.0	65.78	33.91	30.0	.797	4.35	16.9	16.2	.975	1.158	4.48	4.26	6.09
48	1560*	630*	70.0	65.81	34.39	30.0	.786	4.37	16.7	16.3	.969	1.115	4.39	4.28	6.09
49	1510*	300*	70.0	65.86	35.49	30.0	.759	4.41	16.2	16.6	.954	1.091	4.20	4.32	6.09
50	300*	1000*	70.0	63.41	33.44	30.0	.749	4.18	15.5	15.1	.852	1.093	4.19	4.08	6.09
51	320*	620*	70.0	63.60	33.99	30.0	.740	4.21	15.4	15.0	.853	1.085	4.12	4.00	6.09
52	330*	310*	70.0	63.76	34.96	30.0	.720	4.26	15.0	13.8	.847	1.084	3.97	3.58	6.09

*: calculations carried out with equations for laminar flow
+: Temperature Polarization Coefficient; TPC = $(T_{fm}-T_{pm})/(T_{fb}-T_{pb})$

Table 5.7:
Normalized flux and selectivity as a function of the hydrodynamic conditions for module II.

nr.	Re_f [-]	Re_p [-]	T_{fb} [°C]	T_{fm} [°C]	T_{pm} [°C]	T_{pb} [°C]	TPC+ [-]	w_{fme} model [%]	w_{pe} model [%]	w_{pe} exp [%]	flux model [g/m²s]	flux exp [g/m²s]	selectivity model [-]	selectivity exp [-]	selectivity VLE [-]
53	3380	1060*	70.0	68.70	40.76	30.0	.698	4.86	15.9	16.3	3.703	3.666	3.70	3.80	6.09
54	3440	690*	70.0	68.76	42.02	30.0	.668	4.87	15.2	15.7	3.614	3.640	3.49	3.64	6.09
55	3420	340*	70.0	68.82	44.27	30.0	.614	4.90	13.9	14.5	3.435	3.214	3.14	3.30	6.09
56	2210	1070*	70.0	68.21	40.54	30.0	.692	4.81	15.6	14.7	3.608	3.485	3.66	3.42	6.09
56a	2210*	1070*	70.0	65.08	39.30	30.0	.645	4.53	14.0	14.5	3.034	3.466	3.42	3.56	6.09
57	2250	700*	70.0	68.29	41.78	30.0	.663	4.83	15.0	14.6	3.526	3.365	3.47	3.36	6.09
57a	2250*	700*	70.0	65.23	40.45	30.0	.620	4.58	13.5	14.3	2.981	3.348	3.26	3.48	6.09
58	2290	350*	70.0	68.40	43.97	30.0	.611	4.87	13.8	13.4	3.367	3.024	3.13	3.01	6.09
58a	2290*	350*	70.0	65.48	42.47	30.0	.575	4.66	12.7	13.1	2.875	3.007	2.99	3.08	6.09
59	1150*	1150*	70.0	64.13	38.78	30.0	.634	4.48	13.7	12.8	2.886	2.824	3.38	3.14	6.09
60	1250*	750*	70.0	64.39	39.92	30.0	.612	4.54	13.3	13.1	2.857	2.760	3.24	3.18	6.09
61	1180*	360*	70.0	64.57	41.90	30.0	.567	4.62	12.5	12.8	2.743	2.539	2.96	3.03	6.09
62	220*	1190*	70.0	61.12	37.65	30.0	.587	4.40	12.7	11.8	2.428	2.116	3.17	2.89	6.09
63	260*	760*	70.0	61.68	38.80	30.0	.572	4.46	12.5	11.1	2.446	2.217	3.07	2.67	6.09
64	260*	360*	70.0	62.05	40.73	30.0	.533	4.56	11.9	9.7	2.375	2.104	2.83	2.25	6.09

*: calculations carried out with equations for laminar flow
+: Temperature Polarization Coefficient; TPC = $(T_{fm}-T_{pm})/(T_{fb}-T_{pb})$

Table 5.8:
Normalized flux and selectivity as a function of the temperature difference for module I.

nr.	Re_f [-]	Re_p [-]	T_{fb} [°C]	T_{fm} [°C]	T_{pm} [°C]	T_{pb} [°C]	TPC+ [-]	w_{fme} model [%]	w_{pe} model [%]	w_{pe} exp [%]	flux model [g/m²s]	flux exp [g/m²s]	selectivity model [-]	selectivity exp [-]	selectivity VLE [-]
65	4770	800*	80.0	78.50	36.82	30.0	.834	4.71	22.2	24.8	1.865	2.075	5.79	6.67	7.33
66	4240	860*	70.0	68.93	34.57	30.0	.859	4.81	19.8	20.9	1.165	1.163	4.90	5.24	6.09
67	3760	940*	60.0	59.27	32.87	30.0	.880	4.89	16.5	18.7	.674	.654	3.84	4.46	4.57
68	3170	1070*	50.0	49.55	31.61	30.0	.897	4.96	12.4	12.4	.344	.329	2.71	2.71	3.05
69	4240	860*	70.0	68.93	34.57	30.0	.859	4.81	19.8	21.8	1.165	1.170	4.90	5.53	6.09
70	4290	1320*	70.0	69.13	43.57	40.0	.852	4.91	14.5	16.3	.988	1.015	3.29	3.76	4.04
71	4220	1830*	70.0	69.36	52.54	50.0	.841	4.98	10.1	12.8	.749	.803	2.15	2.81	2.50
72	4610	2240	70.0	69.64	60.61	60.0	.903	5.00	7.3	8.5	.462	.481	1.49	1.77	1.56
72a	4610	2240*	70.0	69.67	61.41	60.0	.826	5.00	7.1	8.6	.429	.477	1.44	1.78	1.56

*: calculations carried out with equations for laminar flow
+: Temperature Polarization Coefficient; TPC = $(T_{fm}-T_{pm})/(T_{fb}-T_{pb})$

Table 5.9:
Normalized flux and selectivity as a function of the temperature difference for module II.

nr.	Re_f [-]	Re_p [-]	T_{fb} [°C]	T_{fm} [°C]	T_{pm} [°C]	T_{pb} [°C]	TPC+ [-]	w_{fme} model [%]	w_{pe} model [%]	w_{pe} exp [%]	flux model [g/m²s]	flux exp [g/m²s]	selectivity model [-]	selectivity exp [-]	selectivity VLE [-]
73	3920	1010*	80.0	78.26	45.51	30.0	.655	4.80	17.3	21.8	5.872	6.432	4.13	5.52	7.33
74	3440	1050*	70.0	68.72	40.80	30.0	.698	4.86	15.9	18.3	3.704	3.698	3.69	4.38	6.09
75	2930	1130*	60.0	59.08	37.03	30.0	.735	4.92	13.7	15.3	2.157	1.934	3.06	3.49	4.57
76	2520	1250*	50.0	49.43	34.08	30.0	.767	4.97	10.8	10.8	1.106	.903	2.31	2.32	3.05
76a	2520*	1250*	50.0	48.23	33.78	30.0	.722	4.90	10.2	10.8	1.002	.902	2.21	2.35	3.05
77	3440	1050*	70.0	68.72	40.80	30.0	.698	4.86	15.9	19.2	3.704	3.708	3.69	4.67	6.09
78	3440	1560*	70.0	68.97	48.42	40.0	.685	4.95	11.9	14.6	3.072	2.925	2.59	3.28	4.04
79	3460	2035	70.0	69.16	53.21	50.0	.798	4.98	9.8	11.0	2.582	2.144	2.07	2.37	2.50
79a	3460	2035*	70.0	69.27	55.94	50.0	.667	5.00	8.8	11.1	2.261	2.161	1.82	2.36	2.50
80	3570	2640	70.0	69.54	61.56	60.0	.798	5.00	7.0	7.4	1.496	1.111	1.42	1.53	1.56
80a	3570	2640*	70.0	69.62	63.14	60.0	.648	5.00	6.6	7.5	1.250	1.112	1.33	1.54	1.56

*: calculations carried out with equations for laminar flow
+: Temperature Polarization Coefficient; TPC = $(T_{fm}-T_{pm})/(T_{fb}-T_{pb})$

Chapter 6:

PERVAPORATION PROCESS USING A THERMAL GRADIENT AS THE DRIVING FORCE

A.C.M. Franken, M.H.V. Mulder & C.A. Smolders

Summary

A new process design for pervaporation is described in which a composite membrane, consisting of a selective hydrophilic toplayer and a microporous hydrophobic sublayer, is used (1). The feed mixture is brought into contact with the hydrophilic layer. At the permeate side of the membrane a permeate-absorbing liquid is brought into contact with the porous sublayer. It is essential that the liquid at the permeate side does not penetrate into the pores of the hydrophobic membrane.

The driving force for this process is caused by the thermal gradient that exists between the warm feed side of the membrane and the cold permeate side.

In this design, the equipment generally needed in conventional pervaporation processes to produce a reduced partial pressure at the permeate side and to condense the permeating vapour is no longer necessary. In addition, this design permits recovery of most of the heat from the permeated condensate.

6.1: Introduction

Pervaporation is a membrane process in which a liquid is in direct contact with a dense polymer film (feed side) and in which the permeating product is removed as a vapour at the other side of this film (permeate side) by applying a reduced partial pressure. In most cases this reduced partial pressure is achieved either by creating a vacuum or by employing a sweeping gas.

Pervaporation can be used to separate liquids which are difficult to separate by distillation such as azeotropic mixtures and mixtures with close boiling points. Although some research is going on in the field of separations of hydrocarbons (2-7), most of the research is concentrated on aque-

ous/organic mixtures (7-15). Especially for the dehydration of organic mixtures pervaporation seems to be a promising technique (7-14). Within this field the separation of ethanol/water mixtures is the subject on which most of the research has been focussed (8,9,12,13,15). So far, the only commercial application of the pervaporation process is the dehydration of organic solvents, especially of alcohols, using PVA membranes (16,17).

The separation potential of pervaporation mixtures of organic components and water as well as for non-aqueous organic mixtures is definitely promising in spite of the fact that pervaporation is a relatively complex process compared to other membrane processes such as reverse osmosis. Rautenbach and Albrecht (3,4) state that the specific costs of pervaporation will always be high, because:

- the process requires a heat transfer interface, since the evaporation enthalpy necessary for the phase change of the permeate has to be supplied;
- the modules must be designed for a low pressure drop at the permeate side because the principle of pervaporation is very sensitive to varying permeate pressures.

In this chapter a new process design using a thermal gradient as the driving force is described which minimizes the disadvantages as described above.

6.2: Background

Thermally driven membrane processes are known for more than a century. The first experiments, in which transport of gases as a result of a temperature difference was observed, were carried out by Feddersen in 1873 (18). Lippmann (in 1907) was the first who studied the transport of a liquid across a membrane which separated two solutions of identical composition but different temperatures (18). These processes, which are known as thermo-osmosis, are generally characterized by small solvent fluxes and low selectivities whereas the energy-input is quite large. This explains why thermo-osmosis never has been of great practical interest.

The renewed interest for thermally driven membrane processes has been generated by a relatively new process, **membrane distillation.** Membrane distillation is a distillation process in which two aqueous liquids with

different temperatures are separated by a microporous hydrophobic membrane. In this process the pores of the microporous membrane, which are not wetted by the liquid mixtures at the feed side or the permeate side, act as a vapour phase. The vapour pressure difference ΔP_v, resulting from the temperature difference ΔT across the membrane, causes vapour molecules to be transported from the warm feed side to the cold permeate side.

Membrane distillation is generally used for the production of pure water from aqueous solutions of inorganic material (for instance, desalination of sea water). In contrast with thermo-osmosis, membrane distillation has relatively high fluxes and good selectivities (19,20).

The transport mechanism of membrane distillation involves three steps:

1. evaporation at the feed side of the membrane;
2. transport of the vapour through the pores of the hydrophobic membrane;
3. condensation of the vapour at the permeate side of the membrane.

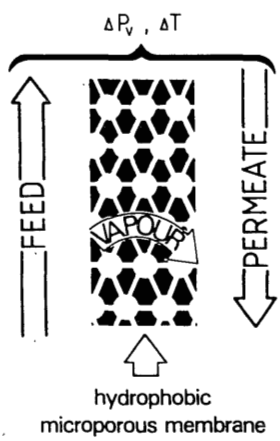

FIGURE 6.1: Membrane distillation.

On the basis of this transport mechanism, it can be understood that the separation mechanism of membrane distillation is formed by the vapour-liquid equilibrium. This also means that the maximum selectivity that can be obtained by membrane distillation is given by this vapour-liquid equilibrium. If a solution of an inorganic salt in water is used only water will pass through the membrane. On the other hand, if a solution of two (or more) volatile components is used then the vapour-liquid equilibrium of this solution determines the selectivity.

The fact that the selectivity of the membrane distillation operation is

determined by the vapour-liquid equilibrium indicates the limited possibilities for the treatment of solutions with several volatile components. Membrane distillation is not a real alternative for distillation, because it cannot be used in difficult separation problems (such as azeotropic mixtures).

Pervaporation processes are known since the beginning of this century and the term 'pervaporation' was introduced in 1917 by Kober (21). The interest in pervaporation processes increased during the 'seventies'. One of the possible alternatives of fossile energy sources is the use of ethanol as fuel. The best known process for rectifying ethanol is distillation. A more economic alternative for the azeotropic distillation of ethanol is pervaporation (17). In pervaporation the product is removed as a vapour at the permeate side by applying a reduced partial pressure. This can be achieved by creating a vacuum or by employing a sweeping gas (figure 6.2).

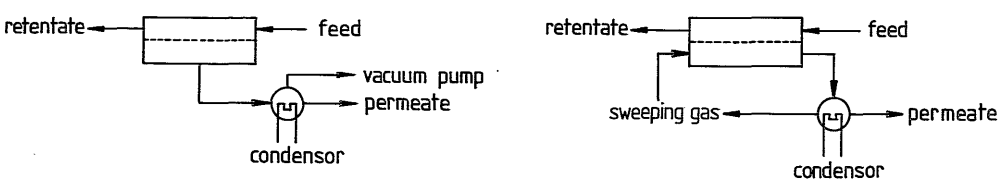

FIGURE 6.2: Pervaporation with downstream vacuum or sweeping gas.

In vacuum operation only a small pressure loss can be allowed at the permeate side, since an increase in partial downstream pressure directly influences flux and selectivity negatively. Vacuum operation is always to be regarded as critical, since large apparatus volumes are necessary, leakage problems may appear, oxygen might diffuse into the apparatus which leads to oxidation, etc. Furthermore, rather expensive equipment is necessary to generate this vacuum.

Application of a sweeping gas downstream does not involve the problems of vacuum apparatus. Nevertheless, the use of sweeping gas and a condensor is technically very costly and, moreover, because of the lower temperature level needed in the condensor, even partial recovery of the heat of evaporation needed for pervaporation is usually not possible.

The transport mechanism of pervaporation essentially involves the following steps:

1. selective sorption of components of a liquid mixture into the membrane at the feed side;
2. selective diffusion through the membrane;
3. desorption into a vapour phase at the permeate side.

In contrast to membrane distillation, the selectivity of the pervaporation process is not determined by the vapour-liquid equilibrium of the liquid mixture, but by the choice of the polymeric material. The selectivity towards a liquid mixture is determined by selective sorption into the membrane and selective diffusion through the membrane. This means that pervaporation can be used to separate organic liquids which are difficult to separate by distillation.

Although in pervaporation a reduced partial pressure at the permeate side can also be achieved by a temperature difference between the feed side and the permeate side of the membrane, this method is not commonly used. In literature this has only been described by Aptel et al. in a membrane operation which was called **'thermo-pervaporation'** (7). The thermo-pervaporation apparatus essentially consists of a pervaporation membrane (supported at the downstream side by a sintered stainless steel plate), which separates the hot liquid feed at the upstream side and a downstream compartment with a cold wall. The liquid that permeates through the membrane evaporates, diffuses through the downstream compartment and condenses against the cold wall. The condensed permeate is drawn off for storage in the container.

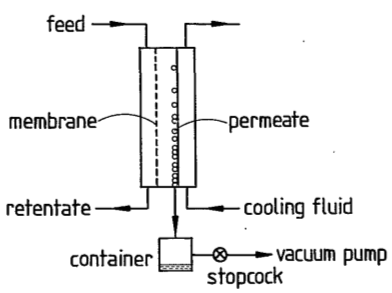

FIGURE 6.3: Thermo-pervaporation apparatus.

Although Aptel et al. claim that the thermo-pervaporation operation presents several advantages over classical pervaporation no practical application of this system has been developed yet. The fact that the results

obtained with thermo-pervaporation are difficult to interpret might be the reason that this membrane operation is not mentioned in literature any more (22).

6.3: Description of the thermally driven pervaporation process

A new process design using a thermal gradient as the driving force has been developed. In this design a composite membrane consisting of a dense permselective hydrophilic toplayer and a hydrophobic microporous sublayer is used. The warm liquid feed is brought in direct contact with the permselective toplayer and the cold permeate-absorbing liquid is brought in direct contact with the porous sublayer at the downstream side of the composite membrane.

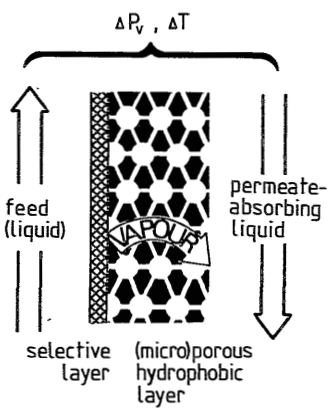

FIGURE 6.4: Pervaporation process using a thermal gradient as the driving force.

The **transport mechanism** of this pervaporation process essentially consists of the following five steps:

1. selective sorption of components of a liquid mixture into the toplayer of the membrane at the feed side;
2. selective diffusion through the toplayer of the membrane;
3. desorption into a vapour phase at the interface of the selective toplayer and the microporous sublayer;
4. transport of vapour through the pores of the hydrophobic sublayer of the membrane;

5. condensation of vapour at the downstream side of the membrane.

In this process the first three steps are identical to the transport mechanism in a conventional pervaporation process which makes use of vacuum or sweeping gas. Furthermore, it can be seen that step 4 and 5 of this mechanism resemble the last two steps of a membrane distillation operation. In fact all water-selective membranes that have been developed for pervaporation processes in general can be used as a permselective toplayer in this specific pervaporation design. The difference between membranes developed for a conventional pervaporation process and this specific design is that a hydrophobic porous sublayer is necessary. However, hydrophobicity of the porous sublayer is not the factor which determines the feasibility of this pervaporation process. The only restriction is that the permeate-absorbing liquid on the downstream side of the membrane **should not penetrate** into the pores of the porous sublayer.

During stationary operation the permeate-absorbing liquid on the downstream side has the same composition as the permeate. Although it is not necessary that the permeate-absorbing liquid has the same composition as the permeate, it is preferable. Simple calculations show that the selectivity of the process alters in such a way that an equilibrium value of the composition of the permeate-absorbing liquid is persued.

The **driving force** for this process is a vapour pressure difference which results from the temperature difference across the membrane. In figure 6.5 the temperature profile and the corresponding vapour pressure profile across the composite membrane are given schematically.

The **temperature profile** across the membrane is established by conductance of heat, by transport of heat through molecules and by evaporation/condensation at the membrane/liquid interfaces. In this temperature profile six steps can be distinguished:

1. transport of heat from the bulk of the feed solution to the membrane;
2. transport of heat through the non-porous toplayer of the membrane;
3. evaporation of the permeating components;
4. transport of heat through the porous sublayer of the membrane;
5. condensation of the permeating components;
6. transport of heat from the membrane surface to the bulk of the permeate-absorbing liquid.

Step 1 and 6 (transport of heat in a flowing liquid) are both influenced by the same parameters. The heat transfer coefficient, h, is influenced

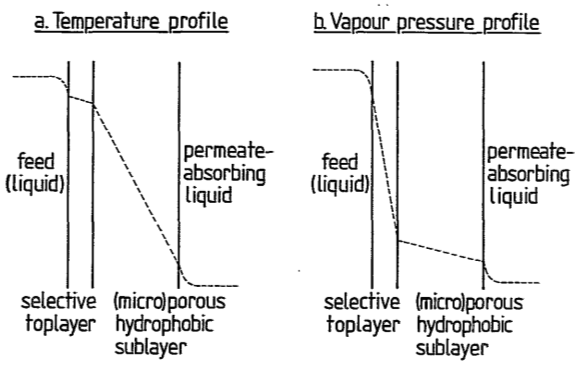

FIGURE 6.5: Temperature profile (a) and partial vapour pressure profile (b) across a membrane.

among others by the temperature level and module parameters, but mainly by the velocity of the flowing liquid.

In the non-porous toplayer of the membrane heat transfer mainly takes place by conductance. Also heat transfer through the permeating liquid takes place, but this is of minor importance.

The heat needed for the evaporation of the permeate has to be supplied by the liquid feed and the heat of condensation is directly supplied to the permeate-absorbing liquid.

Heat transfer by conductance through the porous sublayer has a lower value than the heat transfer by conductance through the non-porous toplayer. Because of the high porosity of the sublayer (in case of Accurel membranes the overall porosity is about 80%), this layer acts as a thermally insulating layer. The effect of the heat transfer by conductance can be illustrated by means of a resistance model as given in figure 6.6.

The heat resistance is given as the membrane thickness divided by the thermal conductivity of the membrane, δ_m/k_m. The heat resistance of the porous sublayer can be calculated by means of the the following formula:

$$(\delta_{sub}/k_{sub}) = \delta_{sub}/(\varepsilon.k_{air} + (1-\varepsilon).k_{PP})) \qquad (6.1)$$

Knowing that k_{air} = 0.02 W/m°C and k_{PP} = 0.18 W/m°C it can be calculated that k_{sub} has a value of about 0.05 W/m°C. If this value is compared with the value of the thermal conductivity of the swollen toplayer (k_{top} = 0.40 - 0.45 W/m°C) and if it is considered that the sublayer is much thicker than

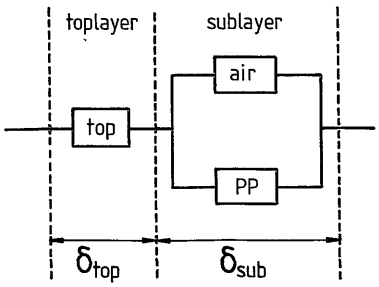

FIGURE 6.6: Heat resistance model.

the toplayer, it can be seen that the heat resistance of the porous sublayer is much higher. For example, if the thickness of the porous sublayer is 100 μm and the thickness of the toplayer is 10 μm, it can be calculated that the heat resistance of the porous sublayer is about 80 times the heat resistance of the swollen toplayer. Because no accumulation of heat occurs, the heat flux through the toplayer is equal to the heat flux through the sublayer. Therefore, the temperature difference across the sublayer is about 80 times higher than the temperature difference across the toplayer.

This phenomenon is very favourable for the separation mechanism of the membrane operation under study. This can be explained by means of figure 6.5b, in which the partial vapour pressure of the components across the membrane is described. The partial vapour pressures at both membrane surfaces are given by the temperatures of the feed solution and the permeate-absorbing liquid respectively. Because the transport of the vapour through the porous sublayer is much faster than the transport of the liquid through the non-porous toplayer, it can be concluded that the vapour leaving the non-porous toplayer is immediately drawn away and transported through the pores of the sublayer. This means that the vapour pressure profile across the porous sublayer is rather flat, whereas the profile across the toplayer is very steep.

Comparing the temperature profile and the vapour pressure profile the following conclusions can be drawn:

- no condensation of permeate will take place inside the pores of the sublayer because the vapour pressure at any point in the membrane is lower than the maximum vapour pressure corresponding to the temperature that exists at that specific point in the membrane;
- the vapour pressure difference across the toplayer of the membrane determines the flux and selectivity of the membrane. If this vapour pressure

difference increases, both flux and selectivity will increase.

Compared to the conventional pervaporation processes this thermally driven pervaporation process has the following **advantages:**

- the equipment costs are lower. The thermally driven pervaporation process can be performed without the equipment needed for vacuum generation or sweeping gas circulation. Also special equipment for the condensation of the vapours and pipelines leading to these condensors are not necessary;
- the transfer of latent heat of vaporization to the evaporation surface (the membrane) is an integrated part of the process. In the thermally driven pervaporation process the heat which provides the driving force of the process is also used for the evaporation of the permeating components;
- lateral mixing of the permeate in the vapour phase does not occur. This means also that no lateral mixing of heat takes place and that a temperature gradient along the membrane can be established. If the process is conducted in counter-current flow a maximum driving force across the membrane will occur at any place in the module;
- when the process is conducted in counter-current flow, recovery of most of the heat of condensation, which is transfered to the permeate-absorbing liquid, is possible. For example, the permeate-absorbing liquid leaving the module can be used for preheating the feed before it enters the module. This is possible because the permeate-absorbing liquid leaving the module can attain a higher temperature than the feed outlet.
- the process is no longer sensitive to downstream pressure losses;
- the diffusion path for the permeating vapour is very short, since it corresponds approximately to only the thickness of the porous second membrane layer;

In general the major advantage of this thermally driven pervaporation process over a conventional pervaporation process is that the membrane process as a whole can be simplified because of the substantially simpler process design.

Like any other new process, this new mode of pervaporation also has its **disadvantages.** Compared to the conventional pervaporation the disadvantages are:

- the permeate-absorbing liquid should not penetrate into the pores of the porous sublayer. This means that the permeate-absorbing liquid must have

a surface tension which is higher than the critical surface tension (23). In practice, this means that only aqueous solutions or solutions of DMSO can be used as a permeate-absorbing liquid if polypropylene membranes are used;

- the flux and selectivity are lower than the intrinsic values that can be reached with conventional pervaporation in which a low vacuum (< 100 Pa) is applied. In thermally driven pervaporation the vapour pressure of the permeate-absorbing liquid is determined by its temperature.

The second disadvantage mentioned above is in fact more an academic problem. In practical applications a vacuum as low as 100 Pascal is not used, because the costs of such a low pressure are much too high. In fact, commercial pervaporation installations make use of a vacuum pump to remove inert gases at the downstream side. Then the pump is disconnected and a condensor is used to maintain the low vapour pressure. In these cases the temperature of the condensor determines the partial vapour pressure, whereas in case of thermally driven pervaporation the temperature of the permeate-absorbing liquid determines the partial vapour pressure.

A typical field of **application** for thermally driven pervaporation is dehydration of organic liquids with a low water content. To prevent wetting of the porous membrane layer by the permeate, the dense toplayer must have a high intrinsic selectivity towards water. Dehydration of mixtures of ethanol/water or acetic acid/water are the best known examples of mixtures that can be separated by this process.

6.4: Experimental

In our investigations, both flat and capillary hydrophobic microporous polypropylene membranes (Accurel, obtained from Enka AG) were used as a sublayer. The flat membranes have a thickness of about 160 µm and the capillary membranes (type R 6/1) have a thickness of about 300 µm.

Three polymers have been used for the dense toplayer: cellulose acetate (Eastman CA 398-3-5), polysulfone (Union Carbide P 3500) and poly(vinyl alcohol) (Aldrich, M_w = 126,000, degree of saponification: 98%). CA and PSf were dissolved in a suitable solvent of analytical grade. Using method 3 for the production of the composite membrane, CA was dissolved in DMSO. PVA was dissolved in ultrafiltrated water.

There are a number of methods to deposit a selective layer onto a microporous membrane. In our investigations the following four methods have been used:

1. casting of a polymer solution onto a glass plate and subsequent evaporation of the solvent;
2. casting of a polymer solution onto a glass plate and subsequent coagulation in a non-solvent bath;
3. casting of a polymer solution onto the microporous sublayer directly;
4. dipcoating ('evaporation-deposition' method (24)).

In the first and second method the remaining homogeneous film is sandwiched with the microporous Accurel membrane to form a bi-layer membrane, which is clamped into the pervaporation cell.

In the third and fourth method it is essential that the solvent in which the polymer is dissolved should not penetrate into the pores of the membrane. In our investigations DMSO and water were used as a solvent.

The composite membranes were tested using both a conventional pervaporation cell (figure 6.7) and a cell suitable for thermally driven pervaporation (figure 6.8).

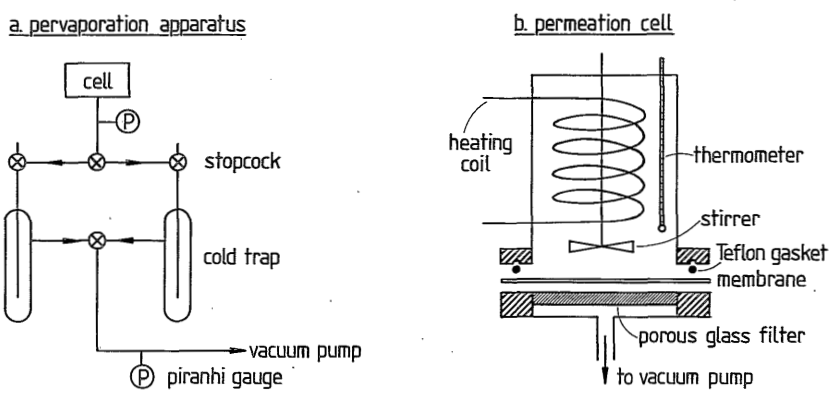

FIGURE 6.7. Conventional pervaporation apparatus:
a. pervaporation apparatus;
b. permeation cell.

In the experiments with flat membranes, the bottom disk of the permeation cell is fitted with porous glass (0.1 m in diameter), to support the membrane. A Teflon gasket is placed on the membrane before the upper part of

the cell is matched. The whole unit is tightened by means of a sovirel clamp. A heating coil is placed into the upper compartment to adjust a preselected temperature and to keep the temperature of the liquid feed constant. A mechanical stirrer was used to minimize the effects of temperature and concentration polarization at the membrane surface. A thermometer is placed in the cell to determine the temperature of the liquid feed.

Capillary membranes were fixed into a glass module and coated on the inside with a dilute PVA solution in water by means of the 'evaporation-deposition method' (24). After drying, the module was given a heat treatment (30 minutes at 130°C).

The permeation cell or the module is connected to two cold traps in parallel. This makes it possible to take samples at any time without interrupting the permeation run. Vacuum at the downstream side is maintained at a pressure of 10 - 100 Pascal by a Crompton Parkinson vacuum pump. The pressure is measured by an Edwards piranhi gauge.

Permeation experiments were carried out for eight hours. After about three hours steady-state conditions were reached. A product sample is taken at least every hour.

The apparatus that is used for the thermally driven pervaporation experiments is given in figure 6.8.

In this mode of operation the feed mixture is kept at a constant temperature in the reservoir that is placed in thermostat 1. The total volume of the feed side is about 3 liters. Iwaki MD 6-Z magnet pumps are used to pump the liquids along the membrane at the feed and at the permeate side with a constant cross-flow velocity. Temperatures are measured by means of thermocouples. The feed mixture is pumped back to the reservoir and recirculated again. The depletion of the feed as a result of the flux through the membrane is supplied by the feed supply vessel.

At the permeate side a cooling coil is used instead of a reservoir, thus giving to a total volume at the permeate side of about 300 ml. The flux is measured by means of an overflow measurement. During the period that no flux is measured the overflow point is connected to the feed supply vessel. In this way the depleted ethanol/water mixture is recirculated.

In the experiments, in which flat membranes were used, a cross-flow cell (made of perspex) is used. The membrane is placed in the cell in such a way that the selective layer of the membrane is in contact with the feed. In this cell the membrane is supported on both sides by a wire-netting with

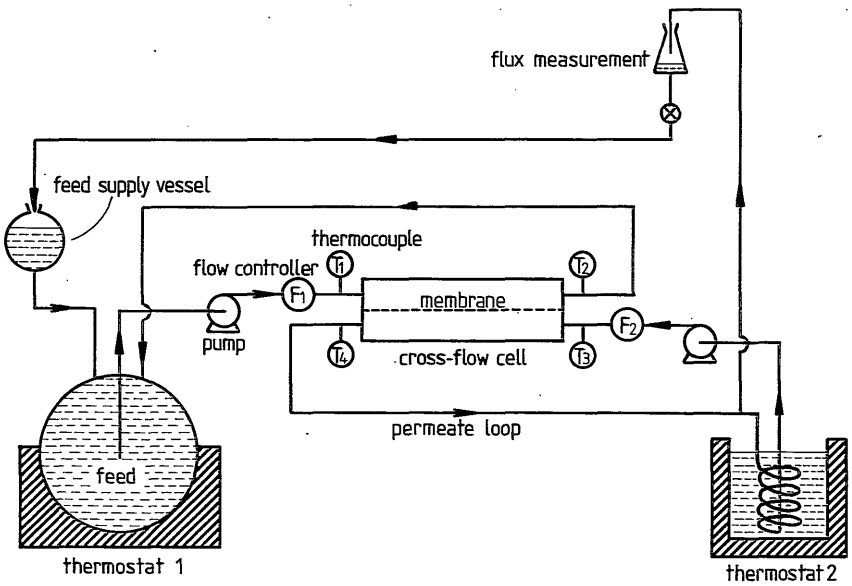

FIGURE 6.8: Thermally driven pervaporation apparatus.

meshes of about 5 mm. Because this process is conducted without any pressure difference, this construction provides a sufficient support.

In the experiments with capillary membranes the modules could be used directly.

In both cases the feed mixture and the permeate mixture are pumped in counter-current flow through the pervaporation cell.

6.5: Results and discussion

Pervaporation experiments with a thermal gradient as a driving force are very time-consuming. In our experiments, the experimental conditions were chosen in such a way that the feed concentration hardly changed during the experiment and that the permeate concentration was measured as a function of the time of operation. The concentration at the permeate side is reaching a steady-state value according to the following exponential function,

$$C_t = C^{\infty} \cdot (1 - \exp^{-(J.A.t/\rho.V)}) \qquad (6.2)$$

It can be calculated that the total permeation yield (expressed by J.A.t/ρ) must be about five times the permeate volume V to reach a steady-state value within 1%. As the permeate volume is about 300 ml, the total permeation yield must be about 1500 ml. With a flux of about 0.1 g/m²s and a membrane area A of 80 . 10^{-4} m², it takes about 500 hours to reach a steady-state value!

Therefore, only a few experiments were carried out with the pervaporation process using the thermal gradient as the driving force. The results are given in table 6.1.

Table 6.1: Pervaporation experiments using a thermal gradient.

exp. nr	preparation method	polymer/ solvent	wt.% ethanol in feed	temperature feed [°C]	temperature perm [°C]	flux J [g/m²s]	selectivity α	thickness selective layer [μm]
1	1	CA/acetone	35	27.0	19.0	0.033	2.4	30
2	2	PSf/DMAc coag. in isopropanol	35	37.5	21.0	0.004	10.0	
3	3	CA/DMSO	35	29.2	20.8	0.055	2.4	10
4			35	38.7	23.3	0.11	3.5	
5			35	47.8	25.2	0.17	4.8	
6			35	48.6	40.4	0.105	2.2	
7	3	CA/DMSO	35	29.3	23.5	0.10	1.9	5
8			35	37.5	26.1	0.19	2.8	
9			35	46.2	29.4	0.30	4.0	
10	4	PVA/water	82	67.0	22.5	0.095	65	
11			80	67.0	43.5	0.070	55	
12	4	PVA/water	82	66.5	22.5	0.050	105	
13			81	68.0	42.5	0.042	90	

The first experiment was performed with a sandwich-membrane prepared by the first method. In this case only one temperature difference has been investigated. The flux was 0.033 g/m²s and the selectivity 2.4. If these results are compared with a conventional pervaporation experiment of the same membrane (J = 0.095 g/m²s and α = 6.0), the thermally driven pervaporation process seems very unattractive. However, it must be realized that the conventional pervaporation experiment was carried out using a low pressure at the permeate side (< 100 Pascal) and that the thermally driven pervaporation

process was carried out using a low feed temperature and a low temperature difference.

In experiment 2 it is demonstrated that besides homogeneous films as a selective layer also asymmetric films can be used. In this experiment an asymmetric polysulfone membrane is sandwiched with a microporous Accurel membrane. A separation factor of 10 is achieved with a flux of 0.004 g/m^2s.

The effect of the temperature and the temperature difference can be seen if experiments 3 till 6 are compared. If the temperature difference increases both flux and selectivity increase (experiments 3 till 5). Comparing experiments 3 and 6 it is shown that in the latter case the flux is higher because of the higher temperature, whereas the selectivity is about the same. This can be explained making use of figure 6.5b. If the vapour pressure at the permeate side is higher, the driving force across the selective layer is lower. This is analogous to conventional pervaporation experiments where both flux and selectivity decrease when the partial vapour pressure at the permeate side of the membrane is increased (25).

Comparing experiments 3 till 6 with experiments 7 till 9, it can be seen that the flux through the membrane is increased by a factor 2 when the thickness of the membrane is reduced by the same factor. It appears that in both cases the selectivity is mainly influenced by the temperature difference. These observations are an indication that the main resistance for transport through the membrane is formed by the selective layer which is in agreement with the transport mechanism.

Some results obtained with the 'evaporation-deposition' method are listed in table 6.1 (experiments 10 till 13). The phenomena, that were observed for the CA membranes, can also be seen for the PVA membranes.

From these results it can be concluded that the best results are obtained with a high feed temperature and a large temperature difference across the membrane. The temperatures for the thermally driven pervaporation process should be in the range of 70 to 100°C for the feed side and in the range of 20 to 50°C for the permeate side in order to achieve an optimal process performance.

Comparison of the results of the thermally driven pervaporation with the results of the conventional pervaporation, listed in table 6.2, shows that both flux and selectivity of the latter mode of operation are higher for the CA membranes. This difference can be explained by the fact that the partial vapour pressure at the permeate side in the conventional mode of operation is as low as 100 Pascal, whereas the vapour pressure in the ther-

mally driven pervaporation is determined by the temperature of the permeate. For instance, a solution of 20 wt% ethanol in water at 20°C has a vapour pressure of about 4000 Pa; at 30°C the vapour pressure is about 7500 Pa. The flux and selectivity of a conventional pervaporation process decreases also when the partial vapour pressure on the permeate side is raised (4,25). For the PVA membranes it is observed that the flux in the thermally driven pervaporation operation is lower than in the conventional type. The selectivity, however, is higher. This latter result cannot be explained directly from the separation mechanism.

Because the partial vapour pressure at the permeate side in a commercial installation will be in the range of 10^3 - 10^4 Pascal, the differences in flux and selectivity between conventional and thermally driven pervaporation will not be as large as indicated in the tables 6.1 and 6.2.

Table 6.2: Conventional pervaporation results (downstream pressure: < 100 Pa).

exp. nr.	preparation method	polymer/ solvent	wt.% ethanol in feed	temperature feed [°C]	flux J [g/m²s]	selectivity α	remarks
14	1	CA/acetone	35	23.0	0.095	6.0	(see exp.1)
15	1	CA/DMSO	35	23.0	0.22	7.0	δ=8 μm
16	4	PVA/water	79	50.0	0.105	45	(same
17			79	59.0	0.18	35	membrane as
18			79	68.0	0.27	30	exp. 10/11)
19	4	PVA/water	81	49.0	0.04	55	(same
20			81	59.0	0.065	47	membrane as
21			80	67.0	0.09	40	exp. 12/13)

In our investigations the cross-flow velocity was chosen in such a way that the effect of temperature polarization is kept as low as possible. The effect of the cross-flow velocity on the flux and the selectivity was measured in membrane distillation experiments (26,27). From these experiments it appeared that the effect of temperature polarization was more pronounced if the cross-flow velocity was lower. The effect of temperature polarization can be discussed qualitatively making use of figure 6.5a. In the heat transport across the membrane step 1 and 6 are affected by the cross-flow velocity. If the cross-flow velocity is lower, the Reynolds number will be lower and this hinders the heat transfer from the bulk of the solution to the mem-

brane surface. As a result the temperature at the membrane surface will be lower at the feed side and will be higher at the permeate side, thus reducing the driving force for pervaporation.

The cross-flow velocity also determines the temperature drop (respectively rise) in the module. In our investigations the temperature difference between the inlet and outlet feed (respectively permeate-absorbing liquid) always was lower than 1°C. The temperatures that are given in the tables are mean temperatures. Although the effect of the temperature drop (respectively rise) is not investigated in this study, its effect is very important for the commercial application of thermally driven pervaporation. Only if a distinct difference occurs between inlet and outlet temperature, recovery of most of the heat of condensation and heat losses due to conductance is possible when the process is conducted in counter-current flow (19).

A phenomenon which should be avoided in membrane distillation is wetting of the microporous hydrophobic membrane (23). If only some of the pores of the membrane are wetted while conducting a membrane distillation process, a leak occurs which spoils the permeate quality, especially when a high product quality is desired (e.g. ultrapure water).

Wetting of a few pores by the permeate-absorbing liquid does not affect the process in case of thermally driven pervaporation. In fact, the only effect is a volume reduction of the vapour 'compartment'. Only if severe wetting of the microporous sublayer occurs (e.g. more than 50% of the pores in the microporous sublayer being wetted), an effect on flux and selectivity might be measured.

Although the effect of wetting in case of thermally driven pervaporation is not so severe as with membrane distillation, care should be taken that a maximum allowable concentration of the organic component in the permeate-absorbing liquid should not be exceeded. For ethanol/water mixtures the maximum allowable concentration at the permeate side for a flat Accurel membrane, as we used in our investigations, is 41 wt.% ethanol (23).

6.6: Conclusions

The general conclusion of this article is that thermally driven pervaporation is a simple and effective mode of pervaporation. The process is especially suitable for the dehydration of aqueous/organic mixtures.

The second conclusion that can be drawn is that the selective layer must have a high selectivity towards water in order to avoid wetting of the porous sublayer by the permeate-absorbing liquid.

6.7: References

1. A.C.M. Franken, M.H.V. Mulder & C.A. Smolders; Pervaporation Process; European Patent EP 218,019 (German Patent DE 3,536,007).
2. I. Cabasso, J. Jagur-Grodzinski & D. Vofsi; A Study of Permeation of Organic Solvents Through Polymeric Membranes Based on Polymeric Alloys of Polyphosphonates and Acetyl Cellulose. II. Separation of Benzene, Cyclohexene and Cyclohexane; Journal of Applied Polymer Science 18 (1974) 2137-2147.
3. R. Rautenbach & R. Albrecht; The Separation Potential of Pervaporation, part 1. Discussion of Transport Equations and Comparison with Reverse Osmosis; Journal of Membrane Science 25 (1985) 1-23.
4. R. Rautenbach & R. Albrecht; The Separation Potential of Pervaporation, part 2. Process Design and Economics; Journal of Membrane Science 25 (1985) 25-54.
5. G. Ellinghorst; Optimale Trennung von Stoffgemischen; Chemische Industrie 7/86 592-594.
6. R.Y.M. Huang & V.J.C. Lin; Separation of Liquid Mixtures by Using Polymer Membranes. I. Permeation of Binary Organic Liquid Mixtures through Polyethylene; Journal of Applied Polymer Science 12 (1968) 2615.
7. P. Aptel, N. Challard, J. Cuny & J. Neel; Application of the Pervaporation Process to Separate Azeotropic Mixtures; Journal of Membrane Science 1 (1976) 271-287.
8. M.H.V. Mulder; Pervaporation, Separation of Ethanol-Water and of Isomeric Xylenes; Ph.D. thesis; University of Twente, 1984.
9. R.Y.M. Huang, Y. Xu, Y. Jin & C. Lipski; Novel Blended Nylon Membranes for the Pervaporation Separation of Acetic Acid-Water and Ethanol-Water Liquid Mixture Systems; proceedings of the Second International Conference on Pervaporation Processes in the Chemical Industry, San Antonio (USA), March 8-11, 1987, p. 225-239.
10. Y.M. Lee, D. Bourgeois & G. Belfort; Selective Organic Transport through Polyvinylidene Fluoride (PVDF) for Pervaporation; proceedings of the Second International Conference on Pervaporation Processes in the Chemical Industry, San Antonio (USA), March 8-11, 1987, p. 249-265.
11. R. Rautenbach & R. Albrecht; On the Behaviour of Asymmetric Membranes in Pervaporation; Journal of Membrane Science 19 (1984) 1-22.
12. I. Cabasso & Z.-Z. Liu; The Permselectivity of Ion-Exchange Membranes for Non-Electrolyte Liquid Mixtures I. Separation of Alcohol/Water Mixtures with Nafion Hollow Fibers; Journal of Membrane Science 24 (1985) 101-109.
13. K.W. Böddekker; Pervaporation durch Membranen und ihre Anwendung zur Trennung von Flüssiggemischen; Fortschritt-berichte VDI, reihe 3: Verfahrenstechnik, nr. 129; VDI Verlag, Düsseldorf 1986.
14. I. Blume & R. Baker; Separation and Concentration of Organic Solvents from Water using Pervaporation; proceedings of the Second International Conference on Pervaporation Processes in the Chemical Industry, San Antonio (USA), March 8-11, 1987, p. 111-125.

15. A. Niemöller, H. Scholz, B. Götz & G. Ellinghorst; Radiation Grafted Membranes for Pervaporation of Ethanol/Water-Mixtures; poster presented at the '5th International Symposium on Synthetic Membranes in Science and Industry'; Tübingen (FRG), September 2-5, 1986.
16. H. Brüschke; Mehrschichtige Membran und ihre Verwendung zur Trennung von Flüssigkeitsgemischen nach dem Pervaporationsverfahren; German Patent DE 3220570.
17. H.E.A. Brüschke & G.F. Tusel; Economics of Industrial Pervaporation Processes; p. 581-586. In: E. Drioli & M. Nakagaki (editors); Membranes and Membrane Processes (Proceedings of the Europe-Japan Congress on Membranes and Membrane Processes; Stresa (Italy), June 18-22, 1984); Plenum Press, New York, 1986.
18. H. Voellmy & P. Läuger; Untersuchungen über Thermoosmose in Flüssigkeiten; Berichte der Bunsengesellschaft Physikalische Chemie 70 (1966) 165-170.
19. K. Schneider & T.J. van Gassel; Membrandestillation; Chemie Ingenieur Technik 56 (1984) 514-521.
20. A.-S. Jönsson, R. Wimmerstedt & A.-C. Harrysson; Membrane Distillation - A Theoretical Study of Evaporation Through Microporous Membranes; Desalination 56 (1985) 237-249.
21. P.A. Kober; Pervaporation, Perstillation and Percrystallization; Journal of American Chemical Society 39 (1917) 944.
22. P. Aptel; personal communication.
23. A.C.M. Franken, J.A.M. Nolten, M.H.V. Mulder, D. Bargeman & C.A. Smolders; Wetting Criteria for the Applicability of Membrane Distillation; Journal of Membrane Science 33 (1987) 315-328 (also chapter 2 of this thesis).
24. A.C.M. Franken, M.H.V. Mulder & C.A. Smolders; The Evaporation-Deposition Method: a Method for the Application of a Homogeneous Permselective Layer onto a Microporous Hydrophobic Sublayer; chapter 7 of this thesis.
25. Q.T. Nguyen; The Influence of Operating Parameters on the Performance of Pervaporation Processes; AIChE Symposium Series nr.248: Industrial Membrane Processes; volume 82 (1986) 1-11.
26. A.C.M. Franken, J.A.M. Nolten, M.H.V. Mulder & C.A. Smolders; Ethanol-Water Separation by Membrane Distillation: Effect of Temperature Polarization. In: B. Sedlacek & J. Kahovec (editors); Synthetic Polymeric Membranes (Proceedings of the 29th Microsymposium on Macromolecules, Prague, July 7-10, 1986); Walter de Gruyter, Berlin - New York, 1987.
27. A.C.M. Franken; chapters 4 and 5 of this thesis.

Chapter 7:

THE EVAPORATION-DEPOSITION METHOD: A METHOD FOR THE APPLICATION OF A HOMOGENEOUS PERMSELECTIVE LAYER ONTO A MICROPOROUS HYDROPHOBIC SUBLAYER

A.C.M. Franken, R.M. Meertens, J.A.M. Nolten, M.H.V. Mulder & C.A. Smolders

Summary

A method to prepare a composite membrane by the deposition of a thin homogeneous permselective layer onto a porous hydrophobic sublayer, called the evaporation-deposition method (1), is described. Several coating variables, among others a chemical treatment of the surface of the sublayer, have been investigated. Results of the application of a poly(vinyl alcohol) (PVA) layer onto microporous polypropylene (PP) capillaries are evaluated by pervaporation experiments.

From the experiments it can be concluded that membranes with high selectivities and moderate fluxes, as well as membranes with high fluxes and moderate selectivities can be obtained.

7.1: Introduction

The first onset for research into composite membranes was given by the development of asymmetric membranes based on the Loeb-Sourirajan recipe (2). This invention led to a search for alternative methods to prepare thin membranes. In contrast to the asymmetric membranes, all the other methods for the preparation of thin membranes (for instance dip-coating (3,4), plasma polymerization (5) and interfacial polymerization (6,7)) have in common that the selective layer is applied onto a porous sublayer in a separate step and usually consists of a material which differs from the sublayer.

In all these methods, the support is not as vitally important as the separating layer itself. The pores in the sublayer have to be small and uniform, and the applied toplayer should have a good adhesion to the sublayer, but except for the requirement that the support must be solvent

resistant in the case of dipcoating and interfacial polymerization, none of these coating methods has specific demands towards the sublayer as far as material properties are concerned.

The thermally driven pervaporation process, as described in the previous chapter, makes use of composite membranes too. In this process the conditions that the sublayer should be hydrophobic and that the toplayer should be selective to water, are essential for the applicability of the process. Therefore, a coating method, in which a water-selective layer is applied onto a hydrophobic membrane, has to be found.

In this chapter an evaporation-deposition method is described, which combines the effect of the hydrophobicity of the sublayer and the solubility of the coating polymer in water. The latter quality guarantees a water-selective final toplayer.

7.2: The evaporation-deposition method

7.2.1: Description of the method

The evaporation-deposition method is in fact a modified dip-coating method for the production of composite membranes. In this method the polymer material for the permselective toplayer is dissolved in a suitable solvent. For the applicability of this coating method it is essential that the solvent does not penetrate into the porous sublayer. The dilute polymer solution is brought in direct contact with one side of the hydrophobic sublayer. At the other side of the sublayer a low vapour pressure is applied. This situation is shown schematically in figure 7.1.

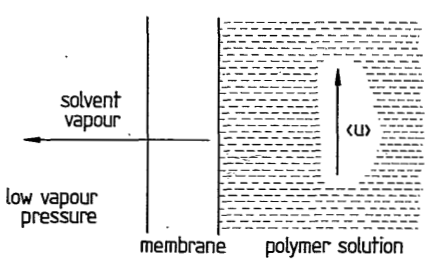

FIGURE 7.1: Schematic representation of the evaporation-deposition method.

A low vapour pressure of the solvent at the uncoated side of the sublayer can be achieved by using a vacuum pump or by using a sweeping gas such as nitrogen. If vacuum is used it should not be too low as to prevent penetration of the polymer solution into the pores of the sublayer. In cases where this already occurs at a relatively high pressure, the sweeping gas method should be used.

Due to evaporation of the solvent through the pores of the sublayer, the polymer concentration at the membrane surface increases. After a certain time the excess polymer solution is removed, leaving a thin film with a high polymer concentration on the surface of the porous sublayer. This film can be dried and crosslinked if necessary, to form the insoluble toplayer of the composite membrane.

7.2.2: Concentration polarization

As a result of evaporation of the solvent through the membrane, the concentration of polymer at the membrane surface increases. In figure 7.2 the effect of concentration polarization is schematically shown by plotting the concentration of polymer as a function of the distance to the membrane.

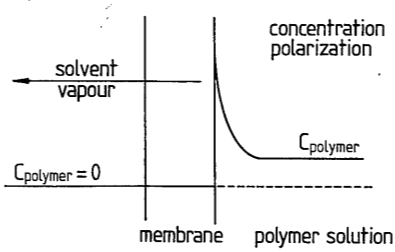

FIGURE 7.2: Concentration polarization as a result of solvent evaporation through the membrane.

The concentration at the membrane surface can be calculated on the basis of mass balances. The equation generally used for concentration polarization is (8):

$$\frac{J_V}{k_M} = \ln\left(\frac{C_m - C_p}{C_b - C_p}\right) \qquad (7.1)$$

In the evaporation-deposition method the rejection of the polymer is 100%, thus leading to the following expression for the concentration at the membrane surface:

$$C_m = C_b \cdot \exp (J_V/k_M) \qquad (7.2)$$

From this equation it can be seen that the concentration of polymer at the membrane surface depends on three parameters:

- the mass transfer coefficient k_M, which is mainly influenced by the tangential flow velocity of the polymer solution and the kind of solute;
- the flux J_V of solvent through the membrane;
- the concentration of the polymer in the bulk of the solution.

The concentration at the membrane surface can be calculated if the above parameters are known for a steady-state situation. The flux J_V and the bulk concentration C_b can be measured and k_M can be calculated using the Leveque equation for mass transfer in the laminar flow region (see chapter 4, equation 4.19).

Taking the values for a typical evaporation-deposition experiment (J_V = 4 x 10^{-7} m^3/m^2s, C_b = 0.03 g/ml, D = 3 x 10^{-11} m^2/s (9) and $\langle u \rangle$ = 0.005 m/s) it can be calculated that the concentration at the membrane surface will be about 5 times higher than the bulk concentration. Taking the uncertainty in the mass transfer coefficient into account, a value varying between 0.10 and 0.20 g/ml is found for C_m. Calculations with other bulk concentrations, but with the same cross-flow velocity, gave values for C_m which are in the same order of magnitude.

Although this calculation is not very precise, it shows that due to evaporation of the solvent an increased polymer concentration at the membrane surface is obtained, which produces a selective membrane after drying and/or crosslinking.

7.2.3: Applicability of the evaporation-deposition method

The applicability of the evaporation-deposition method is limited to hydrophobic membranes in combination with a solvent which does not penetrate into the pores of the membrane. This means that only solvents with high surface tensions can be used. Whether the combination of sublayer and solvent is suitable can be determined by the 'penetrating drop method'

(10). From the experiments given in chapter 3 of this thesis, it can be seen that water, formic acid and DMSO can be used as a solvent if polypropylene is used as the membrane material for the porous sublayer. If PTFE is used as the polymer material, this group of solvents can be extended with DMAc, DMF and 1,4-dioxane.

As the main purpose of this evaporation-deposition method is to fabricate membranes suitable for the pervaporation process as described in the previous chapter, the use of hydrophobic membranes as a sublayer is necessary. On the other hand, the limitation in the use of solvents might lead to the fact that some polymers are excluded as a permselective layer.

The advantages of the evaporation-deposition method are that it is possible to fabricate a composite membrane using a porous support with pores which are much larger than the macromolecules of the polymer employed for the toplayer.

The second advantage is that, due to the evaporation of solvent through the pores of the sublayer, the polymer is deposited at those places where it should be deposited. Also irregularities in the surface of the porous membrane are smoothed due to this coating technique.

The third advantage is that this coating method can be applied to modules directly. Hollow fiber or capillary modules with hydrophobic porous membranes, which are used for microfiltration, ultrafiltration or membrane distillation, can be transformed into devices suitable for pervaporation. Coating a module directly has the advantages that the thin permselective layer is not subjected to mechanical treatments after it is deposited and that a greater flexibility in the production of membrane modules is achieved. By a relatively simple coating procedure a microfiltration module can be transformed into a pervaporation module.

7.3: Experimental

In our investigations poly(vinylidene fluoride) (PVDF) and polypropylene (PP) membranes, supplied by Enka A.G., were used as the hydrophobic microporous support. The characteristics of these membranes are listed in table 7.1.

Experiments with the evaporation-deposition method were carried out with a solution of poly(vinyl alcohol) (PVA) in water. Four different types of PVA were used; their characteristics are listed in table 7.2. In some of

Table 7.1: Characteristics of microporous membranes.

Property	Membrane			
	PV 159	F 0030	R 5/1	Acc. 0.1
Polymer material	PVDF	PVDF	PP	PP
Configuration	cap.	cap.	cap.	flat
Inside diameter (μm)	830	1000	1200	--
Outside diameter (μm)	1230	1500	1800	--
Wall thickness (μm)	200	250	300	100
Max. pore diameter* (μm)	0.25	0.60	0.38	0.40
Porosity* (%)	75	82	80	80

*: as given by the manufacturer; cap.: capillary membranes.

the experiments maleic acid (MA) was added as a crosslinking agent. Maleic acid was obtained from BDH and was used without further purification.

The surface of the microporous polypropylene membranes (both capillaries and flat membranes) was treated with a reactive agent in order to improve the adhesion of the PVA layer to the sublayer. Three types of reagents were used, being fuming sulphuric acid, chromic acid and fuming nitric acid. Fuming sulphuric acid containing about 5% free SO_3 was used at room temperature and was prepared from fuming sulphuric acid containing 30% free SO_3 and concentrated sulphuric acid, both obtained from Merck. The amount of free SO_3 was determined by titration. Chromic acid was prepared by solving 25 g $K_2Cr_2O_7$ in 500 ml sulphuric acid (2.5 molair) and was used at a temperature of 50°C. Fuming nitric acid was obtained from Merck as 100% HNO_3 and was used at a temperature of 40°C. The time of the chemical treatment has been varied. After the treatment the capillaries were rinsed

Table 7.2: Characteristics of poly(vinyl alcohol)s.

Property	PVA 1	PVA 2	PVA 3	PVA 4
Supplier	Aldrich	Aldrich	Aldrich	Merck
Molecular weight* (Dalton)	126,000	95,000	76,000	72,000
Degree of saponification* (%)	98	96	98	98
Solvent	water	water	water	water

*: as given by the supplier.

with an excess of tap water for at least 5 minutes.

Analysis of the modified surfaces was done by observing the change in hydrophilicity of the membrane before and after the chemical treatment. Because a quantitative measurement of contact angles on porous materials is very difficult, only these qualitative observations were carried out. Additional analysis of the surfaces that were treated with fuming sulphuric acid was carried out with an energy dispersive analysis technique (EDAX) and with X-ray photoelectron spectroscopy (XPS). The latter technique was also used for the analysis of the surfaces that were treated with chromic acid or fuming nitric acid.

To investigate the effect of a surface treatment on coating of the microporous membranes, (classical) dip-coating experiments were carried out on flat Accurel membranes with solutions of poly(vinyl alcohol) (PVA), poly(acrylic acid) (PAA), poly(acryl amide) (PAAm) and cellulose acetate (CA). Their properties are listed in table 7.3.

Table 7.3: Polymers used for dip-coating experiments on flat Accurel membranes.

Property	PVA 1	PAA	PAAm	CA
Supplier	Aldrich	Aldrich	Polysciences	Eastman
Polymer material	PVA	PAA	PAAm	CA
Molecular weight* (Dalton)	126,000	250,000	5,000,000	55,000
Degree of acetylation* (%)	-	-	-	39.8
Solvent	water	water	water	DMSO

*: as given by the supplier.

In these experiments the flat Accurel membranes were dipped into a polymer solution in water with polymer concentrations ranging from 0.5 to 5% polymer by weight. The dip-coated membranes were dried in air subsequently. The remaining polymer layer was tested on wetting, adhesion, and thickness.

The wetting tests were carried out using ethanol. If the layer did not homogeneously spread over the sublayer and/or if it contained holes, ethanol penetrates through this layer and wets the sublayer. The wetting of the sublayer can be observed very clearly.

The adhesion was investigated by a simple test in which the composite membrane was torn into two pieces. If the toplayer tears up at the same place as the sublayer a good adhesion is obtained. A rupture at a different place, resulting in a separation of the toplayer and the sublayer indicates a bad adhesion. Another indication for a bad adhesion was obtained from scanning electron microscope photographs, from which it could be seen directly whether the selective layer showed a good adhesion. Examples of such scanning electron microscope photographs, showing a bad, respectively a good, adhesion of a coated PVA layer onto a microporous PP membrane are given in figure 7.4a and 7.4b respectively.

The thickness of the selective layer can also be investigated by scanning electron microscopy (see for instance figure 7.4). In cases the selective layer showed a bad adhesion and the layer could be separated from the sublayer without damaging it, the thickness was measured by means of a micrometer.

Experiments with the evaporation-deposition method were carried out with a 'one-capillary module', consisting of a module made of glass in which one capillary with a length of 200 mm was mounted. In figure 7.3 a schematic representation of this module is given. The selective layer is applied at the inside of the capillary.

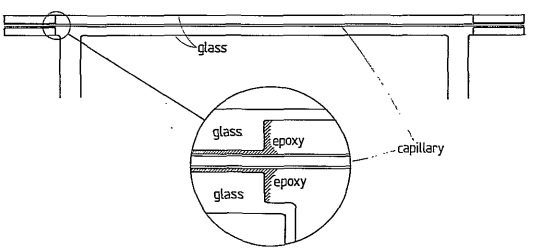

FIGURE 7.3: Schematic representation of a 'one-capillary module'.

The separation characteristics of the modules were tested in a pervaporation set-up. The feed consists of a mixture of 80% of ethanol by weight in water, prepared from ethanol of analytical grade and ultrafiltrated water. The feed is pumped through the bore of the capillaries by an Iwaki MD-6Z magnet pump with a cross-flow velocity of about 0.4 m/s. The temperature of the feed is kept constant by an Eurotherm controller and the inlet

temperature of the module is measured by a thermometer. The module is connected to two cold traps in parallel, which make it possible to take samples without interrupting the permeation run. Vacuum at the downstream side is maintained at a pressure of about 100 Pascal by a Crompton Parkinson vacuum pump. The pressure is measured by an Edwards piranhi gauge. The downstream compartment of the experimental set-up is the same as described in the previous chapter (see figure 6.7b).

7.4: Results

7.4.1: Surface modification

The first results obtained with coating experiments on hydrophobic microporous membranes showed that the adhesion of the polymer layer onto the microporous sublayer was not very good. It appeared that the selective layer could be peeled off or rubbed off with little effort.

All the composite membranes which were prepared by applying a PVA layer onto an untreated hydrophobic membrane showed a bad adhesion. For that reason a surface modification of the capillaries was carried out prior to coating. Restrictive conditions for this chemical treatment are:

- only the inside surface of the fiber must be made hydrophilic;
- no penetration of the chemical agent into the pores of the microporous membrane is allowed;
- the chemical agent should be concentrated because both PP and PVDF have a good chemical resistance;
- the method should be easily applicable to a module.

In literature a number of reagents are known that fit the above requirements, being fuming sulphuric acid (11,12,13), fuming nitric acid (12,14), chromic acid (12,15,16) and permanganate acid (17). All these reagents have a high surface tension which guarantees non-penetration into the pores of the support. The effect of the surface treatment was tried out on the outside of a fiber before the chemical treatment was actually applied on the inside. A few tests were carried out in which it was determined whether the hydrophilicity of the microporous capillary was changed. Once the reaction conditions (time, temperature and concentration) were optimized, the inside surfaces of the capillaries were treated.

The treatment with fuming sulphuric acid gave both a good hydrophilicity and a good adhesion of the PVA layer to the microporous sublayer. Scanning electron microscope photographs and rupture-tests showed that the adhesion of the layer to the microporous capillary was excellent. Figure 7.4b shows an example of the good adhesion of the PVA layer to the microporous PP sublayer which was treated with fuming sulphuric acid before the coating was applied.

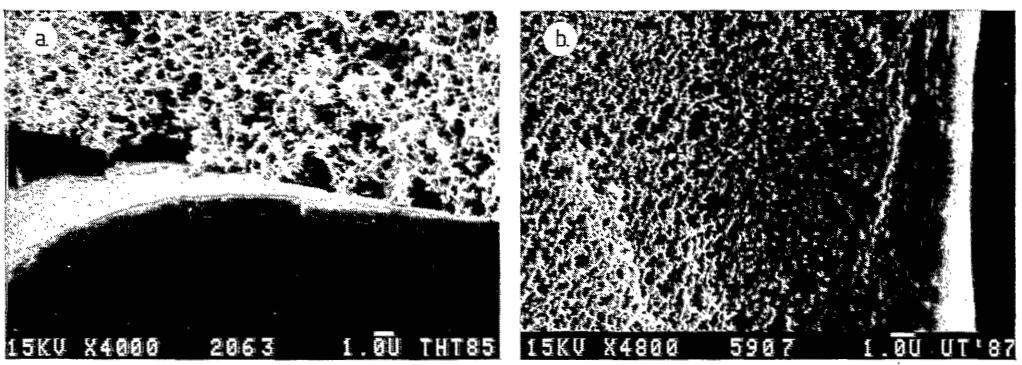

FIGURE 7.4: Scanning electron microscope photographs, showing a bad adhesion (a) and a good adhesion (b) of the PVA layer to the microporous PP membrane:
a. no surface treatment of the sublayer;
b. surface of the sublayer treated with fuming sulphuric acid.

Knowing that the reaction with fuming sulphuric acid was successful, it was still not clear whether this reaction was only a surface reaction, in other words, whether the penetration depth of reaction was limited. The hydrophilicity tests showed already that no penetration of water into the treated sublayers took place, thus indicating that the reaction had not penetrated through the membrane.

To find out which penetration depth was reached, a capillary, which was treated with fuming sulphuric acid for 10 minutes (about ten times as long as usual), was analysed with EDAX. The measurements showed that sulphur could be detected, but that the height of the sulphur peaks was about the minimum level of detection. This is not surprising; EDAX is not a real surface analysis technique since it has a penetration depth in the order of micrometers.

The penetration depth of the electrons in XPS is about 5 to 10 nm. A

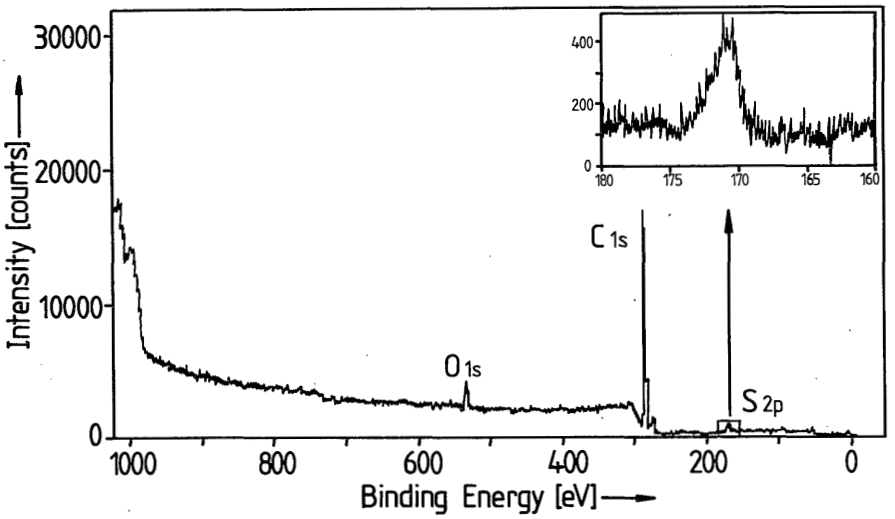

FIGURE 7.5: XPS analysis of a flat PP membrane, which was treated with fuming sulphuric acid for 2 minutes.

typical XPS analysis is shown in figure 7.5, in which an overall scan is given. Detailed scans, as given for sulphur in figure 7.5, are made for all components. The analysis shows that sulphur is significantly present at the surface. Furthermore, it is observed that the sulphur peak (S 2p) is situated at a binding energy level of about 169 ± 1 eV. The chemical shift of this sulphur peak in relation to atomic sulphur is about 4 eV. A binding energy level of 169 eV is specifically ascribed to a $-SO_3H$ group (18). Also the fact that the ratio sulphur to oxygen is about 3, indicates that $-SO_3H$ groups are present at the surface of the treated sublayer.

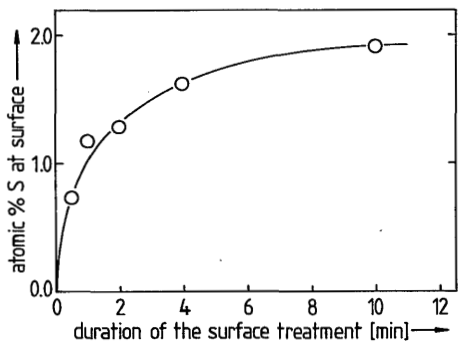

FIGURE 7.6: Atomic percentage of sulphur in the surface layer of a PP membrane found in an XPS analysis as a function of the duration of the surface treatment.

Although it is not possible to obtain quantitative results on the penetration depth of the chemical treatment, some information about the effect of the reaction time could be obtained from the results. In figure 7.6 the atomic percentage of sulphur in the surface layer as a function of the reaction time is given. From this figure it can be observed that the reaction proceeds very fast in the first minutes and that its effect then flattens.

Combining the results of the measurements in which a change of hydrophilicity was observed with the results of XPS and EDAX measurements, it can be concluded that chemical modification of the sublayer by fuming sulphuric acid is restricted to the surface. Furthermore, the reaction proceeds as described in literature, yielding $-SO_3H$ groups at the surface (12,13).

The chemical treatment of aliphatic hydrocarbons by chromic acid yields -OH groups at the surface through the following reaction (12,15, 16):

$$R_3CH \xrightarrow{[O]} R_3COH$$

In this reaction nearly always the C-H bond involved is tertiary, because these bonds are more susceptible to free-radical attack than primary and secondary bonds.

The treatment of the PP membranes with chromic acid increased the hydrophilicity of the fiber. On the other hand the treatment did not give much improvement of the adhesion of the PVA layer to the fiber, which was checked by both scanning electron microscopy and rupture tests.

The effect of the surface treatment was qualitatively measured by observing a change in hydrophilicity. EDAX could not be used to determine oxygen. The results obtained with XPS show an increase of the oxygen content at the membrane surface. Unfortunately these results cannot be used quantitatively as a result of a pollution of the surface with oxides (among others chromium oxides). Through a chemical shift, it could be determined qualitatively that covalently bound oxygen was present at the membrane surface.

According to the theory the reaction of paraffins with fuming nitric acid can result in the formation of a nitrated product (12):

$$R_3CH + HNO_3 \rightarrow R_3CNO_2 + H_2O$$

The effect of the surface treatment by fuming nitric acid was investigated qualitatively by the change of hydrophilicity and by XPS. The first method showed that an increase of the hydrophilicity of the surface was obtained.

XPS analyses of the modified membranes showed, however, that no oxidized nitrogen groups were present at the membrane surface. In these analyses it was found that either no nitrogen could be detected at all or the nitrogen binding energy (N 1s) was situated at 402 eV. Oxidized nitrogen functions have much higher N 1s binding energies: $-ONO_2$ (408 eV), $-NO_2$ (407 eV) and -ONO (405 eV) (18). The peak at 402 eV might be caused by the presence of ionic NO_3^- groups at the membrane surface. Furthermore, in all the analyses of the modified surfaces oxygen was determined. As a result of the chemical shift it could be determined that covalently bound oxygen was present at the membrane surface. Due to the presence of other oxidized products, however, a quantitative analysis is not possible.

The reason that nitration of the membrane surface does not occur might be due to the fact that the reaction conditions are not favourable for this reaction. The temperature at which the surface modification was carried out is 40°C, which is believed to be a much too low temperature for the free-radical mechanism. At these temperatures the oxidation reaction (14) is favoured.

$$2HNO_3 \rightarrow N_2O_5 + H_2O$$

$$R_3CH + N_2O_5 \rightarrow R_3COH + 2NO_2$$

The alcohol group formed is subject to a reaction with the nitric acid again, resulting in the formation of a nitrate ester.

$$R_3COH + HNO_3 \rightarrow R_3CONO_2 + H_2O$$

Nitrate esters are very unstable and will be subject to hydrolysis due to the rinsing with an excess of tap water:

$$R_3CONO_2 + H_2O \rightarrow R_3COH + HNO_3$$

Whether the surface modification proceeds according to the above reaction scheme is uncertain; it merely gives a possible explanation of the results of the XPS analyses of the membranes treated with fuming nitric acid.

7.4.2: Dip-coating experiments on flat membranes

The dip-coating experiments on flat membranes were carried out to investigate the effect of a surface treatment on the hydrophilicity of the sublayer and especially on the compatibility of a polymer solution to the treated membrane. In table 7.4 the results of the dip-coating experiments with respect to the spreading of the dilute polymer solutions in water are given. The polymer concentration in these experiments was varied from 0.5 till 5% by weight. In this table it is indicated whether a liquid film remains stable on the porous sublayer after dipping into a polymer solution.

Table 7.4: Compatibility of a dilute polymer solution in water as a function of the chemical modification of the sublayer.

chemical agent	water	PVA	PAA	PAAm
no surface treatment	-	+/-	--	--
fuming sulphuric acid	+	-	-	-
chromic acid	+	+	-	-
fuming nitric acid	+	++	-	-

Although these tests are only qualitatively, it is shown clearly from this table that an improved spreading of water on a treated membrane does not mean that the same results are obtained for a dilute polymer solution. For instance, a surface treatment with fuming sulphuric acid gives an improved spreading of a water film, but a diminished spreading of a dilute solution of PVA in water. On the other hand a treatment with fuming nitric acid improves both the spreading of water and of a dilute PVA solution.

An untreated membrane behaves like an extremely hydrophobic material when it is brought in contact with PAA and PAAm solutions. Dip-coating experiments resulted in no deposition of polymer at all. All surface treatments show an improvement in compatibility in relation to the untreated membrane. Despite this improvement, the results were still very bad.

7.4.3: Evaporation-deposition experiments (effect of coating parameters)

The experiments with the 'evaporation-deposition-method' were carried out on one-capillary modules using solutions of PVA in water. In these experiments a number of parameters were varied, being:

- applying the layer on the outside or inside of a capillary;
- using sweeping gas or vacuum downstream;
- type of sublayer;
- modification of the surface of the sublayer;
- molecular weight of the PVA / degree of saponification;
- concentration of PVA in the coating solution;
- cross-flow velocity of the polymer solution;
- deposition time;
- drying procedure / gravitational effects during the drying process;
- addition of a crosslinking agent (maleic acid);
- crosslinking conditions.

Some typical results of the evaporation-deposition experiments are listed in table 7.5. The modules were tested for their pervaporation characteristics with a mixture of 80 wt% ethanol in water. In the tables the flux and the selectivity are given. The selectivity is defined as:

$$\alpha = \frac{(\%\ \text{water} / \%\ \text{ethanol})\ \text{in the permeate}}{(\%\ \text{water} / \%\ \text{ethanol})\ \text{in the feed}} \qquad (7.3)$$

A few experiments were carried out in which a layer was applied on the outside of a capillary, all with rather poor results. Because the PVA solution is very sticky, it tends to stick to the wall and, if more capillaries are used, to other capillaries. This effect reduces the surface area and gives weak spots in the selective layer. Therefore, in all further experiments the layer was applied on the inside of the capillary.

Using a vacuum or a sweeping gas downstream did not give any significant differences in the resulting membrane performance.

The coating experiments were carried out on three different types of capillaries. Although their influence was not investigated systematically, it appeared that hardly any influence on the properties of the selective layers could be observed.

The influence of the surface treatment was only investigated on PP capillaries (R 5/1). The results are given in the tables 7.6 and 7.7 and will be discussed later.

Table 7.5: Evaporation-deposition experiments on unmodified supports: influence of coating parameters.

Preparation method:
- type of capillary: see table 7.1;
- type of PVA: see table 7.2;
- MA: maleic acid as a crosslinking agent;
- vacuum (exp.1-6) or sweeping gas (exp.7-9) downstream;
- rotating the module during drying: exp.6-9;
- all coatings were heat treated at T = 130°C for 30 minutes.

Pervaporation test:
- feed: about 80 wt.% ethanol in water;
- downstream pressure: < 100 Pa.

		PVA			cross-flow			pervaporation		
nr.	type of capillary	type	wt%	MA added	<u> [m/s]	time [hr]	thickness [μm]	flux [g/m²s]	α [-]	T [°C]
1	F0030	3	2	-	0.002	5	1	0.11	2	20
2	F0030	3	5	-	0.004	5	7-50	0.005	55	20
								0.022	53	37
								0.050	44	55
3	F0030	3	5	-	0.038	2	< 1	leaking		
4	R 5/1	2	4	+	0.003	0.5	5-25	0.039	39	24
								1.31	23	55
5	R 5/1	4	5	+	0.003	0.5		0.015	45	24
								0.11	40	55
6	F0030	1	3	+	0.004	2	10-20	0.011	130	25
								0.069	77	50
7	PV159	1	3	+	0.004	0.5		0.14	11	23
								0.95	10	55
8	F0030	1	3	+	0.004	0.5		0.021	52	23
								0.27	36	55
9	R 5/1	1	3	+	0.003	0.5		0.025	33	23
								0.19	40	55

Experiments using different molecular weights of PVA showed that a slight improvement of the membrane characteristics was found with increasing molecular weight. About the degree of saponification this investigation

could not give any definitive answer, but from investigations of Spitzen et al. (19) it appeared that a degree of saponification of 100% gave no improvement of membrane characteristics as compared to 98%. If the degree of saponification is less than 90% the selectivity of the membranes was very low (20). In our investigations mostly PVA type 1 (see table 7.2) was used.

The concentration of PVA in solution is one of the most important variables. Although it can be illustrated from the equations for concentration polarization that the concentration at the membrane surface will have a value between 10 and 20% polymer by weight, it is found that the bulk concentration is rather important for the formation of a selective layer. A 2% PVA solution resulted in the formation of a layer with a thickness of about 1 μm, whereas with a 5% solution a layer of about 20 μm thickness is obtained (see table 7.5, experiment 1 and 2). Although the results show a lot of spreading, a sharp increase of the thickness of the layer with increasing polymer concentration was found. To obtain defect-free layers, a concentration of 3 to 5% of PVA (type 1) by weight seems to be necessary.

The effect of the cross-flow velocity of the polymer solution on the thickness of the selective layer is even more important than the effect of the PVA concentration. As the cross-flow velocity directly influences the mass transfer coefficient k_M (k_M is proportional to $\langle u \rangle^{0.33}$), it can be seen from equation 7.2 that the concentration at the membrane surface decreases when the mass transfer coefficient increases. Experimentally it is observed that if the cross-flow velocity is increased one order of magnitude from 0.004 m/s to 0.04 m/s, the thickness of the selective layer decreased from about 20 μm to less than 1 μm (see table 7.5, experiment 2 and 3). It is not a good alternative to use no cross-flow at all during the formation of the layer, because in these cases the capillaries got plugged. Therefore, in our experiments the cross-flow velocity was kept as low as possible resulting in an experimental cross-flow velocity between 3 and 5 mm/s.

From experiments, in which the permeating solvent was collected in a liquid nitrogen trap, it appeared that the flux through the membrane is rapidly decreasing. This decrease holds on for about 15 to 30 minutes, but after about one hour a steady-state flux is reached. In our experiments, the deposition time has been varied from 15 minutes till 6 hours and no significant differences in the membrane properties of the resulting layer

could be found.

After the excess polymer solution is pumped out of the module, nitrogen (containing water vapour) is passed through the capillaries. The main reason for this gas flow is not drying of the applied layer, but removing the excess polymer out of the capillaries and prevent plugging. The main drying effect is achieved at the downstream side as the low partial pressure is maintained after the excess polymer solution has been removed.

The influence of gravitational effects was found to be significant when a module is placed in a horizontal position during the drying process. Due to the fact that the deposited film is not solid, the polymer solution runs off the upper side of the capillary and a thick layer is formed at the 'bottom' side of the horizontal capillary. The effect was more pronounced if the deposited layer was relatively thick (20 μm or more) and could be minimized when the module was rotated during the drying process at a rotation speed of about 1 rpm. If low polymer concentrations were used and/or if the module was kept vertically during the drying process, the influence of gravitational effects was hardly present.

Maleic acid was used as a crosslinking agent; other crosslinking agents were not investigated. Although a selective PVA membrane can be made without the use of a crosslinking agent, its use seems inevitable when a PVA layer is applied onto a microporous capillary. Application of a crosslinking agent is especially important if the composite membrane is subjected to a heat treatment after drying.

The deposited PVA layers are subjected to a heat treatment at a temperature of 130°C for 30 minutes. The pervaporation results of a PVA layer without addition of a crosslinking agent are rather good when no heat treatment is applied. When a heat treatment is applied then leakage occurs in more than 90% of the experiments. If, however, maleic acid is added to the polymer solution, no leakage occurs. On the other hand, a real improvement of the selectivity towards a mixture of ethanol and water is not found, whereas the flux is decreased by about 40%. In cases where no heat treatment is applied the layer does not stick to the microporous support and can be washed out of the module. This makes a crosslinking step inevitable.

7.4.4: Effect of surface modification on evaporation-deposition experiments

The experiments, in which the influence of the surface modification of

the sublayer is studied, are given in table 7.6. In these experiments a number of the variables, which were discussed above, are fixed at a (sub)-optimal value. In table 7.6 the following parameters are varied: the nature of the chemical reagent used for the surface modification, the use of a heat treatment and the addition of a small amount of sulphuric acid to the coating solution.

Table 7.6: Evaporation-deposition experiments: influence of surface modification of PP capillaries and some other variables.

Preparation variables:
- fixed:
  - type of capillary: R 5/1 (see table 7.1);
  - type of PVA: see table 7.2;
  - MA: maleic acid as a crosslinking agent;
  - vacuum downstream;
  - cross-flow velocity: 5 mm/s;
  - deposition time: 30 minutes;
  - module mounted vertical during coating and drying;
- varied:
  - surface modifying agent;
  - H^+: addition of sulphuric acid (pH of coating solution ~ 1);
  - heat treatment at T = 130°C for 30 minutes.

Pervaporation test:
- feed: about 80 wt.% ethanol in water;
- downstream pressure: < 100 Pa.

	modification			PVA					pervaporation		
nr.	acid	time [min]	T [°C]	type	wt%	MA added	H^+ added	heat treatment	flux [g/m²s]	α [-]	T [°C]
11	no modification			1	5	+	-	-	0.23	10	48
								+	0.35	7	48
12	no modification			1	5	+	+	-	0.058	36	48
								+	0.047	42	50
13	SO_3	1	20	1	5	+	-	-	0.12	8	48
								+	0.103	10	48
14	SO_3	1	20	1	5	+	+	-	0.19	6	49
								+	0.17	3	50
15	Cr	30	50	1	5	+	-	-	0.21	18	49
								+	0.19	21	48
16	Cr	30	50	1	5	+	+	-	0.078	27	50
								+	0.078	25	50
17	HNO_3	0.5	40	1	5	+	+	-	0.32	28	51
								+	0.086	49	50
18	HNO_3	1	40	1	5	+	+	-	0.18	26	50
								+	0.125	37	51
19	HNO_3	2	40	1	5	+	+	-	0.15	26	49
								+	0.114	37	50

The effect of the type of chemical reagent on the compatibility of a PVA solution with the treated sublayer has already been discussed qualitatively in section 7.4.2. From dip-coating tests it appeared that the treatment with fuming nitric acid produced the best results compared to the other surface treatments. As the evaporation-deposition method is in fact a modified dip-coating method, the same tendency is expected. If the results in table 7.6 are considered this tendency indeed is found. It must be realized that the results in table 7.6 do not present an extended review of all the experiments that were performed. If, however, the overall range of values is considered (see table 7.7) the same tendency is found.

Table 7.7: Influence of surface treatment on membrane properties.

surface treatment	flux [g/m²s]	α	T [°C]
no treatment	0.05 - 0.10	20 - 40	50
fuming sulphuric acid	0.15 - 0.25	3 - 10	50
chromic acid	0.08 - 0.15	20 - 30	50
fuming nitric acid	0.10 - 0.14	30 - 40	50

From the results in table 7.7 it can be concluded that the best results are obtained with a surface treatment of fuming nitric acid and the worst results with a treatment of fuming sulphuric acid. The same results were also qualitatively obtained with the dip-coating experiments of dilute PVA solutions on flat membranes (see table 7.4).

The addition of sulphuric acid to the coating solution, in such an amount that the pH of the coating solution is about 1, seems to have a positive effect on the selectivity of the toplayer. A definitive conclusion cannot be given, because the effect is not very pronounced and results with PVA membranes have shown that a certain spreading always occurs.

7.4.5: Pervaporation results

The modules, prepared by the evaporation-deposition method, are tested for their separation characteristics in pervaporation. Some of the results have already been given in the tables 7.5 and 7.6. These results together with some results from literature are given in figure 7.7, in which the flux is plotted against the selectivity.

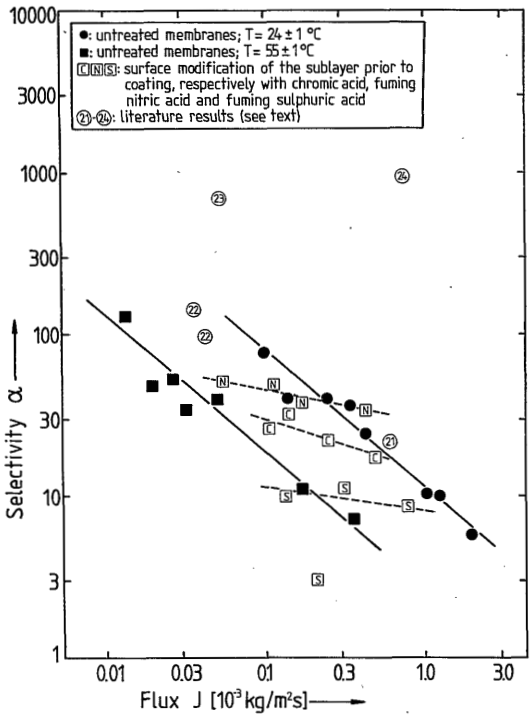

FIGURE 7.7: Pervaporation results.

As far as the results obtained with the unmodified membranes are concerned, it can be concluded from figure 7.6 that a high flux is related to a low selectivity and vice versa. Furthermore, it can be seen that a temperature rise from room temperature (24 ± 1°C) to 55°C gives an increase in flux by a factor 6, whereas the selectivity is only slightly decreased.

When the influence of the surface modification on the pervaporation performance is considered, it appears that the results do not differ as much among each other as the results for the untreated membranes. This is due to the fact that coating conditions were not varied much during these experiments. From figure 7.7 it can be observed that the selectivity for the different surface modifications is about the same, but that the flux can vary considerably for the same coating conditions. Furthermore, it can be seen that the selectivity of the membranes which received a surface treatment with fuming nitric acid is slightly better compared to the value for the chromic acid treated membranes, which on its turn show much better properties than the membranes treated with fuming sulphuric acid.

Compared with the literature results, it appears that our results are

comparable to the results obtained with PVA membranes (see figure 7.7, points 21 and 22). N.B. The number in the open circles also refers to the literature reference.

Some of the results obtained with membranes containing ionic sites are also presented in figure 7.7 (see points 23 and 24). The result presented in point 23 is obtained by Cabasso for sulphonated PE membranes containing Cs^+ as counter-ions (23) and point 24 is taken from Ellinghorst's work, using PAN membranes into which acrylic acid has been grafted and in which the H^+-ions are replaced by K^+-ions (24). These membranes are superior to PVA membranes, but they have the disadvantage that the ions are leached out of the membrane, resulting in a severe loss of selectivity. For instance, the 'unmodified' Ellinghorst-membrane (without K^+ as a counter-ion) has a selectivity of about 10 (24), which makes this membrane, as flux and selectivity are concerned, comparable to a PVA membrane.

7.5: Discussion

The results of the compatibility tests of flat Accurel membranes with dilute PVA solutions are essentially different from those obtained with pure water (see table 7.4). Introducing a hydrophilic group improves the interaction between the treated surface and water. The results show that the nature of the hydrophilic group is not important. The reason for this phenomenon is that in the case of the treated membranes dipole-dipole interactions between water and the surface will occur. Because water can act both as electron donor and acceptor, it makes no difference whether the surface contains electron donor or electron acceptor groups.

The compatibility of a PVA solution with the modified surfaces seems to be determined mainly by the PVA present in solution. The results listed in table 7.4 are obtained for dilute solutions (0.5% by weight) and more concentrated solutions (up till 5% by weight).

A surface treated with fuming sulphuric acid, resulting in $-SO_3H$ groups at the surface, shows a worse compatibility with a PVA solution as compared to an untreated surface. From literature it is known that most sulphonation reactions of polyalkylene surfaces are carried out to improve the printability of the surfaces (13,25). On the other hand, in the field of ultrafiltration sulphonation of hydrophobic membranes is carried out to reduce fouling (26). This effect is ascribed to a reduced interaction be-

tween hydrophobic particles in solution and to an electrostatic repulsion between the negatively charged membrane and negatively charged colloids.

This description can be used as a possible explanation of the phenomenon described above. In an aqueous solution the sulphonic acid group will be present in its ionic form ($-SO_3^-$) and therefore acts as an electron donor. Because PVA through its -OH groups acts as an electron donor, this results in a repulsion between PVA and the sulphonated surface. Furthermore, the resonance structure of the $-SO_3^-$ group is not favourable for the formation of hydrogen bonds. However, if one succeeds in applying a PVA film to the sulphonated PP membrane, an esterification reaction between the sulphonic acid group and a hydroxyl group of the PVA can take place when the film is subjected to a heat treatment. This results in a PVA film which shows an excellent adhesion to the modified PP membrane.

A treatment with chromic acid or fuming nitric acid, yielding both -OH groups at the membrane surface, results in an improved compatibility between the modified film and the PVA solution. Because hydroxyl groups act as electron donor groups, a repulsion between the PVA solution and the modified surface would be expected. On the other hand, hydrogen bonding can take place, which will result in an improved compatibility. According to the results obtained the latter effect is dominating.

Comparing the results of the chromic acid treatment with those of the fuming nitric acid treatment, it appears that the latter results were slightly better. This effect is probably due to a higher degree of oxidation of the surface of the PP membrane in the case of the fuming nitric acid treatment. This assumption is supported by the results from the rupture tests indicating that the PVA layer has a better adhesion to the modified layer if the PP membrane was treated with fuming nitric acid. Moreover, if the sublayer was treated with chromic acid, the rupture tests on the composite membranes show a less good adhesion of the PVA toplayer, which is an indication for a low degree of oxidation of the surface.

In the previous paragraph the (small) difference between the treatments with chromic acid and fuming nitric acid is explained through the difference in degree of oxidation of the PP membrane. A different possibility is the occurence of oxidized nitrogen at the membrane surface. Although oxidized nitrogen could not be observed significantly by means of XPS, a slight increase of the signal at about 408 eV was observed. Whether this increase is a result of wishful thinking or based on reality, has to be determined in future experiments.

The problems occuring with a heat treatment (at T = 130°C for 30 minutes) when no crosslinking agent is added to the polymer solution can be understood if the crystallinity of the PVA layer is taken into account. If thin film composite membranes are subjected to a heat treatment, the thermal expansion coefficient of the support determines also the freedom of lateral expansion of the selective layer. PVA with a high degree of saponification has the ability to form crystalline areas at higher temperatures. Upon cooling the selective layer will not be able to deform in the same way as the support, thus leading to defects in the selective layer. By adding a crosslinking agent the ability of the PVA to crystallize is diminished and, as a less crystalline film is capable to adjust to the differences in thermal expansion, defects in the selective layer are diminished as well.

The occurence of defects was more pronounced if the surface of the sublayer was modified. If a surface treatment is given, the selective layer is firmly fixed to the sublayer during a heat treatment. In this way the ability to adjust to the differences in thermal expansion is reduced and the probability of defects is increased.

Esterification reactions are catalyzed by acids (27). Through the addition of a small amount of sulphuric acid to the coating solution more crosslinks might be realized, thus leading to a lower degree of swelling resulting in a higher selectivity and a lower flux. Since the acidity constant of a maleic acid group which is attached through one ester-bond to a PVA molecule is rather low ($K_a \sim 10^{-5}$), the affinity of such a group to react is low. In the presence of H^+-ions the second esterification reaction will be catalyzed. Whether the reaction actually takes place is uncertain, because it must be considered that an attached molecule is limited in its freedom of movement.

7.6: Conclusions

From our experiments it can be concluded that the evaporation-deposition method is an attractive method for the preparation of composite membranes to be used in the pervaporation process. The method has advantages over other types of coating procedures because microporous membranes can be used as a sublayer. Also the fact that this coating procedure can be applied directly on modules makes this method very attractive for commercial-

ization.

Pervaporation tests on mixtures of ethanol and water have shown that it is possible to obtain selective membranes with moderate fluxes or high-flux membranes with moderate selectivities using this evaporation-deposition method.

A surface treatment of the hydrophobic microporous capillaries with a chemical agent improves the adhesion of the selective layer to these capillaries. The use of nitric acid as a reagent also improves the spreading of a PVA solution on the modified surface, thus resulting in an improved performance of the composite membranes.

7.7: References

1. A.C.M. Franken, M.H.V. Mulder & C.A. Smolders; Verfahren zum Herstellen einer Zweischichtmembran; German Patent DE 3707054.
2. S. Loeb & S. Sourirajan; Sea Water Demineralization by means of an Osmotic Membrane. In: R.F. Gould (editor); Saline Water Conversion II; Advances in Chemistry Series 38 (1962) 117.
3. P.H. Carnell & H.G. Cassidy; The Preparation of Membranes; Journal of Polymer Science 55 (1961) 233-249.
4. P.H. Carnell; Preparation of Thin Polymer Films; Journal of Applied Polymer Science 9 (1965) 1863-1872.
5. H. Yasuda & C.E. Lamaze; Preparation of Reverse Osmosis Membranes by Plasma Polymerization of Organic Compounds; Journal of Applied Polymer Science 17 (1973) 201-222.
6. J.E. Cadotte; Reverse Osmosis Membrane; US Patent 4039440.
7. J.E. Cadotte, R.S. King, R.J. Majerle & R.J. Petersen; Interfacial Synthesis in the Preparation of Reverse Osmosis Membranes; Journal of Macromolecular Science - Chemistry A15 (1981 727-755.
8. H. Strathmann; Trennung von molekularen Mischungen mit Hilfe synthetischer Membranen; Steinkopf, Darmstadt, 1979.
9. J. Bandrup & E.H. Immergut; Polymer Handbook (second edition); Wiley Interscience, New York, 1975.
10. A.C.M. Franken, J.A.M. Nolten, M.H.V. Mulder, D. Bargeman & C.A. Smolders; Wetting Criteria for the Applicability of Membrane Distillation; Journal of Membrane Science 33 (1987) 315-328 (also chapter 2 of this thesis).
11. H.W. Gibson & F.C. Bailey; Chemical Modification of Polymers. 13. Sulfonation of Polystyrene Surfaces; Macromolecules 13 (1980) 34-41.
12. J. March; Advanced Organic Chemistry (Reactions, Mechanisms and Structure); McGraw Hill, Tokyo, 1968.
13. W.E. Wallis & H.G. Hahn; Coating of polyethylene films and articles; US Patent 2,786,780 (Chemical Abstracts 51 (1957) 10125h).
14. J.K. Rieke & C. Moore; Graft copolymers of polyethylene and polypropylene; US Patent 2,987,501 (Chemical Abstracts 55 (1961) 25374b).
15. P. Blais, D.J. Carlsson, G.W. Csullog & D.M. Wiles; The Chromic Acid Etching of Polyolefin Surfaces, and Adhesive Bonding: Journal of Colloid and Interface Science 47 (1974) 636-649.

16. K.B. Wiberg & G. Foster; The Stereochemistry of the Chromic Acid Oxidation of Tertiary Hydrogens; Journal of the American Chemical Society 83 (1961) 423-429.
17. K.B. Wiberg & A.S. Fox; The Mechanisms of Permanganate Oxidation. Oxidation of Tertiary Hydrogens; Journal of the American Chemical Society 85 (1963) 3487-3491.
18. D. Briggs; Applications of XPS in Polymer Technology (chapter 9). In: D. Briggs & M.P. Seah (editors); Practical Surface Analysis by Auger and X-ray Photoelectron Spectroscopy; John Wiley & Sons, 1983.
19. J.W.F. Spitzen, E. Elsinghorst, M.H.V. Mulder & C.A. Smolders; Solution-Diffusion Aspects in the Separation of Ethanol/Water Mixtures with PVA Membranes; Proceedings of Second International Conference on Pervaporation Processes in the Chemical Industry, San Antonio, 1987, pages 209-224.
20. J.W.F. Spitzen; Pervaporation, Membranes and Models for the Dehydration of Ethanol; Ph.D. thesis, University of Twente, 1988.
21. H. Brüschke; Mehrschichtige Membran und ihre Verwendung zur Trennung von Flüssigkeitsgemischen nach dem Pervaporationsverfahren; German Patent DE 3220570.
22. R.Y.M. Huang & N.R. Jarvis; Separation of Liquid Mixtures by Using Polymer Membranes. II. Permeation of Aqueous Alcohol Solutions Through Cellophane and Poly(vinyl Alcohol); Journal of Applied Polymer Science 14 (1970) 2341-2356.
23. I. Cabasso, E. Korngold & Z.-Z. Liu; On the Separation of Alcohol/Water Mixtures by Polyethylene Ion Exchange Membranes; Journal of Polymer Science: Polymer Letters Edition 23 (1985) 577-581.
24. G. Ellinghorst; Optimale Trennung von Stoffgemischen; Chemische Industrie 7 (1986) 592-594.
25. Gevaert Photo-Producten N.V.; Pretreated polyalkylene films; Belgian patent 569,129.
26. D. Bhattacharyya, A.B. Jumawan Jr. & R.B. Grieves; Charged Membrane Ultrafiltration of Heavy Metals from Nonferrous Metal; Journal of the Water Pollution Control Federation 51 (1979) 176-186.
27. T.W.G. Solomons; Organic Chemistry; John Wiley & Sons, New York, 1976.

Appendix

TERMINOLOGY FOR MEMBRANE DISTILLATION

A.C.M. Franken & S. Ripperger

A.1: Introduction

One of the subjects of the 'Round Table' at the 'Workshop on Membrane Distillation' in Rome on 5 May 1986 was nomenclature. The best example for the need of a more uniform language is the name of the process itself. In Rome the following names were used by the authors present: membrane distillation, Trans Membrane Distillation, thermo-pervaporation, pervaporation and membrane evaporation.

At this workshop a committee was formed with the task of preparing a terminology for membrane distillation. The committee consisted of the following members:

V. Calabro	Universita della Calabria	Calabria	I
A.C.M. Franken	University of Twente	Enschede	NL
S. Kimura	University of Tokyo	Tokyo	J
S. Ripperger	Enka (Membrana)	Wuppertal	D
G. Sarti	Universita di Bologna	Bologna	I
R. Schofield	University of New South Wales	Kensington	AUS

In this document terms, definitions and symbols, which are used in the field of membrane distillation, are defined. The basis for this document is formed by the terminology for pressure driven membrane operations (1); whereever this is relevant the terms in this document are defined in the same way.

A.2: Name of the membrane operation

The most suitable name for this operation is **membrane distillation.** This name has the advantage that it is already used by most authors, that it has no commercial ties with a company and that it cannot be confused with other membrane processes.

For the same reasons as mentioned above, the names Trans Membrane Distillation (the commercial name for the Enka process), pervaporation and thermo-pervaporation (already used for other membrane operations (2)) should not be used. Introducing a new name, like membrane evaporation, has the disadvantage that both author and reader will have adjustment problems, that may result in an even greater confusion of tongues.

The name pervaporation is often used by Japanese authors for two different processes: the process of membrane distillation and the process of pervaporation. In our opinion an essential difference exists between these processes.

According to our definition (see chapter 3a), membrane distillation is a process in which the membrane itself has **no influence** on the vapour-liquid equilibrium of the liquids to be separated. On the other hand, pervaporation is a process in which liquid diffuses through a membrane and evaporates at the permeate side of the membrane. The separation characteristics of the pervaporation process are determined by sorption into and diffusion through the membrane.

A.3. Description of the membrane operation

a. Characteristics of membrane distillation

The name 'membrane distillation' should be applied for membrane operations having the following characteristics:

- the membrane should be **porous**;
- the membrane should **not be wetted** by the process liquids;
- **no capillary condensation** should take place inside the pores of the membrane;
- only **vapour** should be transported through the pores of the porous membrane;
- the membrane must not alter the **vapour-liquid equilibrium** of the different components in the process liquids;
- at least **one side** of the membrane should be in **direct contact** with the process liquid;
- for each component the driving force of this membrane operation is a **partial pressure gradient** in the vapour phase.

b. Different embodiments of membrane distillation

Many different embodiments of membrane distillation can be found in literature. For instance, Enka uses a membrane operation in which the liquid on both sides of the membrane is in direct contact with the membrane (3), whereas on the other hand the Swedish National Development Company uses a system in which the vapour is condensed against a cooling-plate (4).

For the different embodiments of membrane distillation the following terms are defined:

- **direct-contact membrane distillation** for a system in which the liquid on both sides of the membrane is in **direct contact** with the membrane and in which the liquid on the downstream side is used as the **condensing medium** (figure A.1).

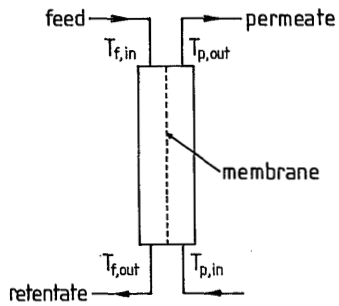

FIGURE A.1:
Direct-contact
membrane distillation.

- **gas-gap membrane distillation** for a system in which the vapour on the downstream side is condensed against a **cooling surface** and in which the condensed liquid on the downstream side **does not have to be** in contact with the membrane (figure A.2). In this configuration the condensation of the permeate takes place **inside** the module.

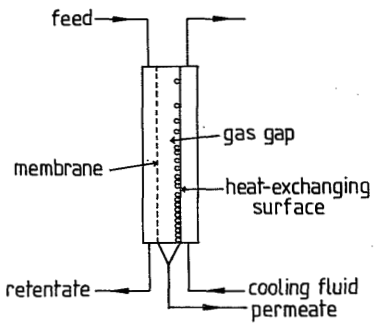

FIGURE A.2:
Gas-gap membrane distillation.

- **low pressure membrane distillation:** in this system a **low pressure** is applied **downstream** and the condensation of the permeate takes place **outside** the module. An other term that can be used in this case is: 'vacuum membrane distillation', but this term is in fact more limiting than low pressure membrane distillation.
- **sweeping gas membrane distillation:** in this system a **sweeping gas** (e.g. nitrogen) is applied **downstream** and the condensation of the permeate takes place **outside** the module.

Note: If the term 'membrane distillation' is used without any further specification, then this term applies to the 'direct-contact'-system. To avoid complications, it is better to use the full term 'direct-contact membrane distillation'.

Example: the system of Enka should be called 'direct-contact membrane distillation' and the system of the Swedish National Development Company should be called 'gas-gap membrane distillation'.

A.4: Membrane characteristics

The membranes, used in membrane distillation, should be characterized by the following membrane (performance) parameters:

a. (polymer) material;
b. thickness of the membrane;
c. porosity of the membrane;
d. nominal pore size;
e. liquid-entry-pressure of water.

a. (polymer) material

The material of which the membrane is made is the most important parameter. At this moment membranes for membrane distillation are all made of polymers, but as one should not exclude other type of materials the term polymer is placed between brackets.

b. thickness of the membrane

This parameter is of importance because it gives information on both the mechanical strength of the membrane and the fluxes to be expected.

c. porosity of the membrane

The porosity of the membrane is defined as the volume of the pores devided by the total volume of the membrane; the symbol for the porosity is ε. A method for the determination of the porosity of (hydrophobic) membranes is suggested in paragraph A.9.

d. nominal pore size

Nominal pore size is important as it can lead to a first approximation of the fluxes to be expected. 'Nominal' pore size is a blanket term incompassing pore sizes estimated from bubble-point tests, gas permeation experiments, or any other convenient technique, and is usually quoted by the membrane manufacturer. Despite the approximate nature of nominal pore size, it conveys useful information, which can be used to make an approximate calculation of the fluxes to be expected.

e. liquid-entry pressure of water

The liquid-entry pressure of water (sometimes faulty called 'wetting pressure') is the pressure (Pa) that must be applied onto pure water before it penetrates into a non-wetted (dry) membrane; the symbol for the liquid-entry pressure of water is LEP_w. A method for the determination of LEP_w of hydrophobic membranes is suggested in paragraph A.9.

These five characteristics are suggested, because they give a visual (a,b) and mechanical (a,b,c) picture of the membrane, while indicating the suitability for membrane distillation (e) and the fluxes to be expected (b,c,d).

As additional information the following membrane characteristics can be given:

f. IPA bubble point;
g. maximum pore size;
h. pore size distribution;
i. pore size morphology;
j. temperature stability;
k. chemical resistance.

f. IPA bubble point

The IPA (isopropylalcohol) bubble point can be measured according to a

standard test method as described in ASTM F-316. This method employs a procedure for determining the maximum pore size and the pore size distribution of a membrane filter by measuring the initial bubble point and gas flow versus pressure through a liquid wet filter. The only difference between the 'IPA bubble point method' and ASTM F-316 is that IPA is used as the wetting liquid instead of water.

g. maximum pore size

The maximum pore size can be calculated by substituting the IPA bubble point pressure into the following formula:

$$\text{pore size} = \frac{4.B.\gamma}{p}$$

in which B: pore size morphology constant;
γ: surface tension of IPA;
p: bubble point pressure.

The pore size morphology constant B is 1 for a circular pore and less than 1 for an elliptical or irregular-shaped pore (7). Because most pores are not circular, the use of the terms 'pore diameter' and 'pore radius' is misleading. Unless membranes with circular pores are used, the term **'pore size'** is recommended.

Note: because the 'pore size morphology constant B' is not known in most cases, it is recommended that the 'IPA bubble point pressure' is given next to the value of the maximum pore size.

h. pore size distribution

The pore size distribution can be measured by means of the standard test method as described in ASTM F-316. A short description of this method is given in point f.

i. pore size morphology

The pore size morphology is closely related to the calculation of the 'maximum pore size' (point g) through the 'pore size morphology constant B'. Therefore, it should be given if the pores are, for instance circular, elliptical or rectangular.

j. temperature stability

The long term stability of a membrane to extreme temperatures should

be given here.

k. chemical resistance

The chemical resistance to solvents, acids and bases is important, especially if the membranes have to be cleaned.

A.5: Process characteristics

The efficiency of a membrane distillation operation can be characterized in many different ways and depends on many different parameters, such as membrane characteristics, module design, hydrodynamic conditions, temperature level, etcetera.

The following parameters are defined to characterize a membrane distillation operation and a membrane distillation process:

a. evaporation efficiency EE;
b. process efficiency PE;
c. concentration factor CF;
d. temperature polarization coefficient TPC.

a. evaporation efficiency EE

This parameter is defined to characterize the efficiency of a membrane distillation operation. The evaporation efficiency EE is defined as:

$$EE = \frac{\text{part of the heat which contributes to evaporation}}{\text{total heat input in the module}}$$

Besides evaporation also a certain heat transfer due to conduction takes place. Therefore, EE is always lower than 1. The value of EE can be calculated very easily. The 'part of the heat which contributes to evaporation' can be calculated by multiplying the measured flux J by the heat of evaporation ΔH_{vap} and the membrane area A. The 'total heat input into the module' can be calculated from a measurement of the caloric value of the incoming and the outgoing feed stream.

b. process efficiency PE

This parameter is used to characterize the efficiency of a membrane

distillation process (N.B. this is a process in which the membrane distillation operation is the most important unit operation). The process efficiency PE is defined as:

$$PE = \frac{\text{heat which contributes to the evaporation of the distillate}}{\text{total heat input of the process}}$$

If the process only consists of a membrane distillation operation then the evaporation efficiency EE is equal to the process efficiency PE. In most cases a heat recovery is advantageously. An example of a membrane distillation process with heat recovery is given in figure A.3.

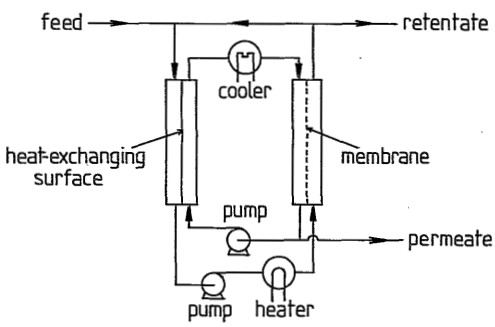

FIGURE A.3: Membrane distillation process with heat recovery.

c. concentration factor CF

The concentration factor CF is defined as the degree of increasing the concentration of a component in a membrane operation. CF can be calculated dividing the concentration of the retentate by the concentration of the feed.

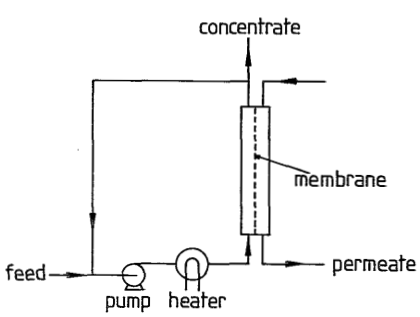

FIGURE A.4: Membrane distillation process with recirculation of the feed.

In formula: $CF = C_r/C_f$. This term is defined in the same way as for pressure driven membrane operations (1).

Due to the low concentration of the solution by one passage of a membrane distillation module, the solution has to be circulated if a concentration of the feed is required (this situation is shown in figure A.4).

d. temperature polarization coefficient TPC

Another phenomenon which occurs in a membrane distillation operation is 'temperature polarization'. Although this term has several disadvantages (its effect cannot be measured directly and the term itself is physically not correct), it is used very often in scientific literature. The value of TPC is given by the temperature difference between the evaporation surface and the condensation surface divided by the temperature difference between the bulk of the feed and the bulk of the permeate.

For direct contact membrane distillation the evaporation surface is formed by the feed-membrane interface and the condensation surface is formed by the permeate-membrane interface. In formula:

$$TPC = \frac{T_{fm} - T_{pm}}{T_{fb} - T_{pb}}$$

It must be stated again that the temperatures at the evaporation (respectively condensation) surface cannot be measured directly. In fact they can only be calculated in special cases when the hydrodynamic conditions on both sides of the membrane are known.

A.6: Definitions

In this chapter a summary is given of the terms that are used in membrane distillation. Whereever this is relevant, the terms are defined in the same way as for pressure driven processes (1).

Bubble point pressure: pressure at which a continuous stream of gas bubbles is pressed through a liquid wet filter.

Bulk temperature T_b: temperature that exists in the bulk phase; in practice

this temperature is equal to the measured temperature.

Circulation loop: a section of a membrane plant containing one or more circulation pumps ensuring adequate cross-flow velocity of the fluid over the membrane (an example is given in figure 4).

Concentration factor CF: the degree of increasing the concentration of a component in a membrane operation; $CF = C_r/C_f$.

Cross-flow velocity u: the velocity of a fluid flowing parallel to the membrane (also called: tangential velocity).

Direct-contact membrane distillation: see chapter 3b.

Evaporation efficiency EE: see chapter 5a.

Feed: the fluid entering a membrane module or plant.

Flux J: amount of permeate, or of any component in the permeate, that is transported through a membrane per unit of membrane area and per unit of time.

Fouling: the deposition of material on the membrane surface and/or in its pores, leading to a change in the membrane performance.

Gas-gap membrane distillation: see chapter 3b.

Liquid-entry pressure LEP: pressure at which the liquid penetrates into a porous membrane (old term to be replaced: 'wetting pressure').

Module: the smallest practical unit containing one or more membranes and supporting structures (old terms to be replaced: permeator, membrane element).

Permeate: the portion of the feed passing through the membrane. Distillate can also be used as a term to describe the 'permeate' of membrane distillation, but it is better to use 'permeate' because it is commonly used in membrane literature.

Pore size: openings in a membrane; this term is prefered to 'pore diameter' and 'pore radius', because all pore shapes can be described by this term.

Porosity: the porosity is defined as the volume of gas that is trapped inside a membrane divided by the total volume of the membrare; a practical definition is given in the appendix 1: 'Determination of membrane characteristics'.

Process efficiency PE: see chapter 5b.

Retentate: the portion of the feed not passing through the membrane (old term: concentrate).

Retention: the ability of a membrane to hinder a component from passing through it or to retain a component in the fluid.

Retention coefficient R: the degree of separation of a certain component from the solvent by the membrane under defined operating conditions; $R = 1-C_p/C_r$. This term should be used if a solution of a solute (e.g. salt) in a solvent (e.g. water) is treated by membrane distillation.

Selectivity α: this term is to be defined as:

$$\alpha = \frac{(\text{wt\% A / wt\% B}) \text{ in permeate}}{(\text{wt\% A / wt\% B}) \text{ in feed}}$$

This term should be used as both components in the membrane distillation system are volatile.

Tangential velocity u: see 'cross-flow velocity'.

Temperature polarization coefficient TPC: see chapter 5.

A.7: Symbols and units

It is very difficult to define symbols in such a way that both author and reader are pleased with it. The discussions between the members of the

nomenclature committee concentrated on the point of the symbols. The discussions about the definition of symbols took about 80% of our discussion time, indicating the difficulty of this matter.

To define the symbols the committee has used the following starting-points:

1. the symbols must be logic and clear to both author and reader;
2. the symbols must be in agreement with the existing membrane literature. The report on the terminology for pressure driven membrane operations (1) is used as a basis for the definition of the symbols;
3. the symbols must be in agreement with the literature on heat transfer. The symbols used in the English literature are used as a basis.

The committee realizes that not everyone will be fully satisfied with the way we defined the symbols for membrane distillation. Nevertheless, we hope that the people working in the field of membrane distillation will use these symbols in their publications.

a. Use of symbols

In this document only those symbols are given which are most frequently used in membane distillation literature. The use of these symbols is strongly recommended.

Latin symbols

A	Membrane area	m^2
C	Concentration	kg/m^3
CF	Concentration factor	--
C_p	Heat capacity	J/kg.K
D	Diffusion coefficient	m^2/s
d	Pore Size	m
EE	Evaporation efficiency	--
ΔH_c	Latent heat of condensation	J/kg
ΔH_{vap}	Latent heat of vaporization	J/kg
h	Heat transfer coefficient	W/m^2K
J	Flux	
	mass flux	kg/m^2s
	molar flux	$kmol/m^2s$
	volume flux	m^3/m^2s
	gas flux	Nm^2/m^2s

k	Thermal conductivity	W/m.K
LEP	Liquid Entry Pressure	Pa
l	Thickness of the air gap	m
M	Molecular weight	Dalton
P	Pressure	Pa
PE	Process efficiency	--
Q	Heat transfer rate	W
Q''	Heat flux	W/m^2
R	Retention coefficient	--
R	Universal gas constant	J/mol.K
T	Temperature	K
TPC	Temperature Polarization Coefficient	--
t	Time	s
U	Overall heat transfer coefficient	W/m^2K
u	Cross-flow velocity	m/s
V	Volume	m^3
w	Weight fraction	--
x	Molar fraction	--

Greek symbols

α	Selectivity	--
γ	Surface tension	N/m
Δ	Difference	--
δ	Membrane thickness	μm
ε	Membrane porosity	--
η	Gas viscosity	Pa.s
μ	Liquid viscosity	Pa.s
π	Osmotic pressure	Pa
ρ	Density	kg/m^3
χ	Membrane pore tortuosity	--

Subscripts

av	Average
b	Bulk
f	Feed
i,j	Index
l	Liquid
m	Membrane

o	Initial, zero
p	Permeate
s	Solute
t	Time
v	Vapour
w	Water

b. use of units

A general rule for the use of units is, that the unit should be as **standard** as possible. This means that in principle SI-units or related units should be used. For instance, the membrane thickness can be given in micrometers instead of meters.

The units which are recommended are given in the 'List of symbols' above.

A.8: References

1. V. Gekas; 'Terminology for pressure driven membrane processes'.
2. P. Aptel et al.; J. Membr. Sc. 1 (1976) 271.
3. K. Schneider & T.J. van Gassel; Chem. Ing. Tech. 56 (1984) 514.
4. Swedish National Development Company; prospect about membrane distillation.
5. W.L. Gore et al.; European Patent EP 88315.
6. I. Cabasso et al.; J. Appl. Pol. Sc. 18 (1974) 2117.
7. R.A. Cotton et al. in 'Membrane filtration; Application, Techniques and Problems' (editor: B.J. Dutka), page 19-39; Marcel Dekker Inc., New York-Basel.

A.9: Determination of membrane characteristics

ad 4b. porosity of the membrane:

The porosity of the membrane is defined as the volume of the pores devided by the total volume of the membrane. The porosity can be measured by making use of a pyknometer, a balance, IPA and water. In this method use is made of the fact that IPA (isopropyl alcohol) penetrates into the pores of the membrane and water does not penetrate into the pores of the membrane.

First, the **density of the polymer material** is calculated using the following formula:

$$\rho_{pol} = \frac{\rho_{IPA} \cdot wt3}{wt1 + wt3 - wt2},$$

in which wt1: weight of the pyknometer with IPA;
wt2: weight of the pyknometer with IPA and membrane;
wt3: dry weight of the membrane.

In the same way the **density of the membrane** can be calculated according to the following formula:

$$\rho_m = \frac{\rho_w \cdot wt3}{wt1 + wt3 - wt2},$$

in which wt1: weight of the pyknometer with water;
wt2: weight of the pyknometer with water and membrane;
wt3: dry weight of the membrane.

The porosity of the membrane can be calculated by the following formula:

$$\varepsilon = 1 - \frac{\rho_m}{\rho_{pol}}.$$

ad 4c. determination of LEP_w:

The following procedure is suggested for the determination of the liquid-entry pressure of water. The apparatus for this measurement is shown in the figure below.

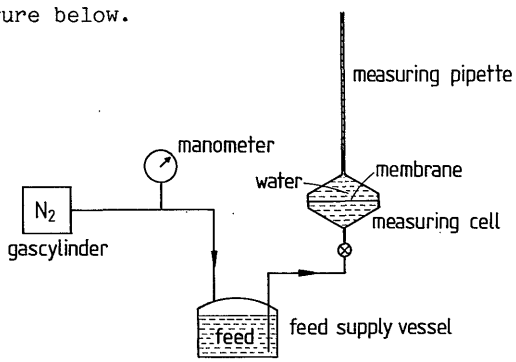

FIGURE A.5: Apparatus for the determination of the liquid-entry pressure.

Measuring procedure:

The dry hydrophobic membrane is placed into the measuring cell and the feed supply vessel is filled with the liquid feed mixture (in this case water). The half-cell which forms the permeate side of the membrane is also filled water. By means of a gascylinder, filled with nitrogen, a slight pressure is applied to the system in order to remove all the gas at the feed side of the membrane. The pressure which is used to remove the gas should of course be lower than the liquid-entry pressure. During the de-gasification of the feed a continuous stream of gas bubbles passes through the membrane. As soon as this stream of gas bubbles stops, there is no more gas in the feed compartment. After the de-gasification of the permeate side the measurement can be started.

During the measurement the pressure is raised stepwise (with 0.1 bar). At each installed pressure one should watch whether a flux through the membrane occurs. The minimum pressure at which a (continuous) flux is observed is called 'liquid-entry pressure'.

SUMMARY

In this thesis several aspects of the membrane distillation process and the thermally driven pervaporation process have been described. Both processes differ essentially from each other as far as their mechanism of separation and their applicability is concerned. From a practical point of view, however, there seems to be hardly any difference between the two processes. The only difference in the experimental set-up of the process is the presence of a permselective layer in the thermally driven pervaporation process.

In fact, the initial proposal for the research project was to develop composite membranes for the membrane distillation process in order to avoid wetting of the hydrophobic membrane, which can take place if organic liquids or surfactants are present in the feed or in the permeate. The application of a **permselective** hydrophilic toplayer onto a porous hydrophobic membrane went beyond the scope of this proposal. Not only wetting of the hydrophobic membrane is avoided, but, moreover, the permselectivity of the toplayer changes the mechanism of separation in such a way that a different process is obtained. This process, called thermally driven pervaporation, can be used for the dehydration of aqueous organic components.

In **chapter 1** a general introduction into membrane technology is given. Special attention is payed to thermally driven membrane processes, pervaporation and the preparation of composite membranes.

The characterization of the microporous sublayer was studied in chapters 2 and 3. In these chapters the criteria for the applicability of a membrane distillation operation and a thermally driven pervaporation process are described.

In **chapter 2** theoretical considerations about wetting of homogeneous smooth materials are given and a critical solute concentration is calculated. For porous materials no such theoretical relation can be derived. Therefore, an experimental method, called penetrating drop method, is developed. By means of this method the maximum allowable concentration of an organic component in water, at which the liquid is on the verge of penetration into the membrane, can be determined. On basis of these measurements, the maximum allowable concentration under process conditions can be calculated.

Wetting of porous membranes is influenced by i) the membrane material,

ii) the nature of the penetrating liquid and iii) the structure of the porous material. In **chapter 3** it is shown that all kinds of structures of porous membranes can be classified into two basic types of structures: the 'sharp-edged' and the 'rounded' pore structure. Theoretical considerations on the penetration of a liquid into both types of pore structures are experimentally checked using the 'penetrating drop method'. It is shown that membranes with a 'sharp-edged' pore structure show more liquid-repellency than those with a 'rounded' pore structure.

The next two chapters discuss the possibility of separating a mixture of ethanol and water by membrane distillation. In **chapter 4**, a model, in which vapour-liquid equilibria data are combined with an effect of temperature polarization and concentration polarization, is described. From these calculations it was shown that the flux and the selectivity of the membrane distillation operation hardly change any more for changing hydrodynamic conditions once the flow at both sides of the membrane has become turbulent. Furthermore, it was calculated that both flux and selectivity increase if the temperature difference between the feed side and the permeate side of the membrane increases.

In **chapter 5** membrane distillation experiments with ethanol/water mixtures are presented and the experimental selectivities and fluxes are compared with the calculated values. A good agreement between model and experiments was found.

The thermally driven pervaporation process, in which a composite membrane consisting of a hydrophilic selective toplayer and a porous hydrophobic sublayer is used, is described in **chapter 6**. The driving force for this process is caused by the thermal gradient existing between the warm feed side of the membrane and the cold permeate side of the membrane. The characteristics of this new process design and its advantages over other pervaporation designs are described. Composite membranes, comprised of a toplayer of cellulose acetate or poly(vinyl alcohol) and a microporous polypropylene sublayer, were tested on their separation characteristics using the thermally driven pervaporation process as well as a pervaporation process with vacuum downstream.

In **chapter 7** a newly developed method for the application of a homogeneous permselective layer onto a porous hydrophobic sublayer, called the evaporation-deposition method, is described. Several coating variables, among others a chemical treatment of the surface of the microporous sublayer, are discussed. Results of the application of a poly(vinyl alcohol)

layer onto microporous polypropylene capillaries are evaluated by pervaporation experiments. With this coating-method membranes with high selectivities and moderate fluxes, as well as membranes with high fluxes and moderate selectivities can be obtained.

The report on 'Terminology for Membrane Distillation' as published by the European Society of Membrane Science and Technology is given as an **appendix** to this thesis.

SAMENVATTING

In dit proefschrift worden diverse aspecten van het membraandestillatieproces en het thermisch gedreven pervaporatieproces besproken. Wat betreft het scheidingsmechanisme en de toepassingsmogelijkheden verschillen beide processen essentieel van elkaar. Desondanks lijken beide processen op het eerste gezicht vrijwel identiek te zijn. Het enige verschil in experimentele omstandigheden is de aanwezigheid van een selectief polymeerlaagje op het hydrofobe microporeuze membraan in het thermisch gedreven pervaporatieproces.

Als organische oplosmiddelen of oppervlakte-aktieve stoffen in de voeding of het permeaat aanwezig zijn, kan bevochtiging van het hydrofobe microporeuze membraan optreden. Vanuit deze achtergrond is het oorspronkelijke voorstel van het onderzoeksproject als volgt geformuleerd: het ontwikkelen van composietmembranen voor membraandestillatie.

Het aanbrengen van een **selectieve** hydrofiele toplaag op een hydrofobe poreuze onderlaag ging verder dan met het projectvoorstel werd beoogd. Het effect van de selectieve toplaag is dat niet alleen de bevochtiging van de onderlaag wordt voorkomen, maar dat bovendien het scheidingsmechanisme van het membraanproces op een dusdanige manier verandert dat men niet meer van membraandestillatie kan spreken, maar het proces met pervaporatie dient aan te duiden. Dit thermisch gedreven pervaporatieproces kan worden toegepast voor het ontwateren van organische oplosmiddelen.

In **hoofdstuk 1** wordt een inleiding over membraantechnologie in het algemeen gegeven, waarbij speciale aandacht wordt besteed aan thermische membraanprocessen, pervaporatie en de bereiding van composietmembranen.

De karakterisering van de hydrofobe microporeuze onderlaag komt aan de orde in de hoofdstukken 2 en 3, waar de criteria voor de toepasbaarheid van membraandestillatie en het thermisch gedreven pervaporatieproces worden geformuleerd.

In **hoofdstuk 2** worden theoretische beschouwingen over de bevochtiging van gladde homogene oppervlakken gegeven van waaruit de kritische oppervlaktespanning en de daarbij behorende concentratie van organisch oplosmiddel in water kan worden berekend. Deze berekeningen kunnen echter niet zonder meer op poreuze materialen worden toegepast. Daarom is er een experimentele methode, genaamd "penetrating drop method", ontwikkeld. Met behulp van deze methode kan de maximaal toegestane hoeveelheid van een

organische component in water, waarbij de vloeistof op de rand van binnendringen in het poreuze membraan is, worden gemeten. Op basis van deze metingen kan de maximaal toegestane hoeveelheid van de organische component tijdens het membraandestillatie of het thermisch gedreven membraanproces worden berekend.

De bevochtiging van poreuze membranen wordt beinvloed door de volgende factoren: i) het membraan materiaal, ii) de aard van de bevochtigende vloeistof en iii) de structuur van het poreuze materiaal. In **hoofdstuk 3** wordt beschreven dat alle verschillende poriestructuren van poreuze membranen in principe kunnen worden geklassificeerd als twee typen: een "scherpe" ('sharp-edged') en een "ronde" ('rounded') poriestructuur. De theoretische afleidingen over het binnendringen van een vloeistof in beide typen van poriestructuren worden experimenteel geverifieerd met behulp van de "penetrating drop method". Uit de onderzoekingen blijkt dat een vloeistof minder gemakkelijk binnendringt in membranen met een "scherpe" poriestructuur dan in membranen met een "ronde" poriestructuur.

De beide volgende hoofdstukken handelen over de mogelijkheid van het scheiden van een mengsel van ethanol en water met behulp van membraandestillatie. In **hoofdstuk 4** wordt een model beschreven, waarin het effect van temperatuur- en concentratiepolarisatie wordt gecombineerd met de gegevens van het vloeistof-damp evenwicht. Uit de berekeningen blijkt dat het veranderen van de hydrodynamische omstandigheden nauwelijks enig effect heeft op de flux en de selectiviteit van het membraandestillatieproces als er turbulente stroming aan beide zijden van het membraan optreedt. Verder kan er theoretisch worden afgeleid dat de flux en de selectiviteit van het membraandestillatieproces toeneemt als het temperatuurverschil tussen voedingszijde en permeaatzijde van het membraan toeneemt.

In **hoofdstuk 5** worden de resultaten van membraandestillatie-experimenten met ethanol/water mengsels gepresenteerd en worden de experimentele waarden van flux en selectiviteit vergeleken met de berekende waarden. Er wordt een goede overeenkomst tussen model en experimenten gevonden.

Het thermisch gedreven pervaporatieproces, waarbij gebruik wordt gemaakt van een composietmembraan bestaande uit een hydrofiele selectieve toplaag en een poreuze hydrofobe onderlaag, wordt beschreven in **hoofdstuk 6.** De drijvende kracht voor dit proces wordt veroorzaakt door de temperatuurgradient tussen de warme voedingszijde en de koude permeaatzijde van het membraan. De kenmerkende eigenschappen van dit nieuwe procesontwerp en de voordelen ten opzichte van andere procesuitvoeringen van pervaporatie

worden beschreven. De scheidingseigenschappen van composietmembranen, bestaande uit een toplaag van cellulose-acetaat of polyvinylalcohol en een microporeuze onderlaag van polypropyleen, worden bepaald met behulp van het thermisch gedreven pervaporatieproces en een pervaporatieproces waarbij gebruik wordt gemaakt van vacuum aan de permeaatzijde.

In **hoofdstuk 7** wordt een nieuwe coatingsmethode, genaamd "evaporation-deposition method", voor het aanbrengen van een homogene selectieve polymeerlaag op een poreuze hydrofobe onderlaag beschreven. Diverse coatingsvariabelen, onder andere een chemische modificatie van het oppervlak van de microporeuze onderlaag, worden behandeld. Aan de hand van pervaporatie-experimenten worden de scheidingseigenschappen van een composietmembraan, waarbij een selectieve laag van polyvinylalcohol op microporeuze capillairen van polypropyleen is aangebracht, bepaald. Met behulp van deze coatingsmethode kunnen zowel membranen met een hoge flux en een relatief lage selectiviteit als membranen met een hoge selectiviteit en een relatief lage flux worden verkregen.

Een rapport over standaardisering van begrippen voor membraandestillatie, getiteld "Terminology for Membrane Distillation", is als **appendix** aan dit proefschrift toegevoegd. Dit rapport is gepubliceerd door de "European Society of Membrane Science and Technology".

LIST OF PUBLICATIONS

- Preferential sorption versus preferential permeability in pervaporation;
M.H.V. Mulder, T. Franken & C.A. Smolders;
Journal of Membrane Science 22 (1985) 155.

- On the mechanism of separation of ethanol/water mixtures by pervaporation. II. Experimental concentration profiles;
M.H.V. Mulder, A.C.M. Franken & C.A. Smolders;
Journal of Membrane Science 23 (1985) 41.

- Pervaporationverfahren;
A.C.M. Franken, M.H.V. Mulder & C.A. Smolders;
German Patent DE 3536007 (July 1986).

- Ethanol/Water Separation by Membrane Distillation: Effect of Temperature Polarization;
A.C.M. Franken, J.A.M. Nolten, M.H.V. Mulder & C.A. Smolders;
In: B. Sedlacek & J. Kahovec (editors); Synthetic Polymeric Membranes, pages 531-540; De Gruyter, Berlin, 1987.

- Wetting criteria for the Applicability of Membrane Distillation;
A.C.M. Franken, J.A.M. Nolten, M.H.V. Mulder, D. Bargeman & C.A. Smolders;
Journal of Membrane Science 33 (1987) 315.

- Terminology for Membrane Distillation;
A.C.M. Franken & S. Ripperger;
European Society for Membrane Science and Technology, January 1988.

- Verfahren zum Herstellen einer Zweischichtmembran;
A.C.M. Franken, M.H.V. Mulder & C.A. Smolders;
German Patent DE 3707054 (February 1988).

- Pervaporation Process;
A.C.M. Franken, M.H.V. Mulder & C.A. Smolders;
European Patent EP 218,019.

- Process for the production of a bilayer membrane;
  A.C.M. Franken, M.H.V. Mulder & C.A. Smolders;
  United States patent application RWP 24619.

- Separation of isomeric xylenes. A fundamental approach;
  M.H.V. Mulder, A.C.M. Franken & C.A. Smolders;
  (to be published).

- Influence of the structure of a microporous membrane on its wettability;
  A.C.M. Franken, J.A.M. Nolten, D. Bargeman, M.H.V. Mulder & C.A. Smolders;
  (to be published in Journal of Colloid & Interface Science).

- Ethanol/water separation by membrane distillation. 1. Model;
  A.C.M. Franken, M.H.V. Mulder & C.A. Smolders;
  (to be published in Journal of Membrane Science).

- Ethanol/water separation by membrane distillation. 2. Experimental results;
  A.C.M. Franken, J.A.M. Nolten, M.H.V. Mulder & C.A. Smolders;
  (to be published in Journal of Membrane Science).

- Pervaporation process using a thermal gradient as the driving force;
  A.C.M. Franken, M.H.V. Mulder & C.A. Smolders;
  (to be published in Journal of Membrane Science).

- The evaporation-deposition method: a method for the application of a homogeneous permselective layer onto a microporous hydrophobic layer;
  A.C.M. Franken, R.M. Meertens, J.A.M. Nolten, M.H.V. Mulder
  & C.A. Smolders;
  (to be published in Journal of Membrane Science).

LEVENSLOOP

Ton Franken werd geboren op 9 mei 1957 te Klarenbeek. Hij behaalde in 1975 zijn Atheneum-B diploma aan het Veluws College te Apeldoorn. In datzelfde jaar begon hij zijn studie Chemische Technologie aan de toenmalige Technische Hogeschool Twente, nu Universiteit Twente, te Enschede.

Hij behaalde in januari 1981 het baccalaureaatsdiploma (vakgroep Anorganische Chemie en Materiaalkunde) en in september 1983 het ingenieursdiploma (vakgroep Macromoleculaire Chemie en Materiaalkunde).

Van 1 november 1983 tot 1 mei 1985 verrichte hij zijn vervangende dienstplicht in de onderzoeksgroep van prof. C.A. Smolders en aansluitend trad hij als wetenschappelijk assistent in dienst van de Technische Hogeschool Twente bij dezelfde onderzoeksgroep. Tot 1 mei 1988 verrichte hij het onderzoek dat in dit proefschrift is beschreven.

Na zijn promotie zal hij in dienst treden van het Centre for Membrane and Separation Technology aan de University of New South Wales te Sydney, Australië.